

Explorations in Generalized Quasi-topological Gravities

by

Mengqi Lu

A thesis
presented to the University of Waterloo
in fulfillment of the
thesis requirement for the degree of
Doctor of Philosophy
in
Physics

Waterloo, Ontario, Canada, 2025

© Mengqi Lu 2025

Examining Committee Membership

The following served on the Examining Committee for this thesis. The decision of the Examining Committee is by majority vote.

External Examiner: Manu Paranjape
Professor, Dept. of Physics, University of Montreal

Supervisor(s): Robert Mann
Professor, Dept. of Physics and Astronomy, University of Waterloo

Internal Member: Niayesh Afshordi
Professor, Dept. of Physics and Astronomy, University of Waterloo

Internal-External Member: Florian Girelli
Professor, Dept. of Physics and Astronomy, University of Waterloo

Other Member(s): Avery Broderick
Professor, Dept. of Physics and Astronomy, University of Waterloo

Author's Declaration

This thesis consists of material all of which I authored or co-authored: see Statement of Contributions included in the thesis. This is a true copy of the thesis, including any required final revisions, as accepted by my examiners.

I understand that my thesis may be made electronically available to the public.

Statement of contributions

This thesis is based on the following published and forthcoming articles.

- Chapter 2 is based on:
 - Pablo Bueno, Pablo A. Cano, Robie A. Hennigar, Mengqi Lu, and Javier Moreno. *Generalized quasi-topological gravities: the whole shebang*. *Class. Quant. Grav.*, 40(1):015004, 2023. [30]
- Chapter 3 is based on:
 - Mengqi Lu and Robert B. Mann. *Maxwell construction and multi-criticality in un-charged generalized quasi-topological black holes*. *Class. Quant. Grav.*, 41(1):015016,2024. [120]
- Chapter 4 is based on:
 - Mengqi Lu, Jiayue Yang, and Robert B. Mann. *Gravitational Wormholes*. *Universe*, 10:257, 2024. [121]
 - Mengqi Lu, Jiayue Yang, and Robert B. Mann. *Existence of vacuum wormholes in Einsteinian cubic gravity*. *JHEP*, 03:073, 2025. [122]
- Contributions not included in the thesis:
 - Mengqi Lu and Robert B. Mann. *Lagrangian Partition Functions Subject to a Fixed Spatial Volume Constraint in the Lovelock Theory*. *Entropy*, 26(4):291, 2024. [119]
 - Ming Zhang, Wen-Di Tan, Mengqi Lu, Dyuman Bhattacharya, Jiayue Yang, and Robert B. Mann. *Finite-cutoff Holographic Thermodynamics*. 7 2025. [170]

Abstract

This thesis presents a comprehensive study of Generalized Quasi-Topological Gravities (GQTGs), a broad class of higher-curvature extensions of Einstein gravity in arbitrary spacetime dimensions. These theories are distinguished by possessing second-order linearized field equations around maximally symmetric backgrounds and admitting static, spherically symmetric black hole solutions characterized by a single metric function $f(r)$ obeying a second-order differential equation. We rigorously demonstrate that, at order n in curvature, exactly $n - 1$ inequivalent GQTG densities exist in dimensions $D \geq 5$, among which only one belongs to the Quasi-topological subclass for which the field equations reduce to an algebraic equation for $f(r)$. In contrast, we find strong evidence that only a unique such density exists for each order in four dimensions, which is not of the Quasi-topological kind.

We analyze the thermodynamic properties of black holes in these theories and confirm that the first law of thermodynamics is satisfied. Moreover, we provide evidence that the black hole thermodynamics is fully encoded in the same embedding function that determines the maximally symmetric vacua of the theory, offering a unified and simplified framework for studying solutions with arbitrary higher-curvature corrections.

Building on this foundation, we explore the multi-critical thermodynamic behavior of uncharged AdS black holes in GQTGs. Utilizing a reformulated version of Maxwell's equal area law, we identify a geometric criterion for the existence of multicritical (or N -tuple) points in the black hole phase diagram. Applying this criterion, we explicitly construct black hole solutions exhibiting quadruple and quintuple critical points supported by genuine GQTG densities.

Finally, we uncover a novel class of traversable wormhole solutions in four-dimensional Einsteinian Cubic Gravity—a specific GQTG—including examples that are entirely vacuum configurations with no need for exotic matter. These wormholes connect asymptotically AdS regions with a geometric deficit at infinity, interpretable as a global monopole. We demonstrate that these configurations satisfy standard traversability conditions and exhibit a variety of geometries depending on the parameter space.

Acknowledgements

My time at the University of Waterloo has been one of the most formative and meaningful periods of my life. Approximately eight years ago, I began my journey in research as an undergraduate student under the supervision of Dr. Robert Mann. At that time, I was experiencing a difficult period marked by severe depression, which significantly impacted my academic performance. Due to this, I had even contemplated leaving physics after completing my bachelor's degree. However, Dr. Mann, with remarkable generosity and foresight, offered me the opportunity to pursue a master's degree. That pivotal gesture not only allowed me to continue in academia but ultimately set me on the path toward completing my PhD.

For that reason, I am deeply grateful to Dr. Mann, who has served not only as an exceptional research advisor but also as a wise and compassionate mentor. His unwavering enthusiasm, encouragement, and optimism have sustained me throughout this academic journey.

I would also like to express my sincere thanks to Dr. Robie Hennigar, my first collaborator, whose generosity with his time and knowledge has left a lasting impact on my development as a researcher. His patient explanations and thoughtful insights were invaluable, and I have learned much from him—both in terms of research and mentorship.

Special thanks are due to Dr. Ming Zhang for his steadfast support in both academic and personal matters.

I extend my deepest appreciation to all of my friends and collaborators, including Pablo Bueno, Pablo A. Cano, Javier Moreno, Jiayue Yang, Wen-Di Tan, Dyuman Bhattacharya, Rex (Ruan) Zhang, Muzi Li, and Zhenggao Wu.

Finally, I would like to express my heartfelt gratitude to my father, Yonkun Lu. Without his unwavering financial support, I could not have come this far.

Table of Contents

Examining Committee	ii
Author's Declaration	iii
Statement of contributions	iv
Abstract	v
Acknowledgements	vi
List of Figures	ix
List of Tables	xii
1 Introduction	1
1.1 Einstein's theory of General Relativity	2
1.1.1 Stress-energy tensor and energy conditions	4
1.1.2 Geodesic congruences	6
1.2 Black holes	7
1.2.1 Euclidean derivation of Hawking temperature	9
1.2.2 Covariant formalism of black hole entropy	11
1.2.3 Black hole phase transitions	14
1.3 Wormholes	15
1.4 Modified theories of gravitation	16
2 Structure of GQTGs	21
2.1 How many types of GQTGs are there?	21
2.1.1 At most $(n + 1)$ order- n densities	22

2.1.2	At most $(n - 1)$ order- n densities	24
2.1.3	Uniqueness of Quasi-topological densities	26
2.1.4	Exactly $(n - 1)$ order- n densities	27
2.2	Black Hole Thermodynamics	31
2.2.1	The first law for general GQTGs	31
2.2.2	A unified picture of the thermodynamics?	33
2.3	Comments	36
3	Multicriticality of black holes	37
3.1	Thermodynamics of GQTG black holes	37
3.2	Geometric interpretation of interphase equilibrium	40
3.3	Multiple phases and N -tuple critical points	42
3.4	Einstein-power-Maxwell AdS black holes	45
3.5	Comments	47
4	Vacuum wormholes in GQTGs	56
4.1	An overview of the main results	56
4.2	Basic strategy	57
4.3	Initial value problems	59
4.4	Wormhole identification	60
4.5	Traversability of the wormhole	61
4.6	Wormhole Candidates	62
4.7	Comments	64
5	Final remarks	65
	References	66
	APPENDICES	78
A		79
A.1	Explicit covariant genuine GQTG densities for $n = 4, 5, 6$ in $D = 5, 6$	79
A.2	Physical constraints for GQTG black holes	88
A.3	Field Equations	90
A.4	Taylor Series Solution at $u = 0$	91
A.5	Taylor Series Solution at $u = u_{\text{th}}$	91

List of Figures

1.1	Kruskal–Szekeres diagram	8
3.1	The Maxwell equal-area construction implies $P = P^*$ divides AaBbC into two regions AaB and BbC with equal areas. The red curve indicates the trajectories of the plots if $K'' = 0$	42
3.2	A quadruple point A is constructed in $D = 7$ with $f_\infty = 1.001359562$, $P^* = 0.07466400248$, $T^* = 0.2615575508$, $\alpha_{4,2} = -1.983132445$, $\alpha_{5,2} = -0.6595495180$, $\alpha_{6,2} = 0.1064022549$, $\alpha_{7,2} = -0.02347725421$, $\alpha_{8,2} = 0.002665217984$. Four exact radii $\{1, 1.07, 1.239, 1.4\}$ are taken as input. The black hole has positive γ^2 everywhere while the entropy is almost positive everywhere except the red region near $T = 0$. Behaviors around A and B are indicated by the two subfigures respectively. The point C_1 is one of the cusps, and in the next figure 3.3, we show the rest 5 which are accumulated around A . So it is a quadruple point with an extremely far-away cusp.	49
3.3	The figure shows further magnifications about the quadruple point A in figure 3.2. The points C_2 to C_6 are five cusps, and the remaining one is indicated in figure 3.2. These cusps are extremely narrow so that they look like lines. Regarding this fact, we further zoom in around A and color curves passing A for better distinguishability. Nearing A , those curves are closer to each other. Staring at the right part of the right subfigure and moving carefully enough, we can see that three curves intersect A , but it is actually four, because the green and red curves between orange and brown ones overlap. Moving a bit far away from A , namely in the dotted box, the red and green curves become more distinguishable.	50

3.4	A quintuple point A appears in $D = 7$ with $f_\infty = 0.9982618066$, $P^* = 0.03402189695$, $T^* = 0.1648652352$, $\alpha_{3,2} = 1, \alpha_{4,2} = 6.232655784$, $\alpha_{5,2} = 1.096317618$, $\alpha_{6,2} = 0.2676712136$, $\alpha_{7,2} = -0.2079188594$, $\alpha_{8,2} = 0.09653639807$, $\alpha_{9,2} = -0.02640506854, \alpha_{10,2} = 0.003268616550$, where $\alpha_{3,2}$ is set to 1 in advance, and the rest of the parameters are computed after five exact radii $\{1, 1.07, 1.21, 1.4, 1.6\}$ are taken as input. The upside of this adjustment is that we can find a physical quintuple point with negative free energy more easily. Blue and red colors indicate regions with positive and negative entropy respectively; solid and dashed curves partition the points with positive and negative γ^2 respectively. Two subfigures show different extents of magnification about the quintuple point A and a further magnification is shown in the next figure 3.5 to clarify that A is truly a quintuple point.	51
3.5	This figure shows further magnifications about the quintuple point A in figure 3.4. We can clearly see the intersection of 5 curves appears at A . . .	52
3.6	This figure shows that the Gibbs free energy corresponds to the equation of state (3.29) with $Q = 1.2368, P^* = 0.0020878, b_5 = -1.0973, b_9 = 1.5937, b_{13} = -1.2746, b_{17} = 0.40172$ which intersects with $T^* = 0.034711$ at $r_+^{(1)} = 1, r_+^{(2)} = 1.04, r_+^{(3)} = 1.1, r_+^{(4)} = 1.4, r_+^{(5)} = 1.9, r_+^{(6)} = 2.9, r_+^{(7)} = 4$	53
3.7	The figure shows the Gibbs free energy corresponds to the equation of states (3.29) with $Q = 1.2424, P^* = 0.0020704, b_5 = -1.1233, b_9 = 1.6535, b_{13} = -1.3338, b_{17} = 0.42279$ which intersects with $T^* = 0.034555$ at $r_+^{(1)} = 1, r_+^{(2)} = 1.04, r_+^{(3)} = 1.1, r_+^{(4)} = 1.42, r_+^{(5)} = 1.9, r_+^{(6)} = 2.93, r_+^{(7)} = 4$	54
3.8	This figure shows that the Gibbs free energy corresponds to the equation of state (3.29) with $Q = 1.2431, P^* = 0.0020692, b_5 = -1.1285, b_9 = 1.6683, b_{13} = -1.3512, b_{17} = 0.42992$ which intersects with $T^* = 0.034544$ at $r_+^{(1)} = 1, r_+^{(2)} = 1.0424, r_+^{(3)} = 1.1, r_+^{(4)} = 1.4243, r_+^{(5)} = 1.9, r_+^{(6)} = 2.93, r_+^{(7)} = 4$	55
4.1	A wormhole solution with a positive mass M (4.16) is constructed subject to $\beta = 0.091, F_2 = 1, F_4 \approx -0.281186 \in (-1, 0), F_5 = 0.1, u_{\text{th}} \approx 3.19114$. The increasing and decreasing solid black curves correspond to the numerical solutions for $F(u)$ and $n(u)$ respectively. Dashed curves are truncations of the series (4.17). Truncation orders are 7, 12, 20 for the respective blue, pink, and purple curves for F ; and 8, 13, 21 for n . We see that pink and purple series curves overlap with the numeric ones for almost the entire domain of u , indicating the speed of convergence for the series (4.18). . . .	61
4.2	Solutions for different F_4 's. Rising and descending curves of the same color respectively correspond to $F(u)$ and $n(u)$ of a solution. The increasing and decreasing curves originating at $u = 0$ respectively correspond to $F(u)$ and $n(u)$. The wormhole solution in Figure 4.1 is in black, with $\beta = 0.091, F_2 = 1, F_4 \approx -0.281186, F_5 = 0.1$. The purple and the blue curves only differ the black ones in F_4 (purple: $F_4 = -0.1$; blue: $F_4 = -0.31$).	63

4.3	Wormhole candidates. The same labeling convention as in Figure 4.1 is applied here. Left: $\beta = 0.2, F_2 = F_5 = 1, F_4 \approx -0.635778, u_{\text{th}} \approx 0.937102$; Right: $\beta = 0.05, F_2 = F_5 = 1, F_4 \approx -0.648749, u_{\text{th}} \approx 3.36473$	63
4.4	Relations between wormhole mass M and throat size r_{th} for $\beta = 0.05$ (purple) and 0.091 (pink). Both of them have the same $F_2 = 1$, and F_4 is obtained by the prescription in Section 4.6.	64

List of Tables

- 3.1 The table shows a general pattern that the pressure follows when some genuine GQTG densities ($k \geq 2$) are turned on. The top element of each column indicate the power of $1/r_+$, and each row contains all possible couplings with a constant sum of subscripts. The table tells what powers of $1/r_+$ in the expression of pressure are influenced by which couplings. For example, if $\alpha_{5,2}$ is the only non-zero coupling, then the pressure will contain three monomials of the form $1/r_+^7, 1/r_+^8, 1/r_+^9$ in addition to P_0 ; if $\alpha_{7,4}$ is turned on as well, then two extra monomials $1/r_+^{10}, 1/r_+^{11}$ will be introduced and both of $\alpha_{5,2}$ and $\alpha_{7,4}$ contribute to coefficient of the term $1/r_+^9$ 48

Chapter 1

Introduction

Over the past century, Albert Einstein’s theory of General Relativity (GR)[69] has established that gravity arises from the curvature of spacetime. GR has proven remarkably successful in describing phenomena at low energies and in weak gravitational fields. Early experimental confirmations include the observed deflection of light by massive bodies[64, 65] and the measurement of time dilation[81], both in precise agreement with GR. In 2016, LIGO detected gravitational waves from a binary black hole merger[1], and in 2019 the Event Horizon Telescope (EHT) captured the first image of a black hole[51]. These landmark observations, together with earlier tests, demonstrate that GR remains highly successful in the classical regime. However, efforts to reconcile GR with quantum mechanics revealed a fundamental incompatibility: GR is non-renormalizable, meaning the divergences that arise in a Feynman diagram expansion cannot be removed by a finite set of counterterms. As a result, GR can only be treated as an effective theory, valid up to a certain energy scale but expected to break down at higher energies.

The difficulties in finding a consistent quantum theory of gravity may come from gravity itself—Einstein’s theory needs to be modified. In 1967, inspired by quantum field theory, Andrei Sakharov argued that the quantum effects of matter induce suitable extra higher curvature terms in the action [149]. In 1976, Kellogg Stelle proved that some higher-curvature gravities are renormalizable [154], making such theories candidates for a quantum theory of gravity. String-theoretic versions of quantum gravity motivate the possibility of higher dimensional spacetimes, and the addition of higher-curvature corrections allows for broader generalizations of the Einstein-Hilbert action to dimensions larger than four. These higher-curvature theories provide toy models for studying the AdS/CFT correspondence and allow for holographic study of Conformal Field Theories (CFTs). In cosmology, an extra squared Ricci scalar R^2 term in the effective action can perfectly induce Starobinsky inflation [153]. These higher-curvature theories also provide toy models for studying the AdS/CFT correspondence and allow for holographic study of Conformal Field Theories (CFTs). Thus, there is no natural reason why higher curvature terms should be eliminated from consideration in gravity.

But the inclusion of higher order curvature terms usually comes at a price – it can yield equations of motion containing higher derivatives in the metric that give rise to instabilities

and negative energy modes [138, 165]. Notably, this inconsistency with GR is absent in some classes of higher-curvature theories [117, 118, 152, 164] in which only a massless spin-2 graviton can propagate to infinity. This subclass of higher-curvature gravity theories is considerably more promising than the others and thus warrants further investigation.

Generalized quasi-topological gravities (GQTGs), a class of recently proposed higher-derivative theories, satisfies the requirements noted above. Theories in the GQTG class characterize generalizations of GR in any dimension and to any order in curvature insofar as they contain non-hairy black hole solutions and second-order-differential equations for the metric in any linearized maximally symmetric background [29, 30, 131].

The main purpose of this thesis is to review some of my contributions to this topic. In this chapter, we basically review a few important concepts in GR, such as how to compute thermodynamic variables of black holes, and give a formal definition of GQTGs. The Chapter 2 is about my work [30] on the identification of GQTGs; the Chapter 2 is based on my work [120] on constructing multicriticality points for GQTG black holes; the Chapter 4 is related to my work [121, 122] which finds the existence of a vacuum traversable wormhole in GQTGs.

1.1 Einstein's theory of General Relativity

The modern viewpoint on gravitation is deeply rooted in Einstein's theory of gravity, where gravity is interpreted as the manifestation of spacetime curvature. As motivated by the Equivalence Principle, the gravitational field is described by a four-dimensional pseudo-Riemannian manifold \mathcal{M} , and the local flatness (locally Minkowski) of a manifold guarantees an inertial reference frame exists at any point in the spacetime.

The whole dynamics of gravity is built on the extra mathematical assumptions. In GR, the Koszul connection ∇ that is associated to \mathcal{M} is postulated to be torsionless and metric compatible, namely,

$$\Gamma_{bc}^a = \Gamma_{cb}^a, \quad \nabla_a g_{bc} = 0, \quad (1.1)$$

where Γ_{bc}^a are the connection coefficients for ∇ . Therefore, the Riemannian tensor $R^a{}_{bcd}$ and the connection are totally determined by a Lorentzian metric tensor g_{ab} via

$$\Gamma_{bc}^a = \frac{1}{2} g^{ad} (\partial_b g_{cd} + \partial_c g_{bd} - \partial_d g_{bc}), \quad (1.2)$$

$$R^a{}_{bcd} = \partial_c \Gamma_{bd}^a - \partial_d \Gamma_{bc}^a + \Gamma_{fc}^a \Gamma_{bd}^f - \Gamma_{fd}^a \Gamma_{bc}^f, \quad (1.3)$$

and the metric tensor can be considered as a fundamental quantity measuring the gravitational field. The Riemannian tensor has identities

$$R_{abcd} = R_{cdab} = -R_{bacd} = -R_{abdc}, \quad (1.4)$$

and its only non-trivial contraction is the Ricci tensor given by

$$R_{bc} \equiv R^a{}_{bac} \quad (1.5)$$

being symmetric in the two indices.

In order to obtain the dynamics of g_{ab} , we have to find the stationary point of the action schematically,

$$S = S_{\text{grav}} + S_{\text{mat}}. \quad (1.6)$$

The matter action S_{mat} contains all non-gravitational fields. We first focus on the part S_{grav} which is postulated to be the Einstein-Hilbert action

$$S_{\text{grav}} = \frac{1}{16\pi G} \int_{\mathcal{M}} d^4x \sqrt{-g} R, \quad g \equiv \det g_{ab}, \quad (1.7)$$

with $R \equiv g^{ab}R_{ab}$ the Ricci scalar and G the Newton's constant. The appearance of $\sqrt{-g}$ ensures the integral is defined properly so that the action is a scalar on the manifold \mathcal{M} .

After some lengthy algebra, the change in S_{grav} under variation of the metric is given by

$$\delta S_{\text{grav}} = \frac{1}{16\pi G} \int \sqrt{-g} d^4x (G_{ab} \delta g^{ab} + \nabla_a \delta v^a), \quad \delta v^a \equiv \nabla_b (-\delta g^{ab} + g^{ab} g_{cd} \delta g^{cd}). \quad (1.8)$$

Besides the desired Einstein tensor

$$G_{ab} \equiv R_{ab} - \frac{1}{2} R g_{ab} \quad (1.9)$$

there is a total-derivative term involving the first derivatives of δg_{ab} at the boundary. This brings us a little trouble, as the term doesn't vanish identically for the Dirichlet condition ($\delta g_{ab} = 0$ at the boundary) implying the physical path is non-stationary. This can be fixed by adding (1.8) a Brown-York boundary term to cancel all first derivatives of δg_{ab} , but for now let's ignore this issue and we will come back to this latter.

One fundamental symmetry the action (1.7) has is diffeomorphism invariance, which means physics doesn't depend on the specific labeling of spacetime points. For the diffeomorphism $x^a \rightarrow x^a + \xi^a$, the change in the action is a total derivative (the measure d^4x doesn't change)

$$\delta_\xi (R \sqrt{-g}) = \sqrt{-g} \nabla_a (R \xi^a). \quad (1.10)$$

This is a general result for actions with integrand being some scalar times a volume form. The change in g^{ab} arises due to the diffeomorphism should be given by the Lie derivative $\mathcal{L}_\xi g^{ab}$,

$$\delta_\xi g^{ab} = \mathcal{L}_\xi g^{ab} = \nabla^a \xi^b + \nabla^b \xi^a. \quad (1.11)$$

By comparing (1.10) and (1.8) with δg^{ab} being replaced by $\delta_\xi g^{ab}$, we yield the contracted Bianchi identity

$$\nabla^a G_{ab} = 0, \quad (1.12)$$

and the off-shell conservation law

$$\nabla_a J^a = 0, \quad (1.13)$$

for the Noether current,

$$J^a \equiv 2G^{ab} \xi_b - R \xi^a + \delta_\xi v^a. \quad (1.14)$$

As $\nabla_a J^a = 0$ holds off-shell, restrictively speaking, it should be regarded as an identity rather than a conservation law. One special advantage for such a current is that there exists a Noether potential J^{ab} such that

$$J^a \equiv \nabla_b J^{ab}. \quad (1.15)$$

In the case of GR, one standard choice of Noether potential is

$$J^{ab} = \frac{1}{16\pi G} (\nabla^a \xi^b - \nabla^b \xi^a). \quad (1.16)$$

The matter action S_{mat} gives the rest part of field equation. Varying it with respect to g^{ab} yields

$$\delta S_{\text{mat}} = - \int \frac{1}{2} T_{ab} \delta g^{ab} \sqrt{-g} d^4 x, \quad (1.17)$$

where T_{ab} is the stress-energy tensor defined as

$$T_{ab} \equiv - \frac{2}{\sqrt{-g}} \frac{\delta S_{\text{mat}}}{\delta g^{ab}}. \quad (1.18)$$

Therefore the full field equation for gravity is

$$G_{ab} = 8\pi G T_{ab}. \quad (1.19)$$

We see immediately that the matter action S_{mat} sources gravity, or in other words, it curves the spacetime.

Additionally, since G_{ab} is divergence-free due to the Bianchi identity, the stress-energy must satisfy

$$\nabla^a T_{ab} = 0, \quad (1.20)$$

as well. This means S_{mat} should also be diffeomorphism-invariant. In fact, this is not as restrictive as it sounds, as we discussed earlier, for any action schematically

$$S_{\text{mat}} = \int \sqrt{\gamma} d^D x L_{\text{mat}} \quad (1.21)$$

with L_{mat} a scalar, and $\sqrt{\gamma} d^D x$ a volume form of D dimensions, is diffeomorphism-invariant as long as the equation of motion for fields is satisfied. This makes the interpretation of (1.20) different from (1.12)—it is a conservation law rather than an identity.

1.1.1 Stress-energy tensor and energy conditions

The interpretation of the stress-energy tensor T_{ab} can be exemplified by considering the matter action for a single particle of mass m :

$$S_p = -m \int \sqrt{-g_{ab} \frac{dx^a}{d\lambda} \frac{dx^b}{d\lambda}} d\lambda, \quad (1.22)$$

where λ is used to parametrize the trajectory $x^a(\lambda)$ of the particle. As S_p is reparameterization invariant, taking the coordinate time t as λ , the variation of S_p with respect to g_{ab} reads (μ is the spacial index)

$$\delta S_p = \frac{1}{2}m \int \frac{u^a u^b}{u^t} \delta g_{ab}(x^\mu(t), t) dt, \quad (1.23)$$

where $u^a = dx^a/d\tau$ (τ proper time) are the components of the four-velocity satisfying $u_a u^a = -1$. In the argument of δg_{ab} , we separates the trajectory $x^a(t)$ into the spatial components x^μ and the time component t , which enables us to rewrite δS_p as

$$\delta S_p = -\frac{1}{2}m \int_{\mathcal{M}} d^4x \frac{u_a u_b}{u^t} \delta^{(3)}(x^\mu - x^\mu(t)) \delta g^{ab}(x). \quad (1.24)$$

We could further simplify it by inserting the identity $1 = \int d\tau \delta(t - t(\tau)) dt/d\tau$:

$$\delta S_p = -\frac{1}{2}m \int_{\mathcal{M}} d^4x \int d\tau \delta^{(4)}(x^c - x^c(t(\tau))) u_a u_b \delta g^{ab}(x), \quad (1.25)$$

yielding T_{ab} describing the energy and momentum of the particle

$$T_{ab} = \frac{m}{\sqrt{-g}} \int d\tau \delta^{(4)}(x^c - x^c(t(\tau))) u_a u_b. \quad (1.26)$$

In classical physics, energy density is typically non-negative. To translate this idea into the context of GR, we assume T_{ab} to satisfy energy conditions. Because an observer (timelike or lightlike) with a four velocity v^a measures the energy density to be $T_{ab} v^a v^b$, we define the weak energy condition (WEC) as

$$T_{ab} v^a v^b \geq 0 \quad (1.27)$$

for any future-directed timelike vector v^a , and the null energy condition (NEC) by simply replacing v^a by an arbitrary null vector k^a :

$$T_{ab} k^a k^b \geq 0. \quad (1.28)$$

Sometimes we relax the positive energy condition a little bit to assume the strong energy condition (SEC) where

$$(T_{ab} - \frac{1}{2}Tg_{ab})v^a v^b \geq 0 \quad (1.29)$$

holds for all timelike v^a . Both NEC and SEC can be reformulated into geometric relations $R_{ab} k^a k^b \geq 0$ and $R_{ab} v^a v^b \geq 0$ respectively via Einstein's equation, which will be used in deriving the focusing theorem of geodesic congruence. In quantum scenarios, these conditions can be violated.

1.1.2 Geodesic congruences

The variation of S_p with respect to x^a leads to the free motion of a particle in the spacetime with g_{ab} . For an affinely parameterized trajectory $x^a(\tau)$, its motion satisfies the geodesic equation

$$u^a \nabla_a u^b = 0. \quad (1.30)$$

It should be mentioned that, even though (1.30) is derived from a massive particle, it works for massless particles as well. Then the integral curve $x^a(\tau)$ generated by u^a is the trajectory of the particle. Now consider a small enough region of the spacetime filling with timelike geodesics $x^a(\tau)$. We can always define ξ^a as a deviation vector field pointing between two neighboring geodesics in the congruence satisfying

$$u^a \xi_a = 0, \quad \mathcal{L}_u \xi^a = \mathcal{L}_\xi u^a. \quad (1.31)$$

The first constraint makes u^a ($u^a u_a = -1$) and ξ^a are orthogonal; while the second one implies ξ^a is integrable and thus generates a coordinate as well. This is justified by the fact that an orthogonal coordinate system always exists in a sufficiently small neighborhood. To proceed, we introduce a tensor B_{ab} that encodes the evolution of ξ^a along the geodesic congruence:

$$u^a \nabla_a \xi^b \equiv B^b_a \xi^a, \quad (1.32)$$

which measures the failure of ξ^a being parallel transported along the congruence. Based on the second constraint in (1.31), the tensor B_{ab} can be expressed as

$$B_{ab} = \nabla_b u_a. \quad (1.33)$$

The interpretation of B_{ab} can be seen from decomposing it into three parts:

$$B_{ab} \equiv \frac{1}{3} \Theta h_{ab} + \sigma_{ab} + \omega_{ab}, \quad (1.34)$$

where h_{ab} is the induced metric on the surface Σ normal to u^a , given by

$$h_{ab} = g_{ab} + u_a u_b. \quad (1.35)$$

The expansion scalar $\Theta \equiv \nabla_a u^a$ is the trace of B_{ab} measuring the expansion of Σ along the congruence, the second term contains all symmetric and traceless parts of B_{ab} measuring the shear effect of Σ along the congruence, the last contains all totally anti-symmetric term characterizes rotation of Σ along geodesics. Taking derivative of Θ with respect to the proper time, we yield

$$\frac{d\Theta}{d\tau} = u^b \nabla_b (\nabla_a u^a). \quad (1.36)$$

Expanding the double derivative via

$$(\nabla_a \nabla_b - \nabla_b \nabla_a) u^c = R^c_{abd} u^d, \quad \forall u^a, \quad (1.37)$$

bring us to

$$\frac{d\Theta}{d\tau} = -B^{ab} B_{ab} - R_{ab} u^a u^b. \quad (1.38)$$

Expanding B_{ab} yields the Raychaudhuri equation

$$\frac{d\Theta}{d\tau} = -\frac{1}{3}\Theta^2 - \sigma^{ab}\sigma_{ab} + \omega^{ab}\omega_{ab} - R_{ab}u^a u^b. \quad (1.39)$$

For geodesics that are hypersurface-orthogonal, namely u^a is a gradient of some scalar function, the rotation tensor ω_{ab} vanishes due to Frobenius's theorem. As the shear tensor is purely spatial, so $\sigma^{ab}\sigma_{ab} \geq 0$. All these imply if the strong energy condition $R_{ab}u^a u^b \geq 0$ holds, the expansion scalar θ always decreases, manifesting the focusing of the timelike congruence. This property demonstrates the attractive nature of gravity when the strong energy condition holds.

For the null geodesics with a four-velocity k^a ($k^a k_a = 0$), we can similarly define a derivation vector field ξ satisfying

$$k^a \xi_a = 0, \quad \mathcal{L}_k \xi^a = \mathcal{L}_\xi k^a. \quad (1.40)$$

This time the induced metric on the hypersurface Σ transverse to k^a becomes

$$h_{ab} = g_{ab} + k_a l_b + k_b l_a, \quad (1.41)$$

where l^a is an auxiliary null vector field and is normalized to $k^a l_a = -1$. The appearance of l^a in the above completeness relation is because of k^a being both orthogonal and normal to the surface Σ resulting another null normal vector field l^a . Thus the transverse surface is 2-dimensional.

Due to the existence of l^a , the tensor $B_{ab} = \nabla_b k_a$ can be further reduced to

$$B'_{ab} = h_{ac} h_{bd} B^{cd}, \quad (1.42)$$

which can be decomposed into

$$B'_{ab} = \frac{1}{2}\Theta h_{ab} + \sigma_{ab} + \omega_{ab} \quad (1.43)$$

with each part the same meaning as before. It should be mentioned that the equation (1.38) holds for the null case and $B^{ab} B_{ab} = B'^{ab} B'_{ab}$. Hence Raychaudhuri's equation for null congruences reads

$$\frac{d\Theta}{d\tau} = -\frac{1}{2}\Theta^2 - \sigma^{ab}\sigma_{ab} + \omega^{ab}\omega_{ab} - R_{ab}k^a k^b. \quad (1.44)$$

If the null energy condition $R_{ab}k^a k^b \geq 0$ holds, then the focusing property of the null congruence is still true for hypersurface-orthogonal congruences ($\omega_{ab} = 0$).

1.2 Black holes

Black holes are amongst the most remarkable predictions of GR, representing solutions to Einstein's field equations with regions where nothing can escape. The simplest black hole, characterized by static spherical symmetry, is described by the Schwarzschild metric:

$$ds^2 = -\left(1 - \frac{2GM}{r}\right) dt^2 + \left(1 - \frac{2GM}{r}\right)^{-1} dr^2 + r^2 d\Omega^2, \quad (1.45)$$

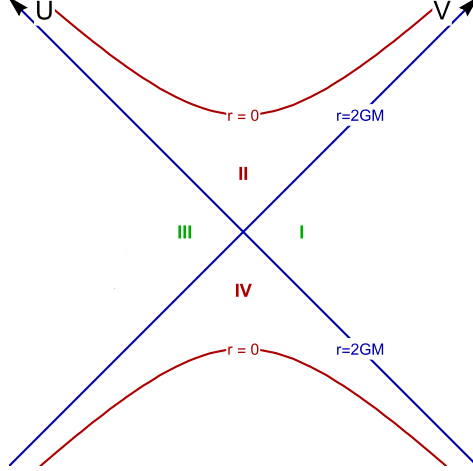


Figure 1.1: Kruskal–Szekeres diagram

where t is the time coordinate, r is a non-negative radial coordinate, and $d\Omega^2 = d\theta^2 + \sin^2\theta d\phi^2$ is the angular line element. The constant M represents the total mass as measured by an observer at infinity.

For $r > 2GM$, the Schwarzschild metric describes a gravitational field sourced by a static, spherically symmetric object, reducing to Newtonian gravity in the weak-field limit for distant observers. The metric retains a Lorentzian signature, with t as the only timelike coordinate. Test particles and light can move freely in this region, either falling toward $r = 2GM$ or escaping to infinity, depending on their initial conditions.

In the interior region where $0 < r < 2GM$, the metric exhibits the defining “black” property: the coordinate t becomes spacelike, and r becomes timelike, decreasing inexorably toward $r = 0$. Therefore, objects entering this region are compelled toward the origin. At $r = 0$, a true curvature singularity emerges, where tidal forces diverge, signaling the breakdown of Einstein’s theory.

The surface at $r = 2GM$, known as the event horizon, separates these regions and is a coordinate singularity in the metric (1.45). This singularity can be eliminated by using Kruskal–Szekeres coordinates:

$$XY = \left(\frac{r}{2GM} - 1 \right) e^{r/(2GM)}, \quad Y/X = e^{t/(2GM)}, \quad (1.46)$$

yielding the metric:

$$ds^2 = \frac{32G^3 M^3}{r} e^{-r/(2GM)} dX dY + r^2 d\Omega^2, \quad (1.47)$$

which smoothly extends the geometry across the horizon, see Figure 1.1. The event horizon, where both r and t coordinates become null, is effectively two-dimensional and possesses striking properties. In the 1970s, Bekenstein, Hawking, Bardeen and Carter established that black holes behave as thermodynamic systems [15, 18, 19, 90], capable of radiating energy via quantum pair production near the horizon—a semiclassical phenomenon now

known as Hawking radiation [90]. This endows the black hole with an effective temperature:

$$T_{\text{H}} = \frac{\hbar c^3}{8\pi G M k_B}, \quad (1.48)$$

inversely proportional to its mass. Subsequently, the Bekenstein-Hawking entropy was derived as:

$$S = \frac{k_B c^3 A}{4\hbar G}. \quad (1.49)$$

where k_B is Boltzmann's constant, \hbar is the reduced Planck constant, and A is the area of the event horizon given by

$$A = \frac{4\pi G^2 M^2}{c^4}. \quad (1.50)$$

Through a direct calculation, we obtain the first law of thermodynamics

$$dM = T_{\text{H}} dS, \quad (1.51)$$

and the Smarr relation [134, 151]

$$M = 2T_{\text{H}} S. \quad (1.52)$$

The latter captures global scaling behaviors of M analogous to the Euler equation for extensive parameters.

1.2.1 Euclidean derivation of Hawking temperature

The Euclidean path integral approach connects quantum statistical mechanics and classical physics via the partition function. It is quite profound that, in 1977, Gibbons and Hawking [85] showed the direct application of path integral to gravity reveals some properties of quantum gravity. As a consequence, the Hawking temperature arises from eliminating the conical singularity for the Euclidean metric at black hole horizon to make the manifold geodesically complete there.

To illustrate, consider a black hole metric of the form

$$ds^2 = -f(r)dt^2 + f(r)^{-1}dr^2 + r^2 d\Omega^2, \quad (1.53)$$

where the horizon is located at r_+ satisfying $f(r_+) = 0$. Performing a Wick rotation $t \rightarrow i\tau$, obtain the corresponding Euclidean metric

$$ds_{\text{E}}^2 = f(r)d\tau^2 + f(r)^{-1}dr^2 + r^2 d\Omega^2, \quad r \geq r_+. \quad (1.54)$$

This geometry is singular at $r = r_+$ unless the imaginary time coordinate τ is assigned a period $\beta = 4\pi/f'(r_+)$. To demonstrate, consider a circle with radius l on a cone parametrized by coordinates r and τ . The center of the circle lies on the tip of a cone ($r = r_+$). To remove the conical singularity, namely, the tip, we should guarantee the geometry to be

locally flat there, which holds only if the perimeter of the circle is $2\pi l$. For our case, the radius l and perimeter are given by

$$l = \int_{r_+}^r f^{-1/2} dr, \quad C = \int_0^\beta f^{1/2} d\tau. \quad (1.55)$$

In the limit of $\Delta r \equiv r - r_+ \rightarrow 0$, they are approximately

$$l \approx 2\sqrt{\frac{\Delta r}{f'(r_+)}} , \quad C \approx \sqrt{f'(r_+)\Delta r}\beta, \quad (1.56)$$

It is straightforward to verify $C = 2\pi l$ only if

$$\beta = 4\pi/f'(r_+). \quad (1.57)$$

This period corresponds to the inverse Hawking temperature (1.48) for Schwarzschild black hole. Alternatively, the temperature can be expressed

$$T = \frac{\kappa}{2\pi} \quad (1.58)$$

in terms of the surface gravity κ defined as the gravitational force measured at infinity needed for an observer hovering on the horizon. This force is constant along the horizon, confirming the temperature interpretation of the black hole. For the null generator ξ^a of the horizon, surface gravity satisfies the equation

$$\xi^a \nabla_a \xi^b = \kappa \xi^b, \quad (1.59)$$

which can be used as an alternative definition of κ .

We conclude this section by addressing the issue in (1.8), where the physical path is not stationary under Dirichlet conditions due to the boundary term δv^a involving first derivatives of the metric. This is resolved by adding the Brown-York boundary term to the gravitational action:

$$S_{\text{grav}} = \frac{1}{16\pi G} \int_{\mathcal{M}} d^4x \sqrt{-g} R + \frac{1}{8\pi G} \int_{\partial\mathcal{M}} d^3x \sqrt{h} K, \quad (1.60)$$

where K is the extrinsic curvature and h is the determinant of the induced metric on the boundary $\partial\mathcal{M}$. This term ensures a well-defined ADM mass for asymptotically flat black holes. In general backgrounds, additional boundary terms [14, 74] are needed in (1.60) for holographic renormalization to regularize the ADM mass. Another motivation for including the boundary term is that the resulting action (1.60) depends only on the first derivatives of the metric, making it suitable for use in the Euclidean path integral formalism. The partition function is:

$$Z = \int \mathcal{D}[g_{ab}] e^{-S_E}, \quad (1.61)$$

where the Euclidean action is:

$$S_{\text{E}} = -\frac{1}{16\pi G} \int_{\mathcal{M}_{\text{E}}} d^4x \sqrt{-g} R - \frac{1}{8\pi G} \int_{\partial\mathcal{M}_{\text{E}}} d^3x \sqrt{h} K. \quad (1.62)$$

The path integral can be evaluated via saddle-point approximation:

$$Z \approx \mathcal{A} e^{-S_{\text{E}}|_{\text{on-shell}}}, \quad (1.63)$$

where S_{E} is evaluated for metrics satisfying the field equations, and \mathcal{A} is a normalization constant. The Helmholtz free energy is:

$$F = -T \log Z. \quad (1.64)$$

Thermodynamic variables are derived as:

$$M = \langle E \rangle = -\frac{\partial}{\partial \beta} \log Z, \quad S = \beta \langle E \rangle + \log Z. \quad (1.65)$$

The thermodynamic energy $\langle E \rangle$ corresponds to the ADM mass M for Schwarzschild black holes (1.45).

Computing M and S via path integrals is often challenging due to complicated boundary contributions. For asymptotically AdS black holes, the Fefferman–Graham expansion of the metric provides a more efficient way to compute the mass. The next section introduces a general method for calculating black hole entropy in arbitrary backgrounds.

1.2.2 Covariant formalism of black hole entropy

A systematic way to derive the entropy of more general stationary black holes carrying angular momentum and charges, based on covariant phase space formalism for field theories, is developed by Wald and Iyer [100, 101, 158]. In this framework black hole entropy arises as a Noether charge associated with the null Killing vector generating the horizon, generalizing the Bekenstein–Hawking entropy to arbitrary diffeomorphism-invariant gravitational theories. We outline the derivation below, assuming no matter fields for simplicity.

Consider a diffeomorphism-invariant gravitational theory described by a scalar Lagrangian L_{grav} that depends solely on the metric g_{ab} and the Riemann curvature tensor R_{abcd} :

$$S = \int d^Dx \sqrt{-g} L_{\text{grav}}. \quad (1.66)$$

We define the generalized Ricci tensor \mathcal{R}_{ab} and P^{abcd} as

$$\mathcal{R}_{ab} \equiv \left. \frac{\partial L_{\text{grav}}}{\partial g^{ab}} \right|_{R_{abcd}}, \quad P^{abcd} \equiv \left. \frac{\partial L_{\text{grav}}}{\partial R_{abcd}} \right|_{g_{ab}}. \quad (1.67)$$

It can be shown easily that \mathcal{R}_{ab} is symmetric and P^{abcd} inherits same symmetries in indices as R^{abcd} . These tensors are related by an easy relation

$$\mathcal{R}^{ab} = P^{acde} R^b_{cde}. \quad (1.68)$$

Varying the action with respect to the metric, treating L_{grav} as a function of g^{ab} and R_{abcd} , yields

$$\delta S = \int_{\mathcal{M}} d^D x \sqrt{-g} (E_{ab} \delta g^{ab} + \nabla_a \delta v^a), \quad (1.69)$$

where E_{ab} is the symmetric tensor analogous to the Einstein tensor, given by

$$E_{ab} \equiv \mathcal{R}_{ab} - \frac{1}{2} g_{ab} L_{\text{grav}} - 2 \nabla^c \nabla^d P_{acdb}, \quad (1.70)$$

and δv^a is a divergence term, reads

$$\delta v^a \equiv 2 P^{cabd} \nabla_b \delta g_{dc} - 2 \delta g_{dc} \nabla_b P^{cabd}. \quad (1.71)$$

For Einstein gravity ($L_{\text{grav}} = R$), this reduces to the standard boundary term (1.8). In addition, the diffeomorphism invariance of the action leads to a Noether current J^a associated with a vector field ξ^a :

$$J^a \equiv 2 E^{ab} \xi_b - L_{\text{grav}} \xi^a + \delta_\xi v^a, \quad (1.72)$$

where $\delta_\xi v^a$ is the variation of v^a under a diffeomorphism generated by ξ^a . There also exists a Noether potential

$$J^{ab} = 2 P^{abcd} \nabla_c \xi_d - 4 \xi_d \nabla_c P^{abcd} \quad (1.73)$$

such that $J^a = \nabla_b J^{ab}$. The current and potential reduce to (1.14) and (1.16) for Einstein's theory respectively.

Here comes the most crucial part. If we look at the Hamiltonian (ADM) formalism of gravity, there exists a symplectic $(D-1)$ -form defined on the covariant phase space as:

$$\omega^a = \delta (\sqrt{-g} \delta_\xi v^a) - \delta_\xi (\sqrt{-g} \delta v^a), \quad (1.74)$$

and encodes the dynamics of the gravitational field via

$$\delta H[\xi] = \int_{\mathcal{C}} d\Sigma_a \omega^a / \sqrt{-g}, \quad (1.75)$$

where \mathcal{C} is a $(D-1)$ -dimensional Cauchy surface, and $d\Sigma_a$ is the directed surface element. We can connect the on-shell ($E_{ab} = 0$) Hamiltonian variation $\delta H[\xi]$ and the current J^a by

$$\omega^a = \delta (J^a[\xi] \sqrt{-g}) + 2 \sqrt{-g} \nabla_b (\xi^{[a} \delta v^{b]}), \quad (1.76)$$

where $\delta_\xi v^a$ is eliminated by (1.72). Thus, the variation of the Hamiltonian becomes:

$$\delta H[\xi] = \delta \int_{\mathcal{C}} d\Sigma_a J^a + 2 \int_{\mathcal{C}} d\Sigma_a \nabla_b (\xi^{[a} \delta v^{b]}). \quad (1.77)$$

For a stationary black hole, the vector field ξ^a can be chosen as a Killing vector field satisfying $\mathcal{L}_\xi g_{ab} = 0$, ensuring the metric is invariant under its flow. This ξ^a generates the horizon, becoming null on the black hole horizon, and corresponds to a linear combination of time translations and rotations at asymptotic infinity. The Cauchy surface \mathcal{C} has two

boundaries: the bifurcation surface \mathcal{S}_{bif} of the horizon (where $\xi^a = 0$) and the boundary at infinity \mathcal{S}_∞ . Applying Stokes' theorem, we obtain:

$$\begin{aligned}\delta H[\xi] &= \delta \int_{\mathcal{C}} d\Sigma_a J^a + \int_{\partial\mathcal{C}} d\Sigma_{ab} (\xi^{[a} \delta v^{b]}) \\ &= -\frac{1}{2} \delta \int_{\mathcal{S}_{\text{bif}}} d\Sigma_{ab} J^{ab} + \frac{1}{2} \delta \int_{\mathcal{S}_\infty} d\Sigma_{ab} J^{ab} + \int_{\mathcal{S}_\infty} d\Sigma_{ab} (\xi^{[a} \delta v^{b]}).\end{aligned}\tag{1.78}$$

The minus sign for the first term arises from its inward orientation relative to the outward normal at \mathcal{S}_∞ . Since $\xi^a = 0$ on \mathcal{S}_{bif} , the term $\xi^{[a} \delta v^{b]}$ vanishes there, yielding the third term alone. For the Hamiltonian to be well-defined, the integral over \mathcal{S}_∞ must be expressible as the variation of a $(D-1)$ -form. Note the Hamiltonian $H[\xi]$ for a Killing vector is conserved, $\delta H[\xi] = 0$ by construction. Therefore the relation (1.78) can be identified with the first law of thermodynamics, and the contributions at infinity are identified as the ‘‘work terms’’:

$$\delta\mathcal{E} - \Omega_{\text{H}}\delta\mathcal{J},\tag{1.79}$$

where \mathcal{E} is the energy (e.g., the ADM mass) and \mathcal{J} is the angular momentum, with Ω_{H} being the angular velocity of the horizon. The first arises from the bifurcation surface is identified as the entropy. Specifically, the Wald entropy is given by:

$$S_{\text{Wald}} = \frac{1}{2} \beta \int_{\mathcal{S}_{\text{bif}}} J^{ab} d\Sigma_{ab}.\tag{1.80}$$

Expanding the area element as

$$d\Sigma_{ab} = (l_a \xi_b - l_b \xi_a) \sqrt{\sigma} d^{D-2}x,\tag{1.81}$$

where l_a is an auxiliary vector field normalized to $\xi^a l_a = -1$. In the case of GR, the potential is given by (1.16). Then the entropy S_{Wald} is evaluated to be

$$S_{\text{Wald}} = -\frac{\beta}{8\pi G} \int d^{D-2}x \sqrt{\sigma} l_a \xi_b \nabla^b \xi^a = \frac{\beta\kappa}{8\pi G} \int d^{D-2}x \sqrt{\sigma} = \frac{A}{4G},\tag{1.82}$$

where (1.59) and $\beta\kappa = 2\pi$ are used.

It is more convenient to recast (1.80) into

$$S_{\text{Wald}} = -2\pi \int_{\mathcal{S}_{\text{bif}}} d^{D-2}x \sqrt{\sigma} P_{ab}{}^{cd} \epsilon^{ab} \epsilon_{cd},\tag{1.83}$$

where ϵ^{ab} is the binormal tensor to the surface \mathcal{S}_{bif} .

The Wald entropy (1.80), which originates from the inner boundary, remains unaffected by the counterterms used to renormalize the ADM mass and is valid for general backgrounds. It generalizes the Bekenstein-Hawking entropy in Einstein gravity to arbitrary diffeomorphism-invariant theories.

1.2.3 Black hole phase transitions

The inclusion of cosmological constant Λ in black hole thermodynamics didn't gain much attention until Hawking and Page [91] found a first-order phase transition between thermal radiation and asymptotically AdS black holes in 1982. This striking result reveals that black holes exhibit behaviors analogous to conventional matter. In the context of the AdS/CFT correspondence, the Hawking–Page transition corresponds to a confinement/deconfinement transition in the dual gauge theory [163]. Another key development in this direction is the recognition that the cosmological constant can be viewed as a variable interpreted as thermodynamic pressure (rather than a constant),

$$P = -\frac{\Lambda}{8\pi G}, \quad (1.84)$$

which was first proposed by Teitelboim and Brown [24, 156]. The variation of the cosmological constant can be interpreted in terms of a massless scalar field, which was first investigated in [86]. With a corresponding thermodynamic volume defined as

$$V \equiv \left(\frac{\partial M}{\partial P} \right)_s, \quad (1.85)$$

the corresponding thermodynamic term can be formally incorporated into the first law [52] and the Smarr relation [42]:

$$\delta M = T\delta S + V\delta P + \dots, \quad (1.86)$$

$$(D-3)M = (D-2)TS - 2VP + \dots. \quad (1.87)$$

It should be mentioned that the thermodynamic volume is independent of geometric volume [62] for most of black holes [53].

With the inclusion of a cosmological constant, the mass M no longer corresponds to the internal energy. Instead, it should be interpreted as the gravitational analogue of the chemical enthalpy H , as its variation takes the same form as that of enthalpy:

$$\delta H = T\delta S + V\delta P. \quad (1.88)$$

This paradigm, often referred to as black hole chemistry [112, 113, 123, 124], opens the door to a rich landscape of phase transitions and critical phenomena reminiscent of those in fluid systems.

Over the past decade, the perspective of black hole chemistry has led to the discovery of a number of rich properties, including Van der Waals phase transitions [111], re-entrant phase transitions [4, 79], superfluid-like phase transitions [63, 95, 97], triple points [5, 79, 98, 99], and multicritical points [120, 155, 166–169]

These phenomena more easily occur in higher-curvature theories as these theories introduce new coupling constants, which can be viewed as thermodynamic parameters controlling the different phases of black holes. In particular, N -th order multicriticality, defined

as a point where N distinct phases merge at a single value of pressure and temperature and generalizing the notion of a triple point (with $N = 3$), was first seen in Einstein gravity coupled to non-linear electrodynamics [155], but was shortly afterward found to be present in multiply rotating Kerr-AdS black holes [167], and in Lanczos-Lovelock gravity [166]. In the latter case multi-critical behaviour can even occur for asymptotically flat black holes [168]. In Chapter 3, we will carry out a general method to construct these points.

1.3 Wormholes

Wormholes are hypothetical solutions to Einstein’s field equations in General Relativity, describing topological structures that connect two distant regions of spacetime or different universes. These structures, often visualized as tunnels or bridges, were first proposed by Ludwig Flamm in 1916. The Einstein-Rosen bridge, introduced by Albert Einstein and Rosen in 1935 [70], represents one of the earliest theoretical models of a wormhole. It arises from the maximally extended Schwarzschild metric, connecting regions I and III (or II and IV) in the Kruskal-Szekeres diagram (see Figure 1.1). However, this wormhole is non-traversable due to its dynamical instability and the presence of a curvature singularity at $r = 0$, where infinite tidal forces would easily destroy any object attempting to pass through.

In 1973, Homer G. Ellis introduced the first wormhole solution [71, 72] free of curvature singularities and event horizons, described by the metric:

$$ds^2 = -dt^2 + d\ell^2 + r(\ell)^2 d\Omega^2, \quad (1.89)$$

where $r(\ell)$ is a function of the proper radial coordinate ℓ , given by:

$$r(\ell) = \sqrt{\rho^2 + \ell^2}, \quad (1.90)$$

and ρ is a constant defining the wormhole throat’s radius.

Approximately fifteen years later, in 1988, Morris and Thorne [132] generalized this concept with a traversable wormhole metric:

$$ds^2 = -e^{2\Phi(r)} dt^2 + (1 - b(r)/r)^{-1} dr^2 + r^2 d\Omega^2, \quad (1.91)$$

where $\Phi(r)$ is the redshift function, and $b(r)$, the shape function, determines the wormhole’s spatial geometry. To illustrate, consider an embedding in flat space with the metric:

$$ds^2 = dz^2 + dr^2 + r^2 d\phi^2. \quad (1.92)$$

The surface

$$z(r) = \pm(r/b(r) - 1)^{-1/2} \quad (1.93)$$

yields a spatial line element matching (1.91). For continuity, there exists a throat radius r_{th} where $z(r_{\text{th}}) = 0$, defining the wormhole’s throat.

The functions Φ and b are subject to specific constraints. Traversability requires the absence of event horizons, so $\Phi(r)$ must remain finite everywhere. The embedding function $z(r)$ must be smooth, implying $dz/dr \rightarrow \infty$ at the throat. Additionally, the throat should be a local minimum of $r(z)$, requiring the flare-out condition $d^2r/dz^2 \geq 0$ at $r = r_{\text{th}}$. In order to avoid the case where passengers talk infinite amount of time to transpass, the proper distance $\ell(r)$ should be well-defined, and thus $1 - b(r)/r \geq 0$ for $r \geq r_{\text{th}}$.

In GR, the Morris–Thorne wormhole requires exotic matter that violates the NEC and SEC in order to exist. This follows directly from Raychaudhuri’s equation. For the metric (1.91), the rotation tensor ω_{ab} , defined in (1.34), vanishes identically for both timelike and null geodesic congruences. From the embedding function $z(r)$, one sees that at the throat—corresponding to a local minimum—future-directed geodesic congruences diverge, in direct contradiction with the focusing theorem discussed in 1.1.2. This indicates repulsive gravity and therefore the necessity of exotic matter violating both NEC and SEC in a wormhole geometry. This requirement has spurred research into modified theories of gravity [17, 54–56, 61, 78, 89, 136], as such theories often incorporate additional structures that may enable the construction of traversable wormholes without the need for exotic matter [23, 71, 72, 147, 148]. Another interesting aspect of 4-dimensional traversable wormholes is that they violate quantum energy inequalities, which may make them non-traversable [157]. In Chapter 4, we will construct a vacuum traversable wormholes in higher-curvature theories, bypassing any additional structures.

1.4 Modified theories of gravitation

Despite its remarkable success, GR also faces challenges in describing physics in the quantum regime. As GR is a four-dimensional theory, it should be have higher-dimensional versions to incorporate bosonic and supersymmetric string theories. Along with the dimension, higher-curvature corrections, terms involving higher powers of the Riemann curvature tensor or its contractions, to the Einstein-Hilbert action (1.6) naturally arise due to string and effective field theories. Furthermore, observational phenomena, such as the accelerated expansion of the universe attributed to dark energy, suggest that these modifications may be necessary. Higher-curvature terms can effectively contribute to the stress-energy tensor, mimicking exotic matter and driving cosmic acceleration. In addition, these modifications enrich gravitational dynamics and provide a framework for testing deviations from GR in extreme environments, and uncover universal or distinctive features of gravitational theories.

The most direct higher-curvature generalizations of GR are the Lanczos [114, 115] - Lovelock [117] (LL) theories. A comprehensive review can be found in [139]. Its Lagrangian is usually expressed as a linear combination of curvature invariants

$$\mathcal{L}_{\text{grav}} = \sum_n \alpha_n \mathcal{R}^{(n)}, \quad \mathcal{R}^{(n)} = \frac{1}{2^n} \delta_{c_1 d_1 \dots c_n d_n}^{a_1 b_1 \dots a_n b_n} R_{a_1 b_1}^{c_1 d_1} \dots R_{a_n b_n}^{c_n d_n}, \quad (1.94)$$

where $\delta_{c_1 d_1 \dots c_n d_n}^{a_1 b_1 \dots a_n b_n}$ is the generalized Kronecker delta, α_n are coupling constants, and the order n here counts the number of Riemannian tensors that involved in the invariant $\mathcal{R}^{(n)}$.

As the lowest two orders of $\mathcal{R}^{(n)}$ gives 1 and R respectively, we usually takes $\alpha_0 \equiv -2\Lambda$ (Λ the cosmological constant) and $\alpha_1 \equiv 1$ to preserve the Einstein limit as all other couplings vanishes.

The deterministic property for LL theory is its generalized Einstein tensor E_{ab} contains up to the second-order derivatives in the metric. As higher-order derivatives can only appears in the third term of E_{ab} , taking $\nabla^c \nabla^d P_{acdb} = 0$ uniquely picks the class of densities (1.94) of dimension D . Alternatively, imposing

$$\nabla^a P_{abcd} = 0 \quad (1.95)$$

gives the same theory although this condition seems to be more restrictive.

For even D , the delta tensor vanishes identically if $n > D/2$, whereas for odd D , it vanishes if $n > (D - 1)/2$. Therefore, given a dimension D , only densities satisfying $n \leq [(D - 1)/2]$ with $[x]$ denoting the smallest integer not smaller than x , don't vanish identically. Thus for $D = 4$, the Ricci scalar and a cosmological constant are the full content of the LL theory, and there is no non-trivial LL generalization of GR in $D = 4$.

The generalized Einstein tensor for each invariant can be easily derived via the principle of variation. It takes the tensorial form:

$$E_b^{a(n)} = -\frac{1}{2^{n+1}} \delta_{bc_1 d_1 \dots c_n d_n}^{aa_1 b_1 \dots a_n b_n} R_{a_1 b_1}^{c_1 d_1} \dots R_{a_n b_n}^{c_n d_n}, \quad (1.96)$$

so the vacuum field equation is simply

$$\sum \alpha_n E_{ab}^{(n)} = 0. \quad (1.97)$$

One interesting property of the above equation is that it reduces to a single equation (algebraic) on $f(r)$ when evaluating on a special static spherically symmetric (SSSS) ansatz:

$$ds_f^2 = -f(r)dt^2 + \frac{dr^2}{f(r)} + r^2 d\Omega_{(D-2)}^2, \quad (1.98)$$

where $d\Omega_{D-2}^2$ is the line element of the $(D - 2)$ -dimensional maximally symmetric space being parametrized by a constant k taking values $k = 1, 0, -1$ for spherical, planar and hyperbolic topologies respectively. This is the property we still want to retain in further generalizations – we want there to always be a vacuum solution of the form (1.98) for new theories.

Here comes the GQTG, which generalizes LL theory in the way mentioned above but restricts the equation of motion for $f(r)$ to be at most of second order. Schematically, the action for theories of such a class can be written as

$$S = \frac{1}{16\pi G} \int d^D x \sqrt{-g} \left[\frac{(D-1)(D-2)}{L^2} + R + \sum_{n=2} \sum_{i_n} L^{2(n-1)} \mu_{i_n}^{(n)} \mathcal{R}_{i_n}^{(n)} \right], \quad (1.99)$$

where the cosmological constant is assumed to be negative and is replaced by

$$\Lambda = -\frac{(D-1)(D-2)}{2L^2}, \quad (1.100)$$

with L some length scale, $\mathcal{R}_{i_n}^{(n)}$ are densities constructed from n Riemann tensors and the metric, the μ_{i_n} are dimensionless couplings, and i_n is an index running over all independent GQTG invariants of order n . To define GQTG invariants, we add an extra degree of freedom to (1.98),

$$ds_{N,f}^2 = -N(r)^2 f(r) dt^2 + \frac{dr^2}{f(r)} + r^2 d\Omega_{(D-2)}^2. \quad (1.101)$$

The formal definition of GQTGs are given as follows. For a given curvature invariant of order n , $\mathcal{R}_{(n)}$, we define $L_{N,f}$ and $S_{N,f}$ as the effective Lagrangian and on-shell action which result from evaluating $\sqrt{|g|}\mathcal{R}_{(n)}$ in the ansatz (1.101)

$$L_{N,f} \equiv N(r)r^{D-2}\mathcal{R}_{(n)}|_{N,f}, \quad S_{N,f} \equiv \Omega_{(D-2)} \int dt \int dr L_{N,f}, \quad (1.102)$$

where we integrated over the angular directions, $\Omega_{(D-2)} \equiv 2\pi^{\frac{D-1}{2}}/\Gamma[\frac{D-1}{2}]$. We will define $L_f \equiv L_{1,f}$ and $S_f \equiv S_{1,f}$, namely, the expressions obtained from setting $N = 1$ in $L_{N,f}$. Now, solving the full nonlinear equations of motion for a metric of the form (1.101) can be shown to be equivalent to solving the Euler-Lagrange equations of $S_{N,f}$ associated to $N(r)$ and $f(r)$ [28, 59, 140], namely,

$$\mathcal{E}^{ab}|_{N,f} \equiv \frac{1}{\sqrt{|g|}} \frac{\delta S}{\delta g^{ab}} \Big|_{N,f} = 0 \quad \Leftrightarrow \quad \frac{\delta S_{N,f}}{\delta N} = \frac{\delta S_{N,f}}{\delta f} = 0. \quad (1.103)$$

We say that $\mathcal{R}_{(n)}$ is a GQTG density if the Euler-Lagrange equation of $f(r)$ associated to L_f vanishes identically, *i.e.*, if

$$\frac{\delta S_f}{\delta f} = 0, \quad \forall f(r). \quad (1.104)$$

This is the same as asking L_f to be a total derivative,

$$L_f = T'_0, \quad (1.105)$$

for some function $T_0(r, f(r), f'(r))$.

The equation satisfied by $f(r)$ for a given GQTG density can be obtained from the variation of $L_{N,f}$ with respect to $N(r)$ as

$$\frac{\delta S_{N,f}}{\delta N} \Big|_{N=1} = 0 \quad \Leftrightarrow \quad \text{equation of } f(r). \quad (1.106)$$

As explained in [27], whenever eq. (1.105) holds, the effective Lagrangian $L_{N,f}$ takes the form

$$L_{N,f} = NT'_0 + N'T_1 + N''T_2 + \mathcal{O}(N'^2/N), \quad (1.107)$$

where T_1, T_2 are functions of $f(r)$ and its derivatives, and $\mathcal{O}(N'^2/N)$ is a sum of terms all of which are at least quadratic in derivatives of $N(r)$. Integrating by parts it follows that

$$S_{N,f} = \Omega_{(D-2)} \int dt \int dr [N(T_0 - T_1 + T_2)' + \mathcal{O}(N'^2/N)]. \quad (1.108)$$

So it is possible to write all terms involving one power of $N(r)$ or its derivatives as a product of $N(r)$ and a total derivative which depends on $f(r)$ alone. Now, it follows straightforwardly that condition (1.106) equates that total derivative to zero. Integrating it once one we are left with [27]

$$\mathcal{F}_{\mathcal{R}(n)} \equiv T_0 - T_1 + T_2' = C, \quad (1.109)$$

where C is an integration constant related to the ADM mass of the solution [10–12, 58]. In particular, for spherical horizons, the precise relation reads

$$C = \frac{M}{\Omega_{(D-2)}}. \quad (1.110)$$

Hence, given some linear combination of GQTG densities, obtaining the equation satisfied by the metric function $f(r)$ amounts to evaluating $L_{N,f}$ as defined in eq. (1.102) and then identifying the functions $T_{i=0,1,2}$ from eq. (1.107). The equation is then given by (1.109). Sometimes we will refer to this equation as the “integrated equation” of $f(r)$ to emphasize the fact that it follows from integrating once (on r) the only non-vanishing component of the actual equations of motion of the theory evaluated on the single-function SSS ansatz.

As argued in [27], the integrated equation is at most second-order in derivatives of $f(r)$. In fact, there are two possibilities as far as the number of derivatives of $f(r)$ are involved: i) theories whose integrated equation involves $f'(r)$ and $f''(r)$; ii) theories whose integrated equation exclusively involves $f(r)$, so the equation is algebraic instead of differential. We shall call theories of the former class “genuine” GQTG densities. Theories of the latter class are called Quasi-topological gravities, and they include GR and LL theories as subcases. However, on general backgrounds the equations of motion will be fourth-order. Quasi-topological gravities are less constrained in the sense that they exist in any space-time dimension $D \geq 5$ for any order in curvature cubic or higher, as explicitly constructed in [29], but genuine GQTGs can exist even in $D = 4$.

GQTGs have by now been the subject of quite intensive investigation [2, 3, 6, 7, 13, 20, 21, 25–28, 31–34, 36–40, 43–48, 60, 66–68, 73, 75–77, 80, 84, 87, 92–94, 96, 102–110, 116, 125–128, 130, 133, 142–145, 150], and many of the interesting properties of these theories are now well-understood. Here we summarize some particularly relevant ones:

1. When linearized around any maximally symmetric background, their equations are identical to those in Einstein gravity, up to a redefinition of Newton’s constant—in other words, they only propagate the usual transverse and traceless graviton in the vacuum [3, 25–28, 93, 94].
2. They possess non-hairy black hole solutions fully characterized by their ADM mass/energy and whose thermodynamic properties can be obtained from an algebraic system of equations.
3. Although the defining property pertains to static spherically symmetric black holes, certain subsets of GQTGs allow for reduction of order in the field equations for other metrics, such as Taub-NUT/Bolt [31], slowly-rotating black holes [2, 87], near extremal black holes [47], and cosmological solutions [6, 7, 43, 48].

4. In the context of gravitational effective field theory, any higher-curvature theory can be mapped, via field redefinition, into some GQTG [29, 36].
5. We can consider arbitrary linear combinations of GQTG densities and the corresponding properties hold, which means, in particular, that GQTG theories have a well-defined and continuous Einstein gravity limit, corresponding to setting all higher-curvature couplings to zero.
6. Extensions away from pure metric theories, including scalars or vector fields, while preserving the main properties are possible [37, 44, 46].

Chapter 2

Structure of GQTGs

This chapter is based on the work [30], which completes the study of structural aspects of GQTGs. GQTGs are proven to exist at all orders of curvature and in all dimensions $D \geq 4$ [29]. In this chapter, we address how many *distinct/inequivalent* GQTGs exist at each order in curvature and in each dimension. Note that by “equivalent GQTGs” we mean as follows: given two genuine GQTG densities of order n , we will say they are “inequivalent” (as far as SSS solutions are concerned) if the quotient of their integrated equations is not a constant,

$$\mathcal{R}_{(n)}^I \text{ inequivalent from } \mathcal{R}_{(n)}^{II} \Leftrightarrow \frac{\mathcal{F}_{\mathcal{R}_{(n)}^I}(r, f(r), f'(r), f''(r))}{\mathcal{F}_{\mathcal{R}_{(n)}^{II}}(r, f(r), f'(r), f''(r))} \neq \text{constant}. \quad (2.1)$$

Otherwise we will say they are “equivalent”. Given two Quasi-topological gravities of order n , we would perform an analogous definition,

$$\mathcal{Z}_{(n)}^I \text{ inequivalent from } \mathcal{Z}_{(n)}^{II} \Leftrightarrow \frac{\mathcal{F}_{\mathcal{Z}_{(n)}^I}(r, f(r))}{\mathcal{F}_{\mathcal{Z}_{(n)}^{II}}(r, f(r))} \neq \text{constant}. \quad (2.2)$$

but we will show later that, in fact, all Quasi-topological gravities of a given order are equivalent. That will not be the case for genuine GQTGs, in whose case we will prove that there exist $(n - 2)$ inequivalent densities for $D \geq 5$.¹

2.1 How many types of GQTGs are there?

In this section we prove that there exist exactly $(n - 2)$ inequivalent genuine GQTG densities and a single inequivalent Quasi-topological one at a given curvature order n in $D \geq 5$. In $D = 4$ there are no Quasi-topological theories and we argue that our proof for the existence of $(n - 2)$ genuine GQTG densities fails in that case, illustrating the fact that a single genuine GQTG density exists in $D = 4$ for $n \geq 3$.

¹The existence of multiple types of GQTG densities was first pointed out in [33], where two inequivalent quintic densities were explicitly constructed in $D = 6$.

2.1.1 At most $(n + 1)$ order- n densities

Let us start our study by putting an upper bound on the possible number of inequivalent GQTG densities existing at a given curvature order n . As argued in [57], evaluated on a metric of the form (1.98), the Riemann tensor can be written as

$$R^{ab}{}_{cd}|_f = 2 \left[-AT_{[c}^{[a}T_{d]}^{b]} + 2BT_{[c}^{[a}\sigma_{d]}^{b]} + \psi\sigma_{[c}^{[a}\sigma_{d]}^{b]} \right], \quad (2.3)$$

where σ_a^b and T_a^b are projectors on the angular and (t, r) directions, respectively.² On the other hand, the dependence on the radial coordinate appears exclusively through the three functions A , B and ψ , which read

$$A \equiv \frac{f''(r)}{2}, \quad B \equiv -\frac{f'(r)}{2r}, \quad \psi \equiv \frac{k - f(r)}{r^2}, \quad (2.4)$$

where $k = 1, 0, -1$ for spherical, planar and hyperbolic horizons respectively.

$$\mathcal{S}_{(n,j)} = \frac{1}{r^{D-1}} \frac{d}{dr} \left[r^{D-1} \psi^{n-j} B^j \right] \quad (2.5)$$

Now, GQTG densities are built from contractions of the metric and the Riemann tensor, so any order- n density of that type will become some polynomial of these objects when evaluated on (1.98), namely,

$$\mathcal{S}|_f = \sum_{l=0}^n \sum_{k=0}^l c_{k,l} B^l \psi^{l-k} A^{n-l}, \quad (2.6)$$

for some constants $c_{k,l}$. The idea is now to determine the most general constants $c_{k,l}$ consistent with the GQTG requirement, which asks $r^{D-2}\mathcal{S}|_f$ to be a total derivative, *i.e.*,

$$r^{D-2}\mathcal{S}|_f = T'_0(r). \quad (2.7)$$

Note that imposing this condition on (2.6) and finding the compatible values of $c_{k,l}$ does not guarantee that the corresponding GQTG densities actually exist, as this does not provide an explicit construction of covariant curvature densities. Doing this does impose, nonetheless, a necessary condition which all actual densities must satisfy. Given a GQTG density, \mathcal{S} , it is useful to define the object $\tau(r)$ through the relation

$$T_0 \equiv r^{D-1}\tau, \quad \text{so that} \quad \mathcal{S}|_f = \frac{1}{r^{D-2}} \frac{d}{dr} \left[r^{D-1}\tau(r) \right]. \quad (2.8)$$

In a sense, $\tau(r)$ is the fundamental building block as long as on-shell GQTG densities are concerned. Observe that since

$$\sum_i \alpha_i \mathcal{S}_i|_f = \frac{1}{r^{D-2}} \frac{d}{dr} \left[r^{D-1} \sum_i \alpha_i \tau_{(i)}(r) \right], \quad (2.9)$$

²These satisfy $T_a^b T_b^c = T_a^c$, $\sigma_a^b \sigma_b^c = \sigma_a^c$, $\sigma_a^b T_b^c = 0$, $\delta_b^a T_a^b = 2$, $\delta_b^a \sigma_a^b = (D-2)$, $\delta_b^a = T_b^a + \sigma_b^a$.

linear combinations of the $\tau_{(i)}$ give rise to linear combinations of GQTG densities in an obvious way.

Now, imposing (2.7) on densities of the form (2.6), we find that there are $(n + 1)$ independent possible densities at a given order n . In terms of the $\tau(r)$, the possibilities turn out to be simply given by $\tau = \tau_{(n,j)}$, where we defined

$$\tau_{(n,j)} \equiv \psi^{n-j} B^j, \quad \text{where } j = 0, 1, \dots, n. \quad (2.10)$$

The corresponding putative on-shell densities read³

$$\mathcal{S}_{(n,j)} \equiv \frac{1}{r^{D-2}} \frac{d}{dr} \left[r^{D-1} \tau_{(n,j)} \right], \quad j = 0, 1, \dots, n. \quad (2.11)$$

Observe that the resulting possibilities are such that A only appears either to the power 1 or to the power 0 when expanding $\mathcal{S}_{(n,j)}$, which is like restricting the sum in l appearing in (2.6) to $l = \{n - 1, n\}$. It follows that any GQTG density in any number of dimensions and at any order in curvature must necessarily be expressible as a linear combination of the above densities when evaluated on the single-function SSS ansatz, namely

$$\mathcal{S}|_f = \frac{1}{r^{D-2}} \frac{d}{dr} \left[r^{D-1} \sum_{j=0}^n \alpha_{(n,j)} \tau_{(n,j)}(r) \right], \quad (2.12)$$

for certain constants $\alpha_{(n,j)}$.

Using the methods developed in [29] —cf. section 5 of that work— it is possible to compute the field equations for the putative theory (2.12) despite the fact that a covariant form of the action is not known. The integrated equation for the metric function $f(r)$ corresponding to a putative density $\mathcal{S}_{(n,j)}$ is given, in the notation of (1.109), by⁴

$$\begin{aligned} \mathcal{F}_{(n,j)} &= \frac{(-1)^{j+1}}{2^{j+1}} r^{D-2+j-2n} (k-f)^{n-j-1} (f')^{j-2} \times \\ &\left[f' \left[j(D-1+j-2n)(k-f)f - (j-1)r(k+(n-j-1)f)f' \right] + j(j-1)r(k-f)ff'' \right]. \end{aligned} \quad (2.13)$$

Observe that this simplifies considerably both for $j = 0$ and $j = 1$. In those cases the dependence on f' and f'' disappears and one finds algebraic equations for $f(r)$,

$$\mathcal{F}_{(n,0)} = -\frac{r^{D-1-2n}}{2} (k-f)^{n-1} [k+(n-1)f], \quad \mathcal{F}_{(n,1)} = \frac{(D-2n)r^{D-1-2n}}{4} (k-f)^{n-1} f. \quad (2.14)$$

An obvious question at this point is: which of these possible densities actually corresponds to the Einstein-Hilbert one, if any. In that case we have $n = 1$, and the two possible

³Note that for the objects $\mathcal{S}_{(n,j)}$ we omit the $|_f$. By this we mean that we literally define $\mathcal{S}_{(n,j)}$ to be the expression that appears in the right-hand side. Actual densities evaluated on the single-function SSS ansatz will reduce to linear combinations of the $\mathcal{S}_{(n,j)}$.

⁴So, for a linear combination of densities, the equation would read $\sum_j \alpha_{(n,j)} \mathcal{F}_{(j)} = C$ where C is an integration constant related to the mass of the solution.

densities and their integrated equations of motion read, respectively,

$$\mathcal{S}_{(1,0)} = -\frac{1}{r^2} [(D-3)(f-k) + rf'] , \quad \mathcal{F}_{(1,0)} = -\frac{r^{D-3}k}{2} , \quad (2.15)$$

$$\mathcal{S}_{(1,1)} = -\frac{1}{2r^2} [(D-2)rf' + r^2f''] , \quad \mathcal{F}_{(1,1)} = \frac{(D-2)r^{D-3}f}{4} . \quad (2.16)$$

Now, the corresponding expressions for the Einstein-Hilbert action (*i.e.*, for a density given by the Ricci scalar $\mathcal{S}_{\text{EH}} \equiv R$) read

$$\mathcal{S}_{\text{EH}}|_f = -\frac{1}{r^2} [(D-2)(D-3)(f-k) + 2(D-2)rf' + r^2f''] , \quad \mathcal{F}_{\text{EH}} = -(D-2)(f-k)r^{D-3} . \quad (2.17)$$

Hence, none of the putative densities coincides with the Einstein-Hilbert one. Rather, it is a linear combination of the two which does, namely,

$$\mathcal{S}_{\text{EH}}|_f = (D-2)\mathcal{S}_{(1,0)} + 2\mathcal{S}_{(1,1)} . \quad (2.18)$$

Even though our approach has selected two possible independent densities susceptible of giving rise to GQTG densities at linear order in curvature, there (obviously) exists a unique possibility corresponding to an actual density, given by the Ricci scalar, which therefore is given by a linear combination of the two. While the $n = 1$ case is somewhat special, this already illustrates the fact that our upper bound of $(n+1)$ densities at order n is not tight and can be improved. For higher n , the only known examples of densities that give rise to algebraic integrated equations for $f(r)$ are Lovelock and Quasi-topological gravities. From our perspective, at a given order n in D dimensions, all available Lovelock and Quasi-topological gravities for such n and D are “equivalent” as far as the equation of $f(r)$ is concerned, which means that they should correspond to a fixed linear combination of $\mathcal{S}_{(n,0)}$ and $\mathcal{S}_{(n,1)}$. In the next subsections we argue that, indeed, the bound of $(n+1)$ densities can be lowered to at most $(n-1)$ GQTG densities of order $n \geq 2$. While amongst the $(n+1)$ candidates identified here there are two which produce algebraic equations, we will see that only a linear combination of the two survives, precisely corresponding to the known Lovelock and Quasi-topological case. The additional putative $(n-2)$ densities would give rise to distinct second-order differential equations for $f(r)$.

2.1.2 At most $(n-1)$ order- n densities

In order to lower our upper bound on the number of available GQTG densities existing at a given order, we can impose some further conditions on our candidate on-shell densities $\mathcal{S}_{(n,j)}$. The first condition comes from imposing that the equations of motion associated to them admit maximally symmetric solutions. When evaluated on such backgrounds, the equations of motion of actual higher-curvature densities reduce to an algebraic equation which involves the cosmological constant, the curvature scale of the background (*e.g.*, the AdS radius) as well as the higher-curvature couplings. More precisely, consider a gravitational Lagrangian consisting of a linear combination of generic higher-curvature

densities of the form given in (1.99). The result for the equations of motion when evaluated for

$$f(r) = \frac{r^2}{L_\star^2} + k, \quad (2.19)$$

which corresponds to pure AdS_D with radius L_\star , is given by

$$\frac{r^{D-1}}{16\pi G} \left[\frac{(D-2)}{L^2} - \frac{(D-2)}{L_\star^2} + \sum_{n=2} \sum_{i_n} \frac{L^{2(n-1)}}{L_\star^{2n}} \mu_{i_n}^{(n)} a_{i_n}^{(n)} \right] = 0, \quad (2.20)$$

for certain constants $a_{i_n}^{(n)}$. Interestingly, as we will see below, this same equation which determines the vacua, also appears to play a key role in the thermodynamics of black holes in the theory. Naturally, the solution for Einstein gravity is simply $L^2 = L_\star^2$, which relates the action scale to the AdS radius in the usual way.

Now, what happens when we consider the integrated equations of a linear combination of candidate on-shell GQTG densities, each contributing as in (2.13), on such a background? It turns out that the result $\sum_j \alpha_{(n,j)} \mathcal{F}_{(n,j)}$ contains two different kinds of terms, one which goes with a power of r^{D-1} , and one which goes with a power of r^{D-3} . As we have seen, actual densities contribute with a single power of the type r^{D-1} , so we must impose that the second kind of term is absent for our putative densities. Removing such a piece amounts to imposing the condition

$$\sum_{j=0}^n \alpha_{(n,j)} (2n - Dj) = 0. \quad (2.21)$$

Hence, we learn that not all the candidate densities can be independent and we reduce the number from $(n+1)$ to n .

There is another condition we can easily impose on our candidate densities. As explained in the first section, GQTG densities have second-order linearized equations around general maximally symmetric backgrounds. This is in contradistinction to most higher-curvature gravities, whose linearized equations involve up to four derivatives of the metric—see *e.g.*, [35] for general formulas. Suppose then that we consider a small radial perturbation on AdS space such that the metric function becomes

$$f(r) = \frac{r^2}{L_\star^2} + k + \varepsilon h(r), \quad (2.22)$$

where $\varepsilon \ll 1$. Now, observe that in our general discussion, the integrated equation of motion for a GQTG density, \mathcal{F}_{S_n} , has been integrated once (on r) with respect to the actual equations of motion of the corresponding density. Hence, the fact that the actual (linearized) equations of motion for GQTG densities are second order for any perturbation on a maximally symmetric background implies that the integrated equations cannot contain terms involving $h''(r)$ (or more derivatives) at leading order in ε . If they did, the actual linearized equations would involve terms of the form $\sim \varepsilon h'''(r)$, in contradiction with the linearized second-order behavior. With this in mind, our strategy now is to insert (2.22)

in a linear combination of integrated equations for our candidate on-shell densities (2.13) and impose that no terms involving $h''(r)$ appear at leading order in ε . By doing so, we find an additional (remarkably simple) condition, which reads

$$\sum_{j=0}^n \alpha_{(n,j)} j(j-1) = 0. \quad (2.23)$$

Imposing it further reduces the number of independent densities from n to $(n-1)$. Hence, we conclude that in D dimensions there exist at most $(n-1)$ inequivalent GQTG theories of order n . Later in subsection 2.1.4 we will prove that in fact there exist exactly $(n-1)$ inequivalent densities for $D \geq 5$. There are many possible ways to choose a basis of on-shell densities so that (2.21) and (2.23) are implemented. For instance, we may choose for the $\tau(r)$ functions defined in (2.8)

$$\tau_{\{n\}}^{\text{QT}} \equiv + (2n - D)\tau_{(n,0)} - 2n\tau_{(n,1)}, \quad (2.24)$$

$$\begin{aligned} \tau_{\{n,j\}}^{\text{GQT}} &\equiv + (j+1)(Dj - 4n)\tau_{(n,j+1)} \\ &\quad + [2D(1 - j^2) - 4n(1 - 2j)]\tau_{(n,j)} + j[D(j+1) - 4n]\tau_{(n,j-1)}, \end{aligned} \quad (2.25)$$

with $j = 2, \dots, n-1$, where we isolated the QT class combination in the first line —see next subsection.

Naturally, constructing actual covariant densities of each of the classes is a non-trivial problem on its own. Explicit formulas for order- n GQTG densities in arbitrary dimensions $D \geq 4$ as well as for order- n QT densities in $D \geq 5$ were presented in [29]. However, these cases only exhausted 2 of the $(n-1)$ classes which we show to exist for $D \geq 5$ in the present paper (one of the genuine GQTG types and the Quasi-topological one).

2.1.3 Uniqueness of Quasi-topological densities

As mentioned above, Quasi-topological densities are a subclass of GQTGs characterized by having an algebraic (as opposed to second-order differential) integrated equation of motion for the metric function $f(r)$ [3, 49, 56, 135, 137]. Theories of that kind are required to satisfy an additional condition besides (1.104), namely [29]

$$\left[\frac{D-2}{r} \frac{\partial}{\partial f''} + \frac{d}{dr} \frac{\partial}{\partial f''} + \frac{(D-3)}{2} \frac{\partial}{\partial f'} + \frac{r}{2} \frac{d}{dr} \frac{\partial}{\partial f'} - r \frac{\partial}{\partial f} \right] \mathcal{Z}|_f = 0, \quad (2.26)$$

which is equivalent to enforcing that the term $\nabla^d P_{acdb}$ from the field equations vanishes on a static spherically symmetric metric ansatz. Imposing this condition on a general linear combination of our candidate densities (2.12) severely constrains the values of the α_j , and we find that $\tau_{\{n\}}^{\text{QT}}$ as defined in (2.24) is in fact the only possibility. Hence, we learn that the only combination of putative densities compatible with the Quasi-topological condition is given by

$$\mathcal{Z}_{(n)}|_f = \frac{1}{r^{D-2}} \frac{d}{dr} \left[r^{D-1} ((2n - D)\tau_{(n,0)} - 2n\tau_{(n,1)}) \right]. \quad (2.27)$$

Now, Quasi-topological gravities with precisely this structure were shown to exist in [29] at all orders in n and for all $D \geq 5$. Therefore, we conclude that the only possible on-shell structure of a Quasi-topological density is given by (2.27). There are no additional inequivalent Quasi-topological densities besides the known ones: if a given higher-curvature density possesses second-order linearized equations around maximally symmetric backgrounds and admits black hole solutions satisfying $g_{tt}g_{rr} = -1$ and such that the equation for $f(r)$ is algebraic, then, the equation that determines such a function is uniquely determined to be

$$\mathcal{F}_{Z_n} = \frac{(D-2n)}{2} r^{D-2n-1} (k-f)^n. \quad (2.28)$$

This naturally includes the subcases of Einstein and Lovelock gravities.

2.1.4 Exactly $(n-1)$ order- n densities

Let us finally proceed to prove that there exist exactly $(n-1)$ inequivalent GQTG densities of order n in dimensions higher than four.

Consider the following combination of “on-shell densities”

$$\mathcal{S}_p^{(k)} = \sum_{i=0}^p \alpha_{p,i}^{(k)} \mathcal{S}_{(p,i)}, \quad k = 1, \dots, k_p \equiv \max(1, p-1), \quad (2.29)$$

where the $\mathcal{S}_{(p,i)}$ are defined in (2.11) and where we assume the constants $\alpha_{p,i}^{(k)}$ to satisfy the constraints found in subsection 2.1.2, namely,

$$\sum_{j=0}^p \alpha_{p,j}^{(k)} (2p - Dj) = 0, \quad \sum_{j=0}^p \alpha_{p,j}^{(k)} j(j-1) = 0. \quad (2.30)$$

At each curvature order p , there are k_p linearly independent solutions and the index k labels each of them.

Now, let us assume that for $p = 1, 2, \dots, n$ we have proven that all of these on-shell densities correspond to the evaluation of actual higher-curvature densities on the single-function SSS ansatz. Namely, there exists a set of Lagrangians $\mathcal{R}_p^{(k)}$ such that

$$\mathcal{R}_p^{(k)} \Big|_f = \mathcal{S}_p^{(k)}, \quad p = 1, \dots, n, \quad k = 1, \dots, k_p. \quad (2.31)$$

With this in mind, let us now consider an order- $(n+1)$ density built from a general linear combination of products of all these lower-order densities, *i.e.*,

$$\tilde{\mathcal{R}}_{n+1} = \sum_{m=1}^n \sum_{k=1}^{k_m} \sum_{k'=1}^{k_{n+1-m}} C_{m,k,k'} \mathcal{R}_m^{(k)} \mathcal{R}_{n+1-m}^{(k')}, \quad (2.32)$$

where we introduced the constants $C_{m,k,k'}$.

We can ask now: is it possible to generate n inequivalent GQTGs of order $(n + 1)$ in this way? In order to answer this question, let us evaluate $\tilde{\mathcal{R}}_{n+1}$ on the single-function SSS ansatz and try to obtain all the possible on-shell GQTGs structures. The evaluation yields

$$\tilde{\mathcal{R}}_{n+1}\Big|_f = \sum_{m=1}^n \sum_{k=1}^{k_m} \sum_{k'=1}^{k_{n+1-m}} \sum_{i=0}^m \sum_{j=0}^{n+1-m} \alpha_{m,i}^{(k)} \alpha_{n+1-m,j}^{(k')} C_{m,k,k'} \mathcal{S}_{(m,i)} \mathcal{S}_{(n+1-m,j)} \quad (2.33)$$

$$= \sum_{m=1}^n \sum_{i=0}^m \sum_{j=0}^{n+1-m} \tilde{C}_{m,i,j} \mathcal{S}_{(m,i)} \mathcal{S}_{(n+1-m,j)}, \quad (2.34)$$

where we defined

$$\tilde{C}_{m,i,j} \equiv \sum_{k=1}^{k_m} \sum_{k'=1}^{k_{n+1-m}} \alpha_{m,i}^{(k)} \alpha_{n+1-m,j}^{(k')} C_{m,k,k'}. \quad (2.35)$$

Now, since we are summing over all the $\alpha_{n,j}^{(k)}$ satisfying (2.30) and $C_{m,k,k'}$ is an arbitrary tensor, note that this equality is equivalent to demanding that $\tilde{C}_{m,i,j}$ is an arbitrary tensor satisfying the following constraints

$$\sum_{j=0}^{n+1-m} \tilde{C}_{m,i,j} [2(n+1-m) - Dj] = 0, \quad \sum_{j=0}^{n+1-m} \tilde{C}_{m,i,j} j(j-1) = 0, \quad (2.36)$$

$$\sum_{i=0}^m \tilde{C}_{m,i,j} (2m - Di) = 0, \quad \sum_{i=0}^m \tilde{C}_{m,i,j} i(i-1) = 0. \quad (2.37)$$

In this way, we do not need to make reference to the $\alpha_{n,j}^{(k)}$ anymore.

Next, it is convenient to rearrange the sum in the following form, in terms of the index $l \equiv i + j$,

$$\tilde{\mathcal{R}}_{n+1}\Big|_f = \sum_{m=1}^n \sum_{l=0}^{n+1} \sum_{j=\max(l-m,0)}^{\min(l,n+1-m)} \tilde{C}_{m,l-j,j} \mathcal{S}_{(m,l-j)} \mathcal{S}_{(n+1-m,j)} \quad (2.38)$$

$$= \sum_{l=0}^{n+1} \sum_{m=1}^n \sum_{j=0}^{n+1-m} \theta(l-j) \theta(j+m-l) \tilde{C}_{m,l-j,j} \mathcal{S}_{(m,l-j)} \mathcal{S}_{(n+1-m,j)}, \quad (2.39)$$

where $\theta(x) \equiv 1$ if $x \geq 0$ and $\theta(x) \equiv 0$ if $x < 0$. Observe that the effect of the theta functions is to enforce that $i \geq 0$ and $i \leq m$, respectively, which in (2.34) is explicit from the i sum. Expanding the product $\mathcal{S}_{(m,l-j)} \mathcal{S}_{(n+1-m,j)}$ we get the following expression,

$$\begin{aligned} \tilde{\mathcal{R}}_{n+1}\Big|_f &= \sum_{l=0}^{n+1} \sum_{m=1}^n \sum_{j=0}^{n+1-m} \theta(l-j) \theta(j+m-l) \tilde{C}_{m,l-j,j} \\ &\times \left[\alpha_{l,m,j} B^{2+l} \psi^{n-1-l} + \beta_{l,m,j} B^{1+l} \psi^{n-l} + \gamma_{l,m,j} B^l \psi^{1-l+n} \right. \\ &\quad \left. + \sigma_{l,m,j} r B' B^l \psi^{n-l} + \zeta_{l,m,j} r B' B^{l-1} \psi^{1-l+n} + \omega_{l,m,j} r^2 (B')^2 B^{l-2} \psi^{1-l+n} \right], \end{aligned} \quad (2.40)$$

where

$$\alpha_{l,m,j} \equiv -4(j-l+m)(-1+j+m-n), \quad (2.41)$$

$$\beta_{l,m,j} \equiv -2[1-4j^2-5l+4m+D(-1+l-n)+4(l-m)(m-n)+n+4j(1+l-2m+n)], \quad (2.42)$$

$$\gamma_{l,m,j} \equiv +(-1+D-2j+2l-2m)(-3+D+2j+2m-2n), \quad (2.43)$$

$$\sigma_{l,m,j} \equiv +2[2j^2-j(1+2l-2m+n)+l(1-m+n)], \quad (2.44)$$

$$\zeta_{l,m,j} \equiv -[4j^2-l(-3+D+2m-2n)-2j(1+2l-2m+n)], \quad (2.45)$$

$$\omega_{l,m,j} \equiv -j(j-l). \quad (2.46)$$

Finally, this can be recast as follows,

$$\tilde{\mathcal{R}}_{n+1} \Big|_f = \sum_{l=0}^{n+1} \left[\Gamma_l B^l \psi^{1-l+n} + \Upsilon_l r B' B^{l-1} \psi^{1-l+n} + \Omega_l r^2 (B')^2 B^{l-2} \psi^{1-l+n} \right],$$

where

$$\begin{aligned} \Gamma_l \equiv & \sum_{m=1}^n \sum_{j=0}^{n+1-m} \left[\theta(l-2-j)\theta(j+m-l+2)\tilde{C}_{m,l-2-j,j}\alpha_{l-2,m,j} \right. \\ & \left. + \theta(l-1-j)\theta(j+m-l+1)\tilde{C}_{m,l-1-j,j}\beta_{l-1,m,j} + \theta(l-j)\theta(j+m-l)\tilde{C}_{m,l-j,j}\gamma_{l,m,j} \right], \end{aligned} \quad (2.47)$$

$$\begin{aligned} \Upsilon_l \equiv & \sum_{m=1}^n \sum_{j=0}^{n+1-m} \left[\theta(l-1-j)\theta(j+m-l+1)\tilde{C}_{m,l-1-j,j}\sigma_{l-1,m,j} \right. \\ & \left. + \theta(l-j)\theta(j+m-l)\tilde{C}_{m,l-j,j}\zeta_{l,m,j} \right], \end{aligned} \quad (2.48)$$

$$\Omega_l \equiv \sum_{m=1}^n \sum_{j=0}^{n+1-m} \theta(l-j)\theta(j+m-l)\tilde{C}_{m,l-j,j}\omega_{l,m,j}. \quad (2.49)$$

Now, in order for this to be a GQTG we must have

$$\tilde{\mathcal{R}}_{n+1} \Big|_f = \mathcal{S}_{n+1}^{(k)} = \sum_{l=0}^{n+1} \alpha_{n+1,l}^{(k)} \mathcal{S}_{(n+1,l)} \quad (2.50)$$

$$= \sum_{l=0}^{n+1} \alpha_{n+1,l}^{(k)} B^{l-1} \psi^{n-l} (lr\psi B' + B\psi(D+2l-2n-3) - 2B^2(l-n-1)) \quad (2.51)$$

$$= \sum_{l=0}^{n+1} \left[B^l \psi^{n-l+1} \left(\alpha_{n+1,l}^{(k)} (D+2l-2n-3) - \alpha_{n+1,l-1}^{(k)} 2(l-n-2) \right) \right. \quad (2.52)$$

$$\left. + \alpha_{n+1,l}^{(k)} lr B' B^{l-1} \psi^{n-l+1} \right], \quad (2.53)$$

for some coefficients $\alpha_{n+1,l}^{(k)}$. Therefore, we have the equations

$$\Gamma_l = \alpha_{n+1,l}^{(k)}(D + 2l - 2n - 3) - \alpha_{n+1,l-1}^{(k)}2(l - n - 2), \quad (2.54)$$

$$\Upsilon_l = l\alpha_{n+1,l}^{(k)}, \quad (2.55)$$

$$\Omega_l = 0, \quad (2.56)$$

for $l = 0, \dots, n + 1$. In addition, the coefficients $\alpha_{n+1,l}^{(k)}$ should satisfy the constraints

$$\sum_{l=0}^{n+1} \alpha_{n+1,l}^{(k)}(2n + 2 - Dl) = 0, \quad \sum_{l=0}^{n+1} \alpha_{n+1,l}^{(k)}l(l - 1) = 0, \quad (2.57)$$

but note that these must arise as consistency conditions in order for the system of equations to have solutions. Then, the question is whether the system of equations for the tensor $\tilde{C}_{m,i,j}$ given by Eqs. (2.36), (2.37), (2.54), (2.55), (2.56) has solutions for *any* value of the $\alpha_{n+1,l}^{(k)}$ satisfying the constraints (2.57). If that is the case, then we have proven the existence of n different GQTGs at order $n + 1$ which, as we saw earlier, is the maximum possible number of GQTGs at that order.

The number of equations to be solved for fixed n —namely, the number of equations required for establishing the existence of n densities of order $(n + 1)$ —and the number of unknowns ($\tilde{C}_{m,i,j}$) read, respectively

$$\# \text{ equations} = \frac{12 + n(11 + 3n)}{2}, \quad \# \text{ unknowns} = \frac{n(n + 2)(n + 7)}{6}. \quad (2.58)$$

The former is greater than the latter as long as $n < 5.10421$ and smaller for greater values of n . Observe that while the number of equations grows as $\sim n^2$, the number of unknowns grows as $\sim n^3$. Here, the number of unknowns is the number of constants available to be fixed in order for the GQTG conditions to be satisfied, and so having more unknowns than equations means that we have more than enough freedom to impose all the conditions. Hence, as long as we are able to show that the $(n - 1)$ different classes of GQTG exist for $n \leq 6$ using other methods, this result shows that they will generally exist for $n > 6$. In practice, solving this system of equations explicitly for any $n \geq 6$ and D is challenging. Nevertheless, the resolution for explicit values of n and D is straightforward with the help of a computer algebra system. Doing this, we have checked that there is a solution for any consistent value of the $\alpha_{n+1,l}^{(k)}$ in any D as long as $n \geq 6$.⁵

In sum, our results here imply that, if $(n - 1)$ inequivalent GQTGs exist for $n = 1, \dots, 6$, then, $(n - 1)$ inequivalent densities will exist for every order $n \geq 6$. In Appendix A.1 we have provided explicit examples of all the inequivalent classes of GQTGs up to $n = 6$ for $D = 5, 6$, so this proves that there are $(n - 1)$ inequivalent GQTGs at every order $n \geq 2$ in those cases. The construction of explicit $n \leq 6$ densities of all the different classes for other values of D can be analogously performed (although it requires some non-trivial computational effort in each case) so we are highly confident that our results apply for general $D \geq 7$ as well.

⁵In practice, we have checked this explicitly for $n = 6$ and general D and for $n = 7, \dots, 20$ in $D = 5, 6, 7$.

On the other hand, note that our argument here does not work in $D = 4$. Indeed, we have found no evidence for the existence of additional inequivalent GQTGs (besides the one known prior to this paper [26, 28, 29, 94]) up to order 6 in that case. This strongly suggests that in $D = 4$ there is a single type of GQTG at every curvature order although a rigorous proof of this fact would require some additional work.

2.2 Black Hole Thermodynamics

In this section we study thermodynamic aspects of GQTGs in an as general a fashion as possible. First we show that the first law of black hole mechanics is satisfied by the black hole solutions of general GQTGs. Then, we will show that thermodynamic magnitudes of at least one class of genuine GQTGs can be, similar to the Lovelock and quasi-topological cases, expressed in terms of the characteristic polynomial that embeds maximally symmetric backgrounds in the theory and the on-shell Lagrangian.

2.2.1 The first law for general GQTGs

Here we wish to understand the first law of thermodynamics for all possible GQTGs. We will begin by working directly with Eq. (2.13), without imposing the constraints on the couplings given in Eqs. (2.21) and (2.23) at this time. The integrated field equations of the putative theory can be written in the form

$$\sum_{n=0}^{n_{\max}} \sum_{j=0}^n \alpha_{n,j} \mathcal{F}_{(n,j)} = -\frac{8\pi GM}{\Omega_{D-2}}, \quad (2.59)$$

where the parameter M is the black hole mass [10–12, 58]. At a black hole horizon, where $f(r_+) = 0$, the above equation can be expanded to yield the following constraints:

$$M = \frac{\Omega_{D-2}}{16\pi G} \sum_{n=0}^{n_{\max}} \sum_{j=0}^n \alpha_{n,j} (j-1) k^{n-j} r_+^{D-2n-1} (-2\pi r_+ T)^j, \quad (2.60)$$

$$0 = \sum_{n=0}^{n_{\max}} \sum_{j=0}^n \alpha_{n,j} (D-2n+j-1) k^{n-j} (-2\pi r_+ T)^j r_+^{D-2n-2}. \quad (2.61)$$

where the temperature satisfies $T = f'(r_+)/4\pi$. The first equation gives the black hole mass in terms of the temperature T and the horizon radius r_+ , while the second provides a relationship between T and r_+ .

The other ingredient we need is the black hole entropy. This should be computed according to Wald's formula (1.83) [100, 158]

$$S = -2\pi \int_{\mathcal{H}} d^{D-2}x \sqrt{\sigma} P_{ab}{}^{cd} \varepsilon^{ab} \varepsilon_{cd}, \quad (2.62)$$

where ε_{ab} is the binormal to the horizon \mathcal{H} . Using the technology introduced in [29], this can be computed without knowledge of the covariant form of the Lagrangian. The key insight is that the tensor $P_{ab}{}^{cd}$ can be computed from the on-shell Lagrangian and must take the form

$$P_{cd}{}^{ab}|_f = P_1 T_{[c}^{[a} T_{d]}^{b]} + P_2 T_{[c}^{[a} \sigma_{d]}^{b]} + P_3 \sigma_{[c}^{[a} \sigma_{d]}^{b]}, \quad (2.63)$$

where

$$P_1 \equiv -\frac{\partial \mathcal{R}_{(n)}|_f}{\partial f''}, \quad P_2 \equiv -\frac{r}{D-2} \frac{\partial \mathcal{R}_{(n)}|_f}{\partial f'}, \quad P_3 \equiv -\frac{r^2}{(D-2)(D-3)} \frac{\partial \mathcal{R}_{(n)}|_f}{\partial f}. \quad (2.64)$$

For the case of the static and spherically symmetric black holes considered here, the horizon binormal is given by $\varepsilon_{ab} = 2r_{[a} t_{b]}$ with r^a and t^b the unit spacelike and timelike normal vectors. A calculation then gives

$$S = -4\pi \Omega_{D-2} r_+^{D-2} \left[\frac{\partial \mathcal{L}}{\partial f''} \right]_{r=r_+} = \frac{\Omega_{D-2}}{8G} \sum_{n=0}^{n_{\max}} \sum_{j=0}^n \alpha_{n,j} j k^{n-j} (-2\pi r_+ T)^{j-1} r_+^{D-2n}. \quad (2.65)$$

It is then straight-forward to show that the first law of thermodynamics

$$dM = T dS \quad (2.66)$$

holds independent of any conditions placed on the couplings $\alpha_{n,j}$. This fact is somewhat surprising because, as discussed earlier, it is only when certain constraints are obeyed by the couplings that a genuine, covariant construction for the Lagrangian can be built based on curvature invariants. However, these same constraints are unnecessary to obtain a valid first law.

Despite the fact that the coupling constraints are not necessary to obtain a valid first law, it is still possible to understand them from a thermodynamic perspective. For this, the natural starting point is the free energy, which reads

$$F = \frac{\Omega_{D-2}}{16\pi G} \sum_{n,j} \alpha_{n,j} k^{n-j} (-2\pi T)^j r_+^{D-1-2n+j}. \quad (2.67)$$

From the free energy, the equation that relates the temperature and horizon radius can be obtained according to

$$\frac{\partial F}{\partial r_+} = 0, \quad (2.68)$$

while the mass and entropy can then be verified to follow in the usual way. The constraints on the couplings enforce the following conditions on the free energy:

$$F - T \frac{\partial F}{\partial T} - \frac{r_+}{D-1} \frac{\partial F}{\partial r_+} \Bigg|_{2\pi T r_+ = -k} = 0, \quad (2.69)$$

$$\frac{\partial^2 F}{\partial T^2} \Bigg|_{2\pi T r_+ = -k} = 0, \quad (2.70)$$

where it is to be noted that the derivatives here are to be computed without assuming any relationship between r_+ and T .

These expressions above, expressing the coupling constraints as properties of the free energy, can be reinterpreted as statements about massless hyperbolic black holes. The static black hole with metric function

$$f(r) = -1 + \frac{r^2}{L_\star^2} \quad (2.71)$$

is pure AdS space in a particular slicing. In terms of the parameters we have been using, this corresponds to $k = -1$, $r_+ = L_\star$ and $T = 1/(2\pi L_\star)$, therefore satisfying the condition $2\pi T r_+ = -k$. In this language, as we will see explicitly below, the first of the two constraints on the free energy actually ensures that the mass of this black hole vanishes. The second constraint on the free energy does not have as direct of an interpretation in terms of the thermodynamic properties of this black hole, but one could imagine it is a statement about fluctuations.

2.2.2 A unified picture of the thermodynamics?

Lovelock and quasi-topological gravities are, by comparison to alternatives, rather simple extensions of general relativity, especially in the context of static, spherically symmetric black holes. Within our parameterization, the coupling constants $\alpha_{n,j}$ to achieve the on-shell Lagrangian for Lovelock and quasi-topological theories amounts to the choice (2.24). For these theories, as has long been known in the case of Lovelock [22, 161, 162], the field equations for a static, spherically symmetric black hole take the form

$$M = \frac{(D-2)\Omega_{D-2}r^{D-1}}{16\pi GL^2}h(y), \quad y \equiv \frac{(f(r) - k)L^2}{r^2}. \quad (2.72)$$

The function $h(x)$ appearing here is the same function that determines the vacua of the theory, *i.e.*, the field equations for the maximally symmetric solutions of the theory. This “embedding function” or “characteristic polynomial” is related to the Lagrangian of the theory evaluated on a maximally symmetric background [32, 35]

$$h(x) = \frac{16\pi GL^2}{(D-1)(D-2)} \left[\mathcal{L}(x) - \frac{2}{D}x\mathcal{L}'(x) \right], \quad (2.73)$$

where here x is related to the curvature of the maximally symmetric background according to

$$R_{ab}{}^{cd} = -\frac{2x}{L^2}\delta_{[a}^c\delta_{b]}^d, \quad (2.74)$$

and $\mathcal{L}(x)$ corresponds to the Lagrangian of the theory evaluated for the curvature (2.74).

The fact that the field equations can be written in terms of the embedding function

naturally leads to some simple and universal expressions for black hole thermodynamics:

$$\begin{aligned} M &= \frac{(D-2)\Omega_{D-2}r_+^{D-1}}{16\pi GL^2}h(y_+), \quad y_+ \equiv -\frac{kL^2}{r_+^2}, \\ S &= -\frac{4\pi\Omega_{D-2}L^2r_+^{D-2}}{D(D-1)}\mathcal{L}'(y_+). \end{aligned} \quad (2.75)$$

These relationships are expressed here in their simplest possible forms, but of course can be massaged using the identity (2.73) and its derivatives, along with the constraint

$$0 = (D-1)kh(y_+) - 2y_+(2\pi r_+T + k)h'(y_+), \quad (2.76)$$

which can be used to compute the temperature, if desired.

It is natural to wonder whether similar relationships hold for the more complicated generalized quasi-topological theories, or whether this result for Lovelock and quasi-topological theories was an artefact of their simplicity. Here we will provide evidence that this is indeed possible, though the situation is more involved than the Lovelock and quasi-topological cases.

Consider the family of theories identified according to the following choices of couplings:

$$\alpha_{n,n-j} = \frac{(D-4)^{j-1}n![(n-j-2)D-4(n-2)]}{2^{2j}j!(n-j)!(n-2)}\alpha_{n,n}. \quad (2.77)$$

In general dimensions, this corresponds to the family of theories for which an explicit covariant formulation was identified in [29]. These couplings satisfy the necessary constraints (2.21) and (2.23), and in addition define a family of GQTG theories for which the free energy can be written as,

$$F = -\frac{(D-2)\Omega_{D-2}r_+^{D-1}}{16\pi GL^2}h(x_+) - \frac{4L^2r_+^{D-3}}{D^2(D-1)}[(D-2)k + (D-4)\pi r_+T]\mathcal{L}'(x_+) \quad (2.78)$$

where

$$x_+ \equiv \frac{8\pi TL^2}{r_+D} - \frac{(D-4)kL^2}{r_+^2D}. \quad (2.79)$$

From this form of the free energy, the full thermodynamic properties for this class of theories can be derived. We obtain for the mass and relationship between the temperature and horizon radius the following two results:

$$\begin{aligned} M &= \frac{(D-2)\Omega_{D-2}r_+^{D-1}}{16\pi GL^2}h(x_+) - \frac{(D-2)\Omega_{D-2}r_+^{D-3}}{4\pi GD}[2\pi r_+T + k]h'(x_+) \\ &\quad + \frac{(D-4)\Omega_{D-2}L^4r_+^{D-5}}{D^3(D-1)}[2\pi r_+T + k]^2\mathcal{L}''(x_+), \end{aligned} \quad (2.80)$$

$$\begin{aligned} 0 &= (D-1)(D-2)h(x_+) - \frac{2(D-2)^2L^2}{r_+^2D}[2\pi r_+T + k]h'(x_+) \\ &\quad - \frac{8(D-4)L^6}{D^3(D-1)r_+^4}[2\pi r_+T + k]^2(16\pi G\mathcal{L}''(x_+)), \end{aligned} \quad (2.81)$$

while the entropy can be simply obtained from the above according to $S = (M - F)/T$.

It is a bit interesting that the thermodynamic properties of black holes can be encoded in terms of the embedding function $h(x)$ and the Lagrangian of the theory $\mathcal{L}(x)$ evaluated on an auxiliary maximally symmetric vacuum spacetime with curvature given by x_+/L^2 . There is one case where this result is somewhat natural, and this is the case of massless hyperbolic black holes where $f = -1 + r^2/L_\star^2$. Of course, this choice of metric function amounts to a pure AdS space in a particular slicing. One has $k = -1$, $T = 1/(2\pi L_\star)$, and $x_+ = L^2/L_\star^2$. In this case, the only non-trivial field equation demands that $h(x_+) = 0$, which in turn demands that $M = 0$.

Next, note that considerable simplification occurs in $D = 4$. In this case, the situation reduces to that first studied in [28]. In that case, the couplings are given by

$$\alpha_{n,n-1} = -\frac{n}{n-2}\alpha_{n,n}, \quad \alpha_{2,j} = 0 \quad \forall j, \quad \text{and} \quad \alpha_{n,j} = 0 \quad \forall j \neq n, n-1, \forall n \geq 3. \quad (2.82)$$

The thermodynamic relations in this case simplify to

$$M = \frac{\Omega_{D-2}r_+^3}{8\pi GL^2}h(x_+) - \frac{\Omega_{D-2}r_+}{8\pi G}[2\pi r_+T + k]h'(x_+), \quad (2.83)$$

$$S = \frac{\Omega_{D-2}kr_+L^2}{6T}\mathcal{L}'(x_+) - \frac{\Omega_{D-2}r_+}{8\pi GT}[2\pi r_+T + k]h'(x_+), \quad (2.84)$$

and the constraint that determines the temperature in terms of the horizon radius reads

$$0 = \frac{-3r_+^2}{L^2}h(x_+) + [2\pi r_+T + k]h'(x_+). \quad (2.85)$$

It seems likely that the thermodynamics of each family of GQTG can be obtained in this way, though we will leave the full analysis for future work. Nonetheless, we can make a few general remarks, based on the connection with massless hyperbolic black holes. For any given family of GQTGs, the mass must have a term proportional to $h(x)$ followed by a series of terms with powers that vanish for the massless hyperbolic black hole. For example, the simplest possibility would be $(2\pi r_+T + k)$ raised to various powers, multiplying derivatives of h and \mathcal{L} . Similarly, the entropy must have a term proportional to $\mathcal{L}'(x)$, followed by a series of terms that vanish for the massless hyperbolic black hole, just as above. Lastly, the argument x must be a function of r_+ , T and k that limits to L^2/L_\star^2 for the massless hyperbolic black hole. For example, allowing for a linear dependence on the parameters, the most general option is the one-parameter family

$$x_+ = \frac{2\pi TL^2\beta}{r_+} + \frac{(\beta - 1)kL^2}{r_+^2}. \quad (2.86)$$

This linear relationship recovers the result for Lovelock/quasi-topological gravity (with $\beta = 0$) and the GQTG family we have presented above (with $\beta = 4/D$). Preliminary calculations have suggested that other GQTG families may require a more complicated dependence than this.

2.3 Comments

In this chapter, we have completed the structural analysis of generalized quasi-topological gravities, proving that at order n in curvature there exist $n - 1$ distinct GQTGs provided $D > 4$. In the case of $D = 4$, our results strongly suggest that there is a single (unique up to addition of trivial densities) GQTG family corresponding to that identified in [28]. To achieve this, we first derived an upper bound, based on the fact that an on-shell GQTG density must be a polynomial in the three independent terms appearing in the Riemann curvature for a static, spherically symmetric background. This upper bound, which holds independent of any knowledge of the covariant form of the densities, was then refined by demanding of the putative theories additional properties that must hold for a true covariant density. Finally, we proved the refined estimate to be exact using arguments based on recurrence formulas, like those introduced in [29]. In order for our argument to hold, it is required that $n - 1$ densities exist for $n = 2, 3, 4, 5, 6$, which then implies existence for all $n > 6$. Such $n - 1$ densities for the lowest curvature orders can be constructed explicitly for $D \geq 5$ but not for $D = 4$, in which case we have verified that there is always a unique density for every $n = 2, \dots, 6$. The argument for higher n then fails for $D = 4$. While it could in principle be possible that additional inequivalent densities exist in $D = 4$ for higher orders—and our construction involving products of lower-order densities was not general enough to capture them—we find this possibility highly unlikely.

In addition, we have provided a basic analysis of the thermodynamic properties of black holes in all possible theories, confirming that the first law is satisfied. Perhaps the most interesting result in this direction is the strong evidence that the thermodynamics of black holes in any GQTG may be expressible in terms of the same function that determines the vacua of the theory, just like in Lovelock and quasi-topological gravities. Why the thermodynamics of black holes in these theories is encoded in the curvature of some axillary maximally symmetric space remains mysterious to us, and may be worth further investigation. More pragmatically, such closed-form and universal expressions provide a simple means by which the thermodynamics could be studied when an infinite number of higher-curvature corrections are simultaneously included.

As a by-product, our work has identified $(n - 2)$ hitherto unknown families of GQTGs in $D > 4$. Going forward, it would be interesting to understand how the properties of black hole solutions differ between these different families, or whether there exist universal features, such as occurs in $D = 4$ [28]. Moreover, the methods we have used to upper bound the number of distinct theories may generalize to allow for a similar analysis to be carried out when there is non-minimal coupling between gravity and matter fields.

Chapter 3

Multicriticality of black holes

A recent interesting discovery in black hole chemistry was that of multicritical points, which refer to special locations in the phase diagram where multiple types of phase transitions coincide, akin to similar concepts in standard thermodynamic systems like water. At an N -tuple critical point, N distinct phases of black holes—such as small, intermediate, and large black holes—can coexist. The first example of an N -tuple point with $N \geq 4$ was discovered in Einstein-power-Maxwell AdS black holes [155]. The approach in [155] exploited the fact that each extremum of the temperature $T(r_+)$ (regarded as a function of horizon radius) corresponded to a cusp in the Gibbs free energy [155, 166]. To realize N distinct phases, each represented by a separate swallowtail structure in the Gibbs free energy diagram, one requires $2N - 2$ distinct extrema. The intersection points of corresponding swallowtails will appear if two adjacent inflections of $T(r_+)$ occur at the same temperature. Extending this to all the inflections will then yield an N -tuple critical point where all such intersections merge.

The content of this chapter is based on the paper [120]. The original purpose of the work is to investigate the existence of multicritical points in GQTG black holes to follow up the previous work on LL theory [166]. We demonstrate the existence of N -tuple critical points of uncharged AdS black holes in GQTG theories. The criticality is shown to have a geometrical interpretation described by Maxwell’s equal area rule. We present a compact reformulation of the area rule and identify a criterion for the emergence such points. Using this criterion, we develop a new method which avoids fine-tuning, and construct several multicritical points with genuine GQTG densities, including quadruple and quintuple points. We also apply our method to construct a quadruple point for Einstein-power-Maxwell AdS black holes to show the efficiency of our method in comparison with the original one used in [155].

3.1 Thermodynamics of GQTG black holes

In this section, we are going to briefly review thermodynamic variables of GQTG black holes obtained in Section 2.2.1. Most importantly, we should introduce a new notation

convention to avoid the suppression of couplings $\mu_{i_n}^{(n)}$ into $\alpha_{n,j}$, which appear in (2.59), (2.60) and (2.62), for simplification. The action for general GQTGs then reads:

$$S_{\text{GQTG}} = \frac{1}{16\pi G} \int_{\mathcal{M}} d^D x \sqrt{-g} \left[-2\Lambda + R + \sum_{n=2} \sum_k \alpha_{n,k} \mathcal{S}_n^{(k)} \right], \quad (3.1)$$

where Λ is the cosmological constant, $\mathcal{S}_n^{(k)}$ are independent densities constructed from different constructions of n Riemann tensors and the metric, $\alpha_{n,k}$ is now redefined the associated k th higher-curvature coupling, and the Newtonian constant G is set to 1 for simplicity.

The on-shell density $\mathcal{S}_n^{(k)}$ is given by

$$\mathcal{S}_n^{(k)} = \sum_{j=0}^n \lambda_{n,j}^{(k)} \mathcal{S}_{(n,j)}, \quad k = 1, \dots, k_n \equiv \max(1, n-1), \quad n \geq 1 \quad (3.2)$$

where k labels one of the $n-1$ inequivalent densities,

$$\mathcal{S}_{(n,j)} \equiv \frac{1}{r^{D-2}} \frac{d}{dr} \left[r^{D-1} \left(\frac{\kappa - f}{r^2} \right)^{n-j} \left(\frac{-f'}{2r} \right)^j \right], \quad (3.3)$$

and $\lambda_{n,j}^{(k)}$ are some constrained coefficients such that $\mathcal{S}_n^{(k)}$ is induced by a real off-shell GQTG density. Here $\kappa = 1, 0, -1$ for spherical, planar and hyperbolic topologies for Ω_{D-2} respectively. Then the constraints (2.30) become

$$\sum_{j=0}^n \lambda_{n,j}^{(k)} (2n - Dj) = 0, \quad \sum_{j=0}^n \lambda_{n,j}^{(k)} j(j-1) = 0. \quad (3.4)$$

All these are just (2.29), (2.11) and (2.30) respectively, but with a different notation. Note that any linear combination of on-shell densities still satisfies (3.2), (3.3) and (3.4); therefore any density can be decomposed into $n-1$ independent densities. In other words, it is sufficient to study one particular choice of $\lambda_{n,j}^{(k)}$.

Incorporating the constraints (3.4), the following choice

$$\lambda_{n,k+1}^{(k)} = (k-1)(Dk - 4n), \quad \lambda_{n,k}^{(k)} = 2D(1 - k^2) - 4n(1 - 2k), \quad \lambda_{n,k-1}^{(k)} = k[D(k+1) - 4n], \quad (3.5)$$

of $\lambda_{n,j}^{(k)}$ form a family of GQTG densities, with the remaining coefficients identical to 0. This simple choice is employed in our analysis but the results in the remaining part of this chapter hold generally.

In our new notation, the equations of motion (2.59) now read

$$\frac{16\pi M}{(D-2)\Omega_{D-2}} = \sum_{n=0}^{n_{\max}} \alpha_{n,k} \sum_{k=1}^{k_n} \sum_{j=0}^n \lambda_{n,j}^{(k)} \mathcal{F}_{(n,j)}. \quad (3.6)$$

All relevant relations for thermodynamic variables are given by

$$M = \frac{\Omega_{D-2}}{16\pi G} \sum_{n=0}^{n_{\max}} \sum_{k=1}^{k_n} \sum_{j=0}^n \alpha_{n,k} \lambda_{n,j}^{(k)} (j-1) \kappa^{n-j} r_+^{d-2n-1} (-2\pi r_+ T)^j, \quad (3.7)$$

$$0 = \sum_{n=0}^{n_{\max}} \sum_{k=1}^{k_n} \sum_{j=0}^n \alpha_{n,k} \lambda_{n,j}^{(k)} (D-2n+j-1) \kappa^{n-j} (-2\pi r_+ T)^j r_+^{D-2n-2}, \quad (3.8)$$

$$S = \frac{\Omega_{D-2}}{8G} \sum_{n=0}^{n_{\max}} \sum_{k=1}^{k_n} \sum_{j=0}^n \alpha_{n,k} \lambda_{n,j}^{(k)} j \kappa^{n-j} (-2\pi r_+ T)^{j-1} r_+^{D-2n}, \quad (3.9)$$

and these originate from (2.60) and (2.62). The couplings of the lowest two orders are set to be $\alpha_{0,1} \equiv -(D-1)(D-2)/(2L^2)$, and $\alpha_{1,1} \equiv 1/2$ for consistency with Einstein gravity. We are going to investigate multicriticality in the context of black hole chemistry, therefore $\alpha_{0,1}$ is identified as pressure P , and its conjugate potential is identified as thermodynamic volume:

$$P \equiv \frac{(D-1)(D-2)}{16L^2}, \quad V \equiv \frac{\Omega_{D-2} r_+^{D-1}}{D-1}. \quad (3.10)$$

All other couplings except for $\alpha_{1,1}$ are also considered as thermodynamic variables, with

$$\Phi_n^{(k)}(r_+, T) \equiv \frac{\partial M(r_+, T, \{\alpha_{p,l}\})}{\partial \alpha_{n,k}} \quad (3.11)$$

as their corresponding conjugate potentials. We therefore yield the first law and Smarr relation in the extended phase space as

$$dM = TdS + VdP + \sum_{n \geq 2} \Phi_n^{(k)} d\alpha_{n,k}, \quad (3.12)$$

$$(D-3)M = (D-2)TS - 2PV + 2 \sum_{n \geq 2} (n-1) \Phi_n^{(k)} \alpha_{n,k}. \quad (3.13)$$

It should be mentioned that the entropy (3.9) is not always positive, and in such situations it has been common to simply discard solutions for which this is the case. However ambiguities exist in the definition of the black hole entropy. For example, adding to the Lagrangian a term proportional to the induced metric on the horizon will, without having an effect on the other properties of the solution, shift the entropy by an arbitrary constant. One example is that of adding an Euler density to the action [129]. We shall therefore retain solutions with $S < 0$ in our considerations, appropriately indicating in the figures where this occurs.

Henceforth we shall consider the Gibbs free energy $G = M - TS$ for investigating phase transitions. The global minimum of G yields the most stable thermodynamic phase at any given temperature.

Before continuing, we note that physical theories should only propagate one type of massless spin-2 graviton on constant curvature backgrounds. This in turn implies the

effective Newtonian constant must have the same sign as the one in general relativity, which means that for the class of metrics (1.98) having asymptotically AdS solutions of the form

$$f(r) = \kappa + f_\infty \frac{r^2}{\ell^2} + \frac{m}{h'(f_\infty)r^{D-3}} + \dots, \quad (3.14)$$

we shall only consider black holes with $f_\infty > 0$, $h'(f_\infty) < 0$ and $\gamma^2 > 0$ ¹ as satisfying the requisite physical criteria. We discuss these issues in appendix A.2.

3.2 Geometric interpretation of interphase equilibrium

We seek to obtain the conditions under which three or more phases merge at a particular temperature and pressure. The Gibbs free energy provides a diagnostic for this. Its global minimum as a function of the temperature T determines the thermodynamically stable state of the system for a given fixed choice of the other thermodynamic parameters. The presence of swallowtails in the Gibbs free energy indicates multiple phases, with first order phase transitions between two distinct phases taking place at the intersection point of the swallowtail. There must be $N - 1$ swallowtails in order to have N distinct phases. Whenever the intersection points of j different swallowtails coincide, then there is a j -th order multicritical point, where $j \leq N$.

Previous methods for finding multiple phases and N -tuple critical points exploited the fact that, regarding temperature as a function of horizon radius, each extremum of $T(r_+)$ corresponds to a cusp in the Gibbs free energy [155, 166]. Hence N distinct phases require $2N - 2$ distinct extrema. If two adjacent inflections of $T(r_+)$ occur at the same temperature, then the intersection points of corresponding swallowtails will merge. If this takes place for all the inflections, then all such intersection points will merge, corresponding to an N -tuple critical point. These critical points can be found by finely tuning the other thermodynamic parameters.

Here we demonstrate an alternate method that is considerably more efficient. We start with a brief review of the Maxwell construction [50]. It is well-known that the multiplicity of the Gibbs free energy $G(P, T)$ corresponds to the non-monotonic behavior of the pressure $P(V, T)$. As illustrated in figure 3.1, a full oscillation AaBbC in the pressure at a fixed temperature T^* leads to a swallowtail on the Gibbs phase diagram. With some abuse of notation, integrating dG along the loop $A \rightarrow b \rightarrow a \rightarrow C$ yields

$$0 = \oint dG = \oint \left. \frac{\partial G}{\partial P} \right|_{T^*} dP = \int V dP = PV \Big|_{V_A}^{V_C} - \int P dV = \int_{V_A}^{V_C} (P^* - P) dV. \quad (3.15)$$

The second equality holds because the temperature is fixed, the fourth one comes from integration by parts, and the last expression follows from $P(V_A) = P(V_C) = P^*$, where P^* characterizes the swallowtail intersection point in the Gibbs phase plot. The geometric interpretation of (3.15) is obvious: P^* corresponds to a pressure that partitions the oscillatory parts of the $P - V$ diagram into equal areas.

¹Those symbols are defined in appendix A.2.

It is useful to define the function $K(V, V_i)$ and its derivative $K'(V, V_i)$ as follows:

$$K(V, V_i) \equiv \int_{V_i}^V (P^* - P)dV, \quad K'(V, V_i) \equiv \frac{\partial K}{\partial V} = P^* - P(V, T^*). \quad (3.16)$$

It is obvious that $K(V_A, V_A) = 0$ and that the last expression of (3.15) can be rewritten as

$$K(V_C, V_A) = 0. \quad (3.17)$$

However for any two points in thermodynamic phase space whose volumes satisfy (3.17), the relation (3.17) alone doesn't imply that their difference in free energy is zero. It is also necessary to ensure that $P(V_C) = P(V_A)$ so that (3.15) holds. In a plot of G vs. P , this requirement is equivalent to the condition that A and C are the same point. This in turn implies that

$$K'(V_A, V_A) = K'(V_C, V_A) = 0 \quad (3.18)$$

$$K'(V_A, V_A) = 0 \quad (3.19)$$

where the first condition ensures that $P(V_A, T^*) = P^*$. Geometrically, (3.17) and (3.18) ensure that A and C are the same point in the Gibbs free energy diagram, and the continuity of K between A and C guarantees that this point is on some closed loop. A true self-intersection point (or double point) therefore emerges.

We note that if the second derivative K''

$$K'' \equiv \frac{\partial^2 K}{\partial V^2} = -\frac{\partial P}{\partial V} \quad (3.20)$$

vanishes at some point then K will no longer be an extremum there. This is illustrated for point C in the rightmost diagram of figure 3.1 by the red curve. The pressure will then be an extremum at this point (as shown in the leftmost diagram in figure 3.1), and the corresponding part of the curve in the free energy diagram will get reflected through P^* , as shown by the red curve in the middle diagram in figure 3.1. By convention, we still regard this as a double point.

These considerations can be easily generalized to any N -tuple point. We say that an N -tuple point exists at (P^*, T^*) if and only if the K -rule is satisfied: namely that the function $K(V, V_0)$ has N real zero points $\{V_n\}$ for some fixed V_0 and K' vanishes for all those roots, namely

$$K(V_n, V_0) = 0, \quad K'(V_n, V_0) = 0, \quad n = 1, 2, \dots, N \quad (3.21)$$

are satisfied by exactly N different values of $\{V_n\}$, including V_0 itself. Since the above argument about multicriticality is quite general, we would expect these discussions apply to any thermodynamic system for any conjugate pair of thermodynamic quantities, such as the temperature and the entropy.

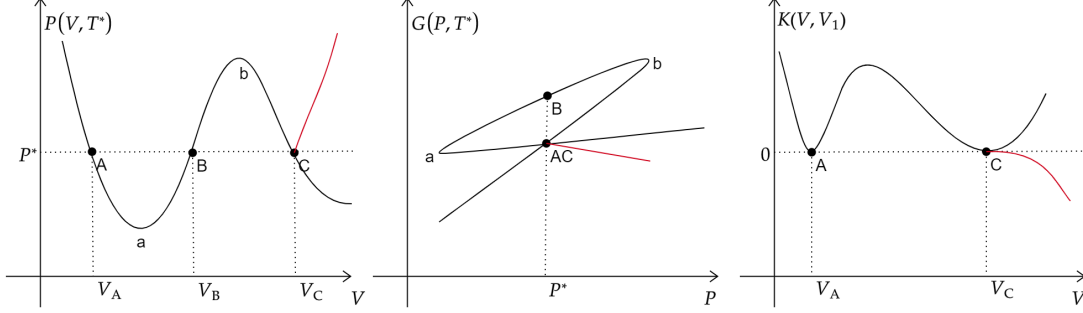


Figure 3.1: The Maxwell equal-area construction implies $P = P^*$ divides AaBbC into two regions AaB and BbC with equal areas. The red curve indicates the trajectories of the plots if $K'' = 0$.

3.3 Multiple phases and N -tuple critical points

We shall now construct multiple phases and N -tuple points for GQTG black holes based on the K -rule introduced in section 3.2. The procedure is simple.

1. Write the function K as

$$K(r_+, r_0) = \int_{r_0}^{r_+} \left[P^* - P(\tilde{r}_+, T^*, \{\alpha_{n,k}\}) \right] \frac{dV(\tilde{r}_+)}{d\tilde{r}_+} d\tilde{r}_+, \quad (3.22)$$

where P is given from (3.8) (which can be regarded as the equation of state) with ℓ^2 replaced by (3.10), V is identified as the thermodynamic volume defined in (3.10), and $\{\alpha_{n,k}\}$ is the set of undetermined couplings.

2. Apply the K -rule to N positive distinct values of r_+ (where r_0 is taken to be any one of these values), then solve for $P^*, T^*, \{\alpha_{n,k}\}$ from the $2N - 1$ independent equations² (3.21). This implies that a minimum number of $2N - 3$ non-zero higher-curvature couplings are required.
3. Check if the solution $P^*, T^*, \{\alpha_{n,k}\}$ provides a real N -tuple point in a sense that exactly N roots solve (3.21) as desired. If not, change the choice of as many horizon radii as needed until a real N -tuple point occurs.

We pause to make a few supplementary comments regarding the feasibility of the method. First of all, K is constructed from P and V instead of T and S because we want K to be a simple function such that the equations in step 2 are solvable: the definition (3.22) fulfills this requirement since K is in fact a polynomial in r_+ . For convenience, K is defined as a function of the radius rather than the volume. It should be pointed out that the density $\mathcal{S}_{n \geq 3}^{(2)}$ is quasi-topological and becomes trivial in $d = 2n$. Therefore, for even dimensions, we exclude $\alpha_{d/2,2}$ from our considerations. We shall also restrict ourselves to spherical black holes with $\kappa = 1$ for simplicity. Since the pressure becomes a polynomial

²Minus one comes from the fact that $K(r_0, r_0) = 0$ is trivial.

in r_+ (with the temperature T considered as a non-dynamical parameter), then Descartes' rule of signs can be applied, which relates the largest number of oscillations in the region $r_+ > 0$ to the number of sign changes in the sequence of a polynomial's coefficients. Thus we discuss the feasibility of our method through studying the possibility for the occurrence of $N - 1$ oscillations in P by manipulating signs of couplings in the next paragraph.

The feasibility of step 2 can be seen by induction. As indicated by (3.8) or table 3.1, switching on an arbitrary genuine GQTG coupling ($k \geq 2$) always introduces three independent terms proportional to different powers of r_+ in the expression for the pressure in addition to

$$P_0 = \frac{(D-2)T}{4r_+} - \frac{(D-3)(D-2)\kappa}{16\pi r_+^2}, \quad (3.23)$$

which is the expression with all higher-curvature couplings set to zero. Since P_0 has one sign change, then turning on any particular coupling can introduce another sign change. Respecting the fact that temperature and the coupling are free, it is possible to make P have a full oscillation, which means that (3.21) has real solutions and a double point can be obtained. Similarly, for critical points involving more phases, we can obtain additional oscillations by including two additional couplings per oscillation, as long as they switch on at least two monomials in r_+ that differ from those already present. Hence not any choice of $2N - 3$ higher-order densities yields an equilibrium state with four phases or more. For example, as bolded in table 3.1, switching on $\{\alpha_{7,2}, \alpha_{8,4}, \alpha_{9,6}, \alpha_{10,8}, \alpha_{11,10}\}$ and keeping other couplings zero only introduces $1/r_+^{11}$, $1/r_+^{12}$, $1/r_+^{13}$ into the pressure. Together with P_0 , a total of five monomials are present in the expression for the pressure, which is only enough to construct a triple point. In this example we must therefore avoid turning on more than three couplings that contribute to the same three powers of r_+ .

The number $2N - 3$ should be considered as the minimum number of couplings required by our method. This may not be the smallest number of couplings needed for the emergence of an N -tuple point in general, since it is possible to have another sign change internally between the three monomials corresponding to the $\alpha_{n,k}$. The explicit form of new terms that are activated by switching on $\alpha_{n,k}$ reads

$$\begin{aligned} (-2)^{k-3} \alpha_{n,k} \left\{ (D+k-2n)(-1+k)(Dk-4n) \frac{\pi^k T^{k+1} \kappa^{n-k-1}}{r_+^{2n-k-1}} \right. \\ + (D+k-2n-1)[D(-1+k^2) + (2-4k)n] \frac{\pi^{k-1} T^k \kappa^{n-k}}{r_+^{2n-k}} \\ \left. + (D+k-2n-2)k(D+Dk-4n) \frac{\pi^{k-2} T^{k-1} \kappa^{n-k+1}}{4r_+^{2n-k+1}} \right\}. \end{aligned} \quad (3.24)$$

We claim that there can be at most one sign change between these three terms. If the sign switches twice, the first two coefficients must have a negative product, namely,

$$(D+k-2n)(-1+k)(Dk-4n)(D+k-2n-1)[D(-1+k^2) + (2-4k)n] < 0.$$

Since we restrict ourselves to genuine GQTG densities ($k \geq 2$) in $D \geq 5$ only, the above can be simplified to

$$(D+k-2n)(D+k-2n-1)(Dk-4n)[D(-1+k^2) + (2-4k)n] < 0. \quad (3.25)$$

Note that the dimension D cannot be any of $2n - k, 2n - k + 1, 2n - k + 2$; otherwise one of the terms would vanish and it would be no longer possible to have two sign changes between two terms. Therefore the first two factors in (3.25) must be positive, which leads to

$$(Dk - 4n)[D(-1 + k^2) + (2 - 4k)n] < 0,$$

finally giving

$$\frac{Dk}{4} < n < \frac{D(k^2 - 1)}{4k - 2}, \quad (3.26)$$

where $k \geq 2$ is applied to determine the directions of inequalities. Meanwhile, we require that the last two terms produce a sign change as well. Through a similar analysis, we arrive at

$$[D(-1 + k^2) + (2 - 4k)n](D + Dk - 4n) < 0,$$

which yields

$$\frac{D(k^2 - 1)}{4k - 2} < n < \frac{D(k + 1)}{4}. \quad (3.27)$$

Our claim is thus proved, since (3.27) contradicts (3.26). Even if there is an extra internal sign change, a half oscillation in the pressure does not necessarily occur, since these variables are not only integers but also constrained relative to each other in a complicated way. However, notice that the range of n in (3.27) is proportional to D , implying that we have a rather large parameter space for n and k . Hence we can still expect that there exists some choices of D, k, n that can give rise to an N -tuple point with less than $2N - 3$ couplings. As a consequence, we would also expect $N - 1$ to be a lower bound on the number of couplings needed for the occurrence of an N -tuple point. Because of these considerations, step 3 is added to guarantee that exactly N phases are obtained.

In order to obtain multiple phases and multi-critical points, the physical constraints and ensuring $P > 0$ everywhere must also be considered. Since it is difficult to find a case with positive γ^2 everywhere, we only impose $\gamma^2 > 0$ in a neighbourhood of each critical point. In practice, we keep manipulating r_+ 's until a critical point satisfying all constraints occurs. Under these considerations, we explicitly obtain a quadruple point (figures 3.2 and 3.3) and a quintuple point (figures 3.4 and 3.5) for two different spherical GQTG black holes. Note that to see the merging of multiple swallowtails requires high precision in computations due to the finely tuned nature of multi-critical points. Both multi-critical points have negative Gibbs free energies, implying stable phase transitions. For the quintuple point, an extra coupling $\alpha_{3,2}$ is fixed to be 1 before running the procedure in order to make physical cases easier to emerge.

Compared with the previous methods, the advantages of our procedure are quite significant. First, the application of the Maxwell construction turns the problem into algebra which enables our method to produce critical points with arbitrarily high precision such that very tiny phase structures can be discovered easily. More importantly, the method is more efficient in the sense that it does not need any fine-tuning procedure such as those previously employed [155, 166–168] where N -tuple points were obtained by manipulating thermodynamic variables so that a common point of inflection occurred between multiple

maxima and minima of the temperature as a function of r_+ . However, due to the additional physical constraint $\gamma^2 > 0$ induced from the non-algebraic nature of equation of motions in genuine GQTGs, finding a physical multicritical point with a large N is still time-consuming.

3.4 Einstein-power-Maxwell AdS black holes

Here we compare our method with methods previously employed in understanding multicritical behaviour. For this illustration, we consider a quadruple point in the Einstein-power-Maxwell theory comparing previous methods used to find it [155] with our proposed approach.

Power-Maxwell theory is a general form of non-linear electrodynamics minimally coupled to $D = 4$ Einstein gravity [82]. The action is

$$S = \int d^4x \sqrt{-g} \left(R - 2\Lambda - \sum_{i=1}^N \alpha_i (F^2)^i \right), \quad (3.28)$$

with $F^2 \equiv F_{\mu\nu} F^{\mu\nu}$ and $F_{\mu\nu} \equiv \nabla_\mu A_\nu - \nabla_\nu A_\mu$, where R is the Ricci scalar. The α_i are dimensional coupling constants ($[\alpha_i] = L^{2(i-1)}$) and A_μ is the U(1) Maxwell field. We recover Einstein-Maxwell theory when $\alpha_1 = 1$ and $\alpha_i (i > 1) = 0$.

For the ansatz (1.98) it is straightforward to find a solution of the form $f(r) = 1 + \sum_{i=1}^K c_i r^{-i} + \frac{r^2}{l^2}$ [155]. The corresponding thermodynamic variables are

$$T = \frac{1}{4\pi r_+} \left[1 + 8\pi P r_+^2 - \frac{Q^2}{r_+^2} - \frac{5b_5 Q}{2r_+^6} - \frac{3b_9 Q}{r_+^{10}} - \frac{13b_{13} Q}{4r_+^{14}} - \frac{17b_{17} Q}{5r_+^{18}} - \frac{7b_{21} Q}{5r_+^{22}} + \dots \right], \quad (3.29)$$

$$S = \pi r_+^2, \quad V = \frac{4}{3} \pi r_+^3, \quad P = \frac{3}{8\pi l^2}, \quad (3.30)$$

where Q is the charge parameter, \dots stands for contributions from higher-powers of F^2 in the action (3.28), and each of the other parameters represent the same physical quantities as before. The field equations imply

$$c_1 = -2M \quad c_i = \frac{4Q}{i+2} b_{i-1}, \quad \text{for } i > 1 \quad (3.31)$$

where

$$b_1 = Q \quad b_5 = \frac{4}{5}Q^3\alpha_2 \quad b_9 = \frac{4}{3}Q^5(4\alpha_2^2 - \alpha_3) \quad (3.32)$$

$$b_{13} = \frac{32}{13}Q^7(24\alpha_2^3 - 12\alpha_3\alpha_2 + \alpha_4) \quad (3.33)$$

$$b_{17} = \frac{80}{17}Q^9(176\alpha_2^4 - 132\alpha_2^2\alpha_3 + 16\alpha_4\alpha_2 + 9\alpha_3^2 - \alpha_5) \quad (3.34)$$

$$b_{21} = \frac{64}{7}Q^{11}(1456\alpha_2^5 + 234\alpha_3^2\alpha_2 + 208\alpha_4\alpha_2^2 - 24\alpha_4\alpha_3 - 1456\alpha_2^3\alpha_3 - 20\alpha_5\alpha_2 + \alpha_6) \quad (3.35)$$

and we can set $\alpha_1 = 1$ without loss of generality.

The Gibbs free energy is again $G = M - TS$ but with the black hole mass now modified to be

$$M = \frac{4}{3}\pi Pr_+^3 + \frac{r_+}{2} + \frac{Q^2}{2r_+} + \frac{b_5Q}{4r_+^5} + \frac{b_9Q}{6r_+^9} + \frac{b_{13}Q}{8r_+^{13}} + \frac{b_{17}Q}{10r_+^{17}} + \frac{b_{21}Q}{12r_+^{21}} + \dots, \quad (3.36)$$

where contributions from higher-powers in F^2 are denoted as \dots again.

The approach³ stated in [155] requires presetting $2N - 1$ intersections $r_+^{(i)}$ to construct an N -tuple point by solving $2N - 1$ equations

$$T(r_+^{(1)}, P^*, \{b_n\}) = \dots = T(r_+^{(2N-1)}, P^*, \{b_n\}) = T^* \quad (3.37)$$

for T^* , P^* , Q , b_n . This yields a numerical expression for the temperature (3.29) each time we change the values of intersections. Hence an N -tuple point (likely) emerges eventually by adjusting the $r_+^{(i)}$ such that $N - 1$ swallowtails of the free energy appear at a single point. The feasibility of our new method can be easily verified by applying a similar analysis in the section 3.3 to (3.29). As a consequence of the rule of signs, $2N - 4$ is the minimum number of couplings required to construct an N -tuple point.

For an illustration, we apply this approach to a quadruple point, and so four non-zero b_n 's are required. For simplicity, we choose them to be $\{b_5, b_9, b_{13}, b_{17}\}$. In order to work out a desired set of b_n 's, we pick intersections $\{1, 1.04, 1.1, 1.4, 1.9, 2.9, 4\}$ (set A) to start with. However, this choice of $r_+^{(i)}$ is not optimal in the sense that only two swallowtails appear in the Gibbs free energy, as shown in figure 3.6, which is far from a quadruple point merger. After a few iterations, we arrive at a better situation displayed in figure 3.7, where all three swallowtails appear. These do not intersect at a single point until all radii are tuned to $\{1, 1.0424, 1.1, 1.4243, 1.9, 2.93, 4\}$ (set B) as illustrated in figure 3.8. Radii with higher precision can be obtained if one iterates the approach many times, but a considerably longer time is inevitably needed.

³There is another method mentioned in the paper that uses extrema. However, they are qualitatively the same since neither of them avoid fine-tuning.

We now consider how things change using our method. We first define the function K as

$$K(r_+, r_0) = \int_{r_0}^{r_+} 4\pi \left[P^* - P(\tilde{r}_+, T^*, \{b_n\}) \right] \tilde{r}_+^2 d\tilde{r} \quad (3.38)$$

where (3.29) and $V = 4\pi r_+^3/3$ are applied to (3.22). Next pick $\{1, 1.1, 1.9, 4\}$ out of the set A to be four different values of r_+ satisfying (3.21). After one implementation of the procedure discussed in section 3.3, we find

$$\begin{aligned} r_+^{(1)} &= 1, & r_+^{(2)} &= 1.042427218, & r_+^{(3)} &= 1.1, \\ r_+^{(4)} &= 1.424291548, & r_+^{(5)} &= 1.9, & r_+^{(6)} &= 2.930025838, & r_+^{(7)} &= 4, \end{aligned} \quad (3.39)$$

which reproduces the set B with considerably higher precision and notably less effort. From this perspective, our approach can be interpreted as a fine-tuning process that automatically identifies all possible proper positions of the $N - 1$ remaining radii in between the preset N radii such that an N -tuple point emerges. All those radii collectively constitute a workable set of $r_+^{(i)}$ which constructs an N -tuple point in the preceding method.

3.5 Comments

In this chapter, we have exploited Maxwell's equal area law to find an interphase equilibrium for black holes with multiple phases, reformulating it into what we call the K -rule. Utilizing the K -rule, we developed a novel approach for constructing N -tuple points in the phase space of black holes.

We applied our results to GQTG theories with $2N - 3$ genuine couplings. Our analysis suggests that the minimum number of couplings required for the formation of an N -tuple point is likely confined between $N - 1$ and $2N - 3$. We presented quadruple and quintuple points to illustrate the effectiveness of the method.

The discovery that black holes can have multiple phases and multicritical behaviour has interesting implications for quantum gravity. The distinct phases correspond to different thermodynamically stable states having different entropy, analogous to the way in which steam and ice are respectively high-entropy and low-entropy states of water. Systems having multicritical behaviour, such as colloids and polymers [83, 141], interact not only through short-range hard-sphere (or hard-cylinder) effects but also through additional soft or long-range interactions comprising multiple length scales [141]. It is reasonable to infer that the fundamental degrees of freedom of a black hole likewise have such complicated interactions, commensurate with recent indications that they are molecular in character [159, 160].

Future work would involve applying the K -rule to other kinds of black hole holes, particularly those whose horizon structures are not spherically symmetric. These include accelerating black holes in non-linear electrodynamics [88], multiply rotating black holes [168], and various black hole solutions in supergravity theories [41].

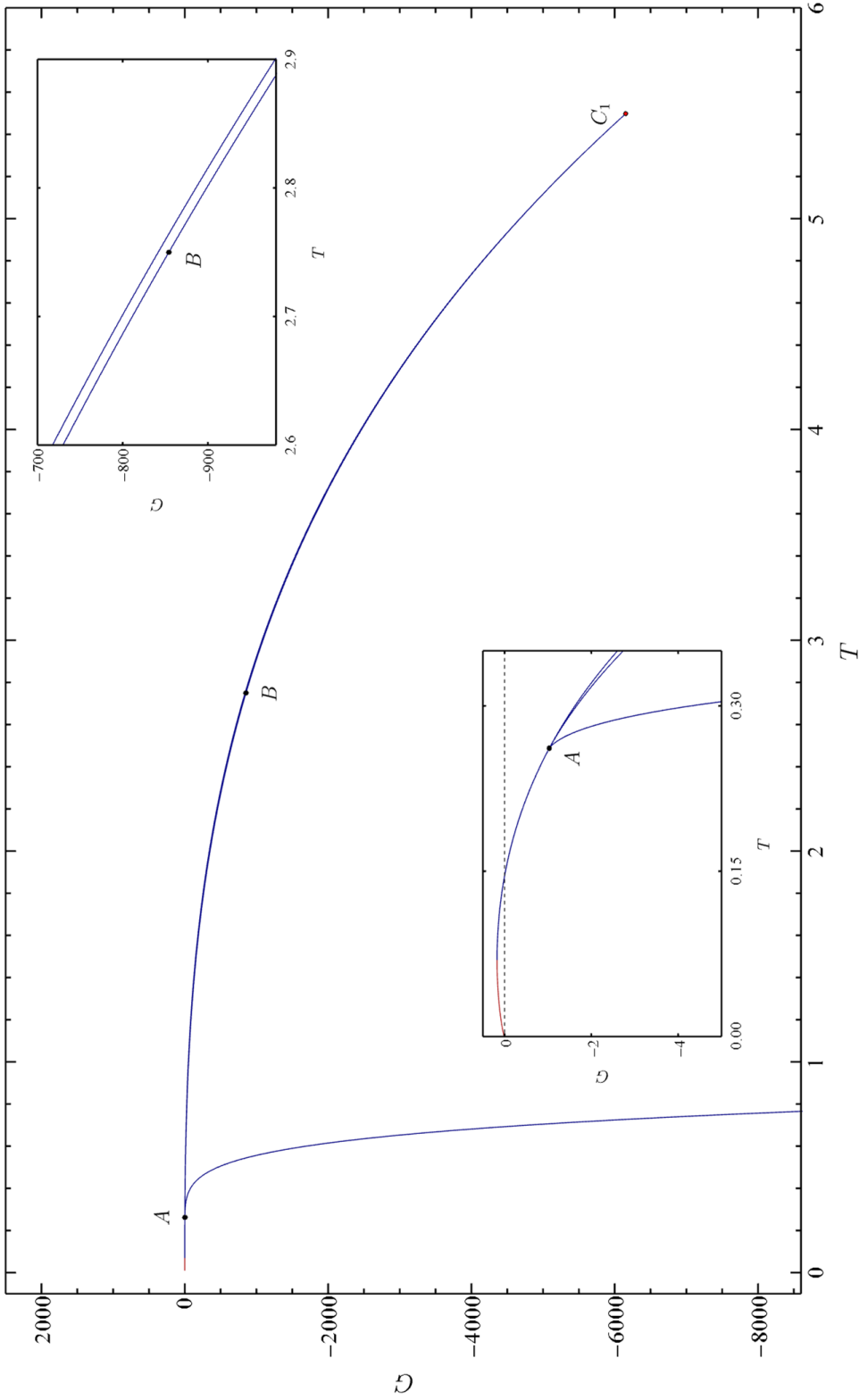


Figure 3.2: A quadruple point A is constructed in $D = 7$ with $f_\infty = 1.001359562$, $P^* = 0.07466400248$, $T^* = 0.2615575508$, $\alpha_{4,2} = -1.983132445$, $\alpha_{5,2} = -0.6595495180$, $\alpha_{6,2} = 0.1064022549$, $\alpha_{7,2} = -0.02347725421$, $\alpha_{8,2} = 0.002665217984$. Four exact radii $\{1, 1.07, 1.239, 1.4\}$ are taken as input. The black hole has positive γ^2 everywhere while the entropy is almost positive everywhere except the red region near $T = 0$. Behaviors around A and B are indicated by the two subfigures respectively. The point C_1 is one of the cusps, and in the next figure 3.3, we show the rest 5 which are accumulated around A . So it is a quadruple point with an extremely far-away cusp.

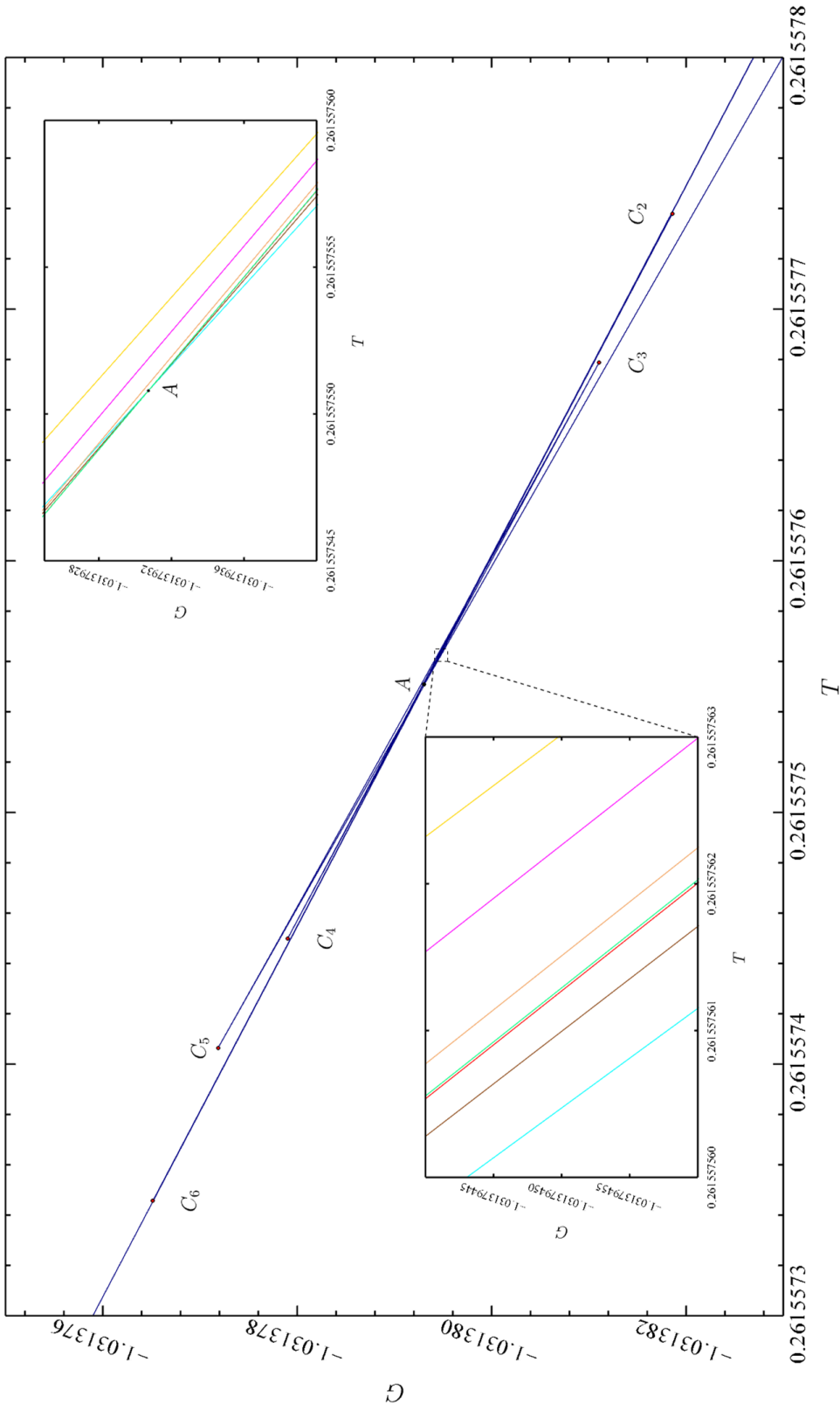


Figure 3.3: The figure shows further magnifications about the quadruple point A in figure 3.2. The points C_2 to C_6 are five cusps, and the remaining one is indicated in figure 3.2. These cusps are extremely narrow so that they look like lines. Regarding this fact, we further zoom in around A and color curves passing A for better distinguishability. Nearing A , those curves are closer to each other. Staring at the right part of the right subfigure and moving carefully enough, we can see that three curves intersect A , but it is actually four, because the green and red curves between orange and brown ones overlap. Moving a bit far away from A , namely in the dotted box, the red and green curves become more distinguishable.

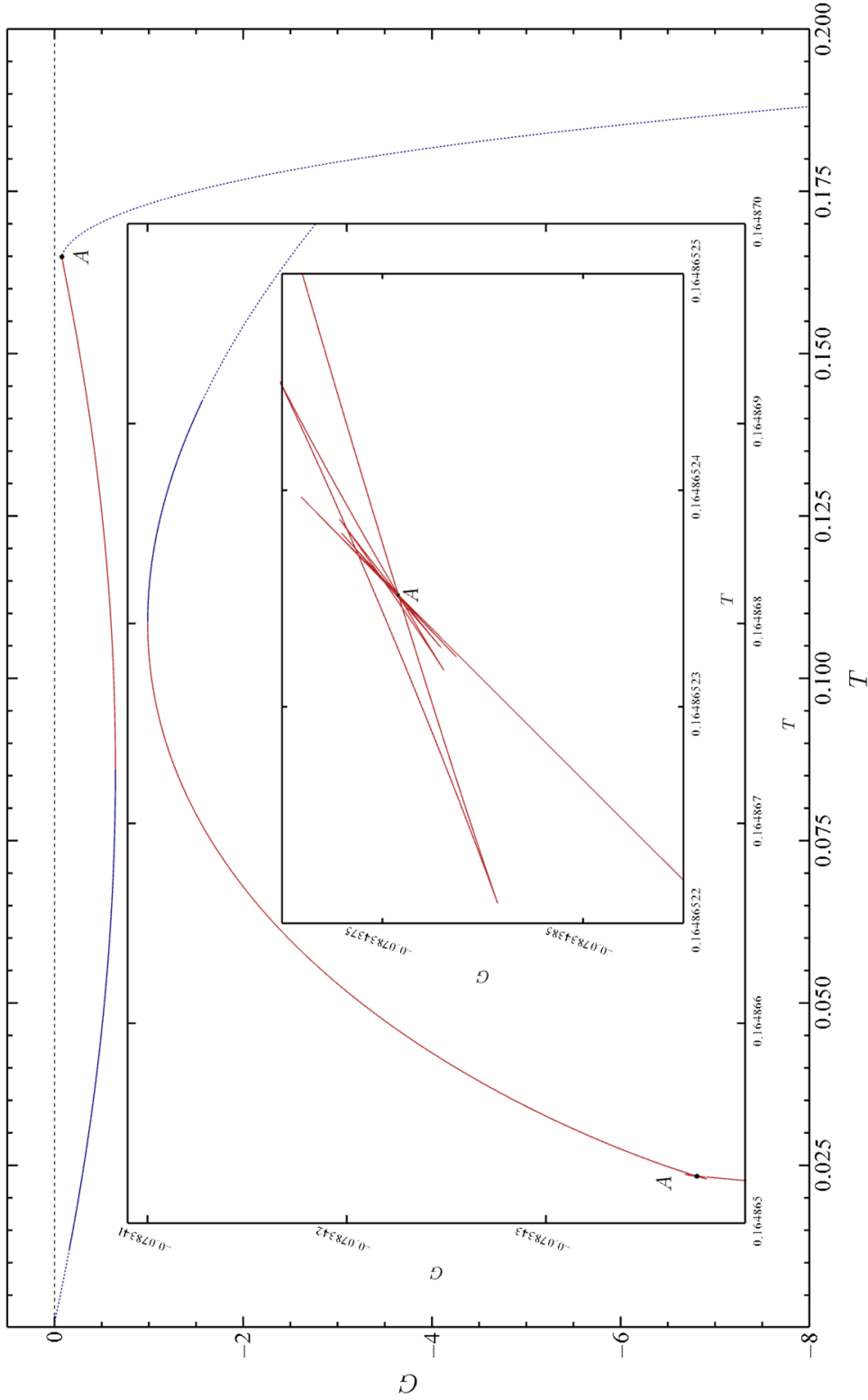


Figure 3.4: A quintuple point A appears in $D = 7$ with $f_\infty = 0.9982618066$, $P^* = 0.03402189695$, $T^* = 0.1648652352$, $\alpha_{3,2} = 1, \alpha_{4,2} = 6.232655784$, $\alpha_{5,2} = 1.096317618$, $\alpha_{6,2} = 0.2676712136$, $\alpha_{7,2} = -0.2079188594$, $\alpha_{8,2} = 0.09653639807$, $\alpha_{9,2} = -0.02640506854$, $\alpha_{10,2} = 0.003268616550$, where $\alpha_{3,2}$ is set to 1 in advance, and the rest of the parameters are computed after five exact radii $\{1, 1.07, 1.21, 1.4, 1.6\}$ are taken as input. The upside of this adjustment is that we can find a physical quintuple point with negative free energy more easily. Blue and red colors indicate regions with positive and negative entropy respectively; solid and dashed curves partition the points with positive and negative γ^2 respectively. Two subfigures show different extents of magnification about the quintuple point A and a further magnification is shown in the next figure 3.5 to clarify that A is truly a quintuple point.

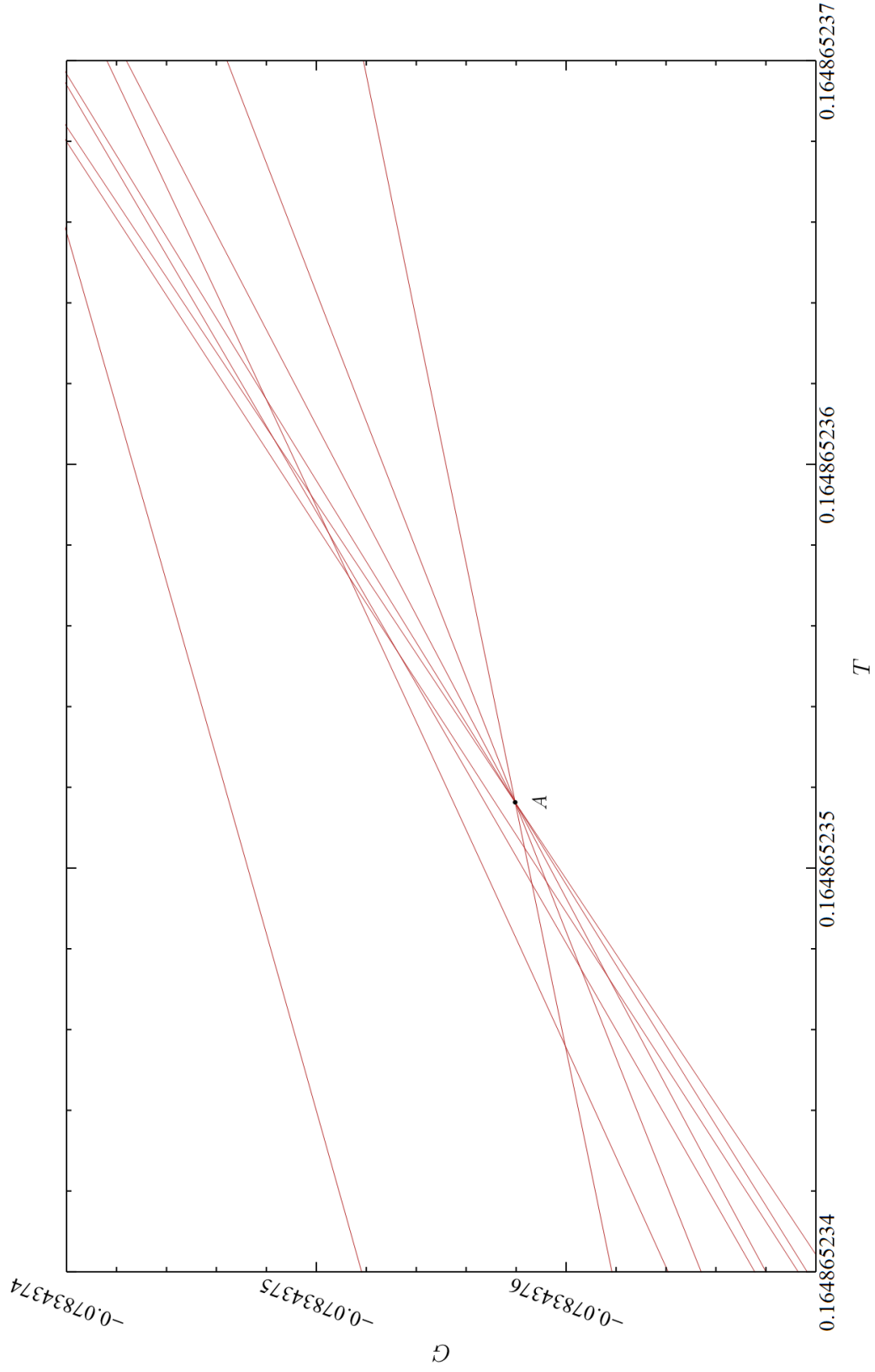


Figure 3.5: This figure shows further magnifications about the quintuple point A in figure 3.4. We can clearly see the intersection of 5 curves appears at A .

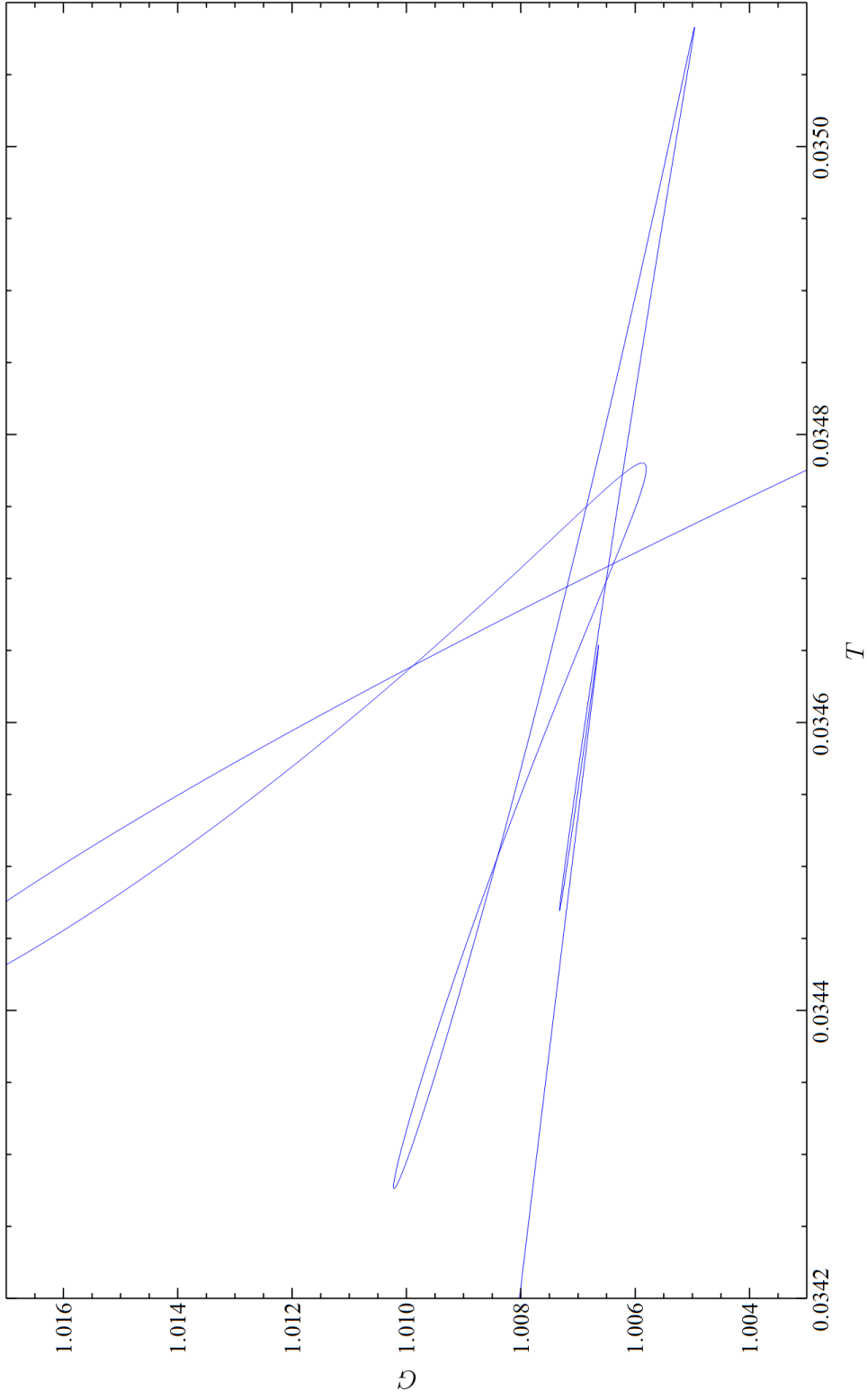


Figure 3.6: This figure shows that the Gibbs free energy corresponds to the equation of state (3.29) with $Q = 1.2368, P^* = 0.0020878, b_5 = -1.0973, b_9 = 1.5937, b_{13} = -1.2746, b_{17} = 0.40172$ which intersects with $T^* = 0.034711$ at $r_+^{(1)} = 1, r_+^{(2)} = 1.04, r_+^{(3)} = 1.1, r_+^{(4)} = 1.4, r_+^{(5)} = 1.9, r_+^{(6)} = 2.9, r_+^{(7)} = 4$.

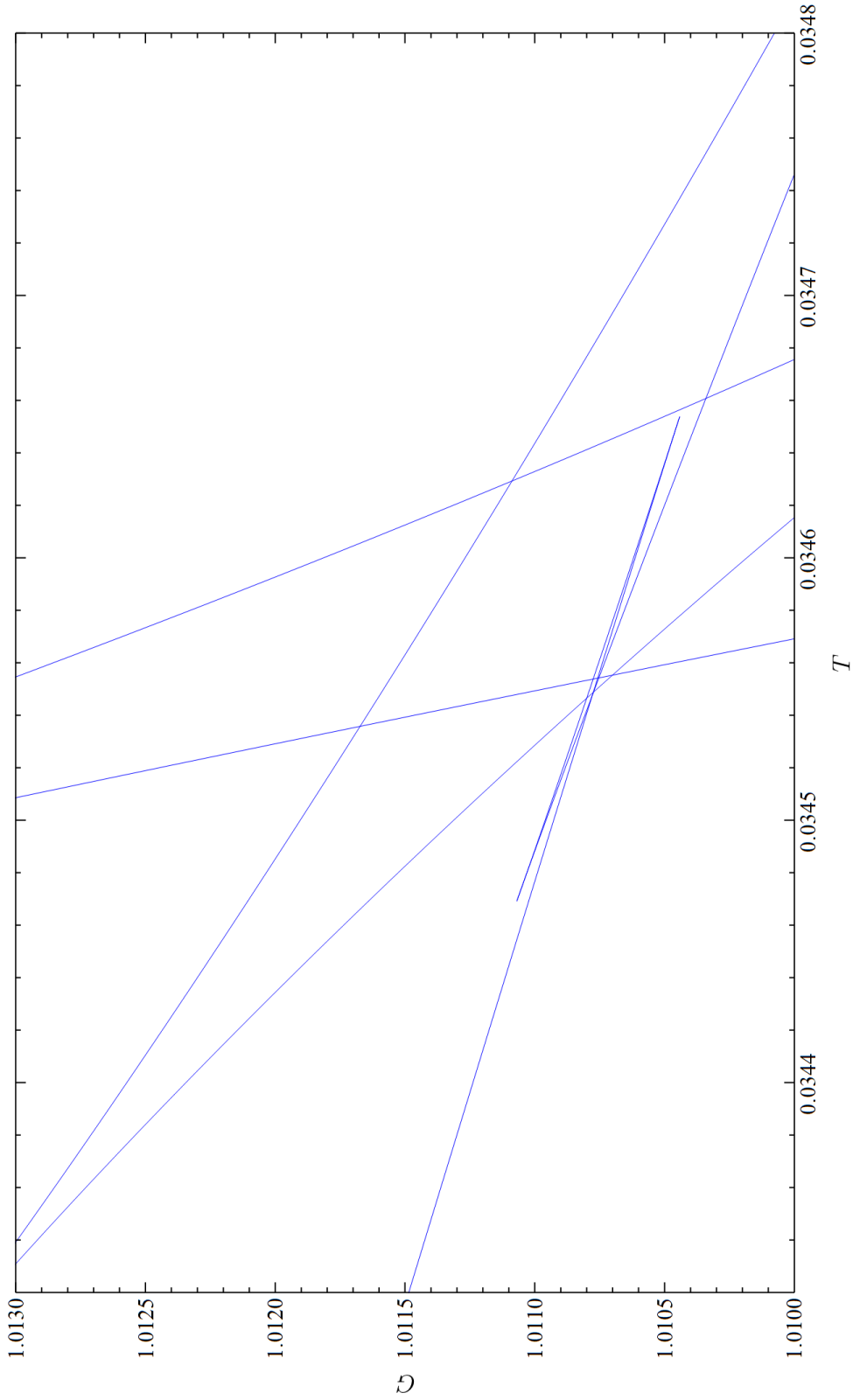


Figure 3.7: The figure shows the Gibbs free energy corresponds to the equation of states (3.29) with $Q = 1.2424, P^* = 0.0020704, b_5 = -1.1233, b_9 = 1.6535, b_{13} = -1.3338, b_{17} = 0.42279$ which intersects with $T^* = 0.034555$ at $r_+^{(1)} = 1, r_+^{(2)} = 1.04, r_+^{(3)} = 1.1, r_+^{(4)} = 1.42, r_+^{(5)} = 1.9, r_+^{(6)} = 2.93, r_+^{(7)} = 4$.

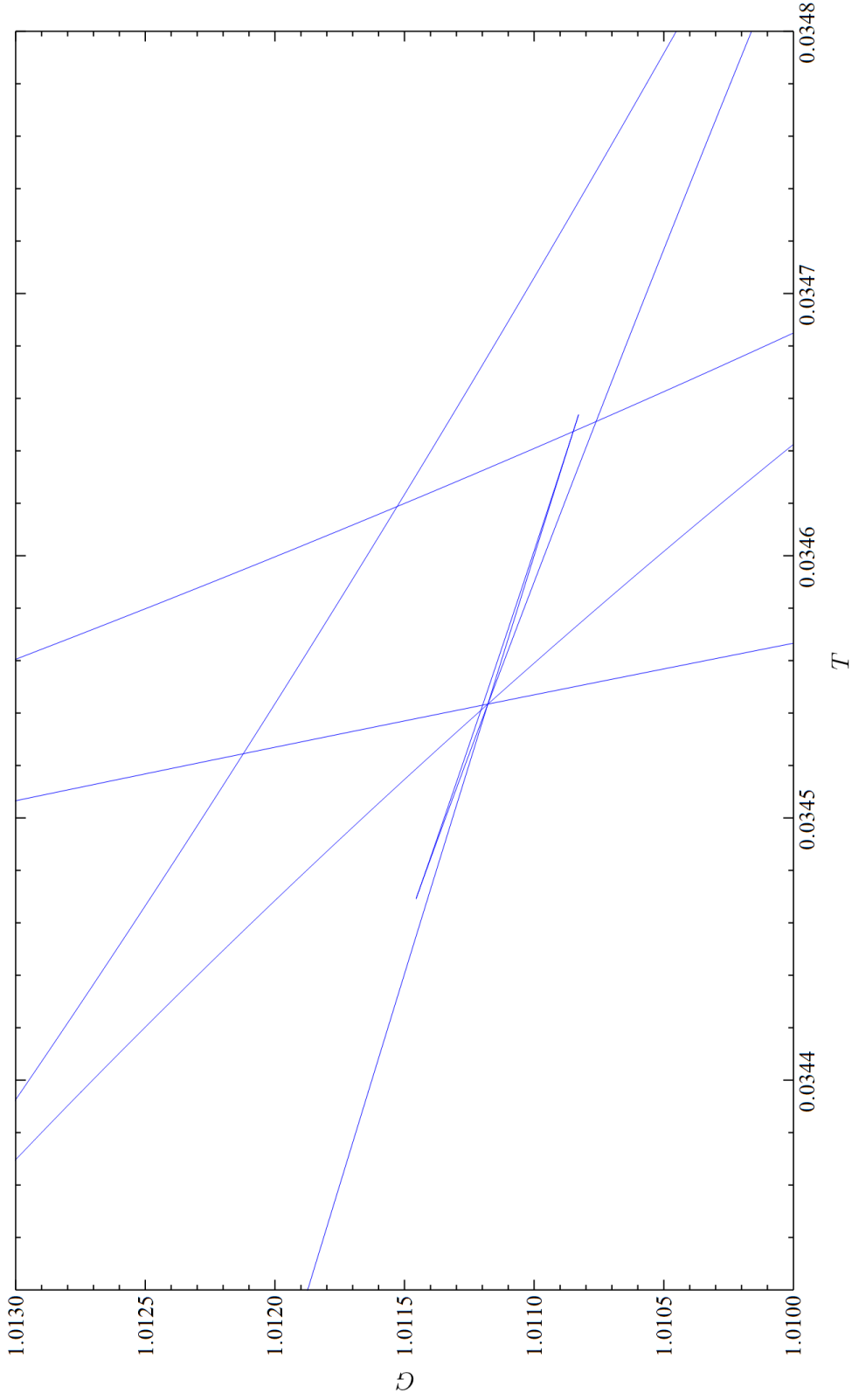


Figure 3.8: This figure shows that the Gibbs free energy corresponds to the equation of state (3.29) with $Q = 1.2431$, $P^* = 0.0020692$, $b_5 = -1.1285$, $b_9 = 1.6683$, $b_{13} = -1.3512$, $b_{17} = 0.42992$ which intersects with $T^* = 0.034544$ at $r_+^{(1)} = 1$, $r_+^{(2)} = 1.0424$, $r_+^{(3)} = 1.1$, $r_+^{(4)} = 1.4243$, $r_+^{(5)} = 1.9$, $r_+^{(6)} = 2.93$, $r_+^{(7)} = 4$.

Chapter 4

Vacuum wormholes in GQTGs

The content of this chapter is based on the work in [121] and [122]. As argued in Section 1.3, the formation of a traversable wormhole in GR requires exotic matter. However, for higher-curvature gravity, gravity itself may behave like exotic matter, as we can always absorb the higher-order terms into the stress-energy tensor T_{ab} . This motivates us to investigate if we can construct a four-dimensional vacuum wormhole solution with the help of Einsteinian cubic gravity (ECG), which is the simplest non-trivial GQTG in four-dimensional spacetime.

4.1 An overview of the main results

Einsteinian Cubic Gravity (ECG) [25, 93] has an action of the general form

$$\mathcal{I} = \frac{1}{16\pi} \int d^d x \sqrt{-g} (-2\Lambda + R + \alpha\mathcal{P} + \beta\mathcal{C} + \gamma\mathcal{C}'), \quad (4.1)$$

where α , β and γ are the respective couplings of the curvature densities \mathcal{P} , \mathcal{C} and \mathcal{C}' , with Λ_0 the cosmological constant. These cubic corrections are given by

$$\mathcal{P} = 12R_a^c R_b^d R_c^e R_d^f R_e^a R_f^b + R_{ab}^{cd} R_{cd}^{ef} R_{ef}^{ab} - 12R_{abcd} R^{ac} R^{bd} + 8R_a^b R_c^c R_b^a, \quad (4.2)$$

$$\mathcal{C} = \frac{1}{2} R R_a^b R_b^a - 2R^{ac} R^{bd} R_{abcd} - \frac{1}{4} R R_{abcd} R^{abcd} + R^{de} R_{abcd} R^{abc}_e. \quad (4.3)$$

$$\mathcal{C}' = R_a^b R_b^c R_c^a - \frac{3}{4} R R_a^b R_b^a + \frac{1}{8} R^3. \quad (4.4)$$

Our primary result is the discovery of a numerical wormhole solution described by a general static spherically symmetric ansatz

$$ds^2 = g_{tt}(r) dt^2 + \frac{dr^2}{g^{rr}(r)} + r^2 (d\theta^2 + \sin^2 \theta d\phi^2), \quad (4.5)$$

within the framework of 4D ECG in the absence of any matter. This implies that the overall effect of gravity must become repulsive near the wormhole throat; otherwise a

timelike/lightlike geodesic congruence would converge and forbid the formation of a throat as we have mentioned in Section 1.3. Indeed, we find (see Appendix 4.6) that the size of the throat marginally increases with increasing mass parameter, indicative of a repulsive effect. The solution we found connects two copies of an asymptotically AdS spacetime (l is the AdS length) with a spherical deficit/surfeit angle $\delta \in (-1, 0)$,

$$r \rightarrow \infty : \quad g_{tt} \sim -\left(\frac{r^2}{l^2} + 1 + \delta\right) + \mathcal{O}(r^{-1}), \quad g^{rr} \sim \frac{r^2}{l^2} + 1 + \delta + \mathcal{O}(r^{-1}), \quad (4.6)$$

analogous to that of a global monopole [16]. This choice of the asymptotic form validates the local analysis of series solutions as it distinguishes the formal series solutions at infinity of a wormhole from its AdS black hole counterparts [121], which turns out to be crucial in the construction. We note for the ansatz (4.5) that \mathcal{C} and \mathcal{C}' are linearly dependent. Henceforth we can set $\gamma = 0$ without loss of generality.

Before proceeding further, let us recall that the Morris-Thorne wormhole metric (1.91) is of the form

$$ds^2 = -e^{2\Phi(r)} dt^2 + (1 - b(r)/r)^{-1} dr^2 + r^2 d\Omega^2. \quad (4.7)$$

Its spatial geometry can be visualized by the surface

$$z(r) = \pm \left(\frac{r}{b(r)} - 1\right)^{-1/2} \quad (4.8)$$

embedding in a flat space. For a smooth and continuous embedding, there exists a throat radius r_{th} at which $z(r_{\text{th}}) = 0$, defining the wormhole's throat. We also require r_{th} to be a local minimum of $r(z)$, leading to the flare-out condition: $d^2r/dz^2 \geq 0$ at $r = r_{\text{th}}$. Finally, the proper radial distance must be well-defined, which requires that the condition $1 - b(r)/r \geq 0$ be satisfied throughout the geometry.

4.2 Basic strategy

Our construction relies on the shooting method, namely, looking for initial conditions satisfying (4.6) at $r = \infty$ such that the wormhole boundary conditions are fulfilled at the throat r_{th} . For this purpose, we take $u \equiv 1/r$, $F(u) \equiv -1/g_{tt}$, $n(u) \equiv -g^{rr}/g_{tt}$ to rewrite the metric ansatz (4.5) as

$$ds^2 = -\frac{1}{F(u)} dt^2 + \frac{1}{u^4} \frac{F(u)}{n(u)} du^2 + \frac{1}{u^2} (d\theta^2 + \sin^2 \theta d\phi^2). \quad (4.9)$$

Then the metric functions satisfying (4.6) are regularized at the initial point $u = 0$ ($r = \infty$), as the initial conditions (4.6) become

$$u \rightarrow 0 : \quad F \sim l^2 u^2 - (1 + \delta) l^4 u^4 + \mathcal{O}(u^5), \quad n \sim 1 + \mathcal{O}(u^3). \quad (4.10)$$

The boundary conditions for a wormhole throat $u_{\text{th}} \equiv 1/r_{\text{th}}$ involve more subtleties. First, according to the metric (4.7) and the continuity for (4.8), we have $g_{tt} > 0$ and

$g_{rr} \rightarrow \infty$ at wormhole throat, which are equivalent to $n = 0$ and F being positive finite at $u = u_{\text{th}}$. Second, since the throat should be a regular point in the spacetime and the non-trivial Riemannian tensor components in a tetrad depend on n', F', F'' only, it suffices to require these derivatives to be finite there.

However, these boundary conditions are more troublesome than they appear to be. The two third order field equations (given in (A.42) in Appendix A.3), obtained from varying the gravitational action (1.99) and using the ansatz (4.9), are linear in $F^{(3)}$ and $n^{(3)}$. These equations can thus be decomposed into 6 first-order equations

$$p' = \xi(F, n, s, p, v, w), \quad w' = \zeta(F, n, s, p, v, w), \quad s \equiv F', \quad p \equiv s', \quad v \equiv n', \quad w \equiv v', \quad (4.11)$$

where ξ and ζ are algebraic functions defined as

$$\begin{aligned} \mathcal{A}\xi \equiv & 8F^7(u^2 - \Lambda_0) - 6F^2nu^8\{s^2u^2v^2(58\alpha + 7\beta) + 8\alpha n^2(p^2u^2 + 26psu + 54s^2) \\ & + 4nsu[4puv(9\alpha + \beta) + 24\alpha s^2 + suw(10\alpha + \beta) + 2sv(62\alpha + 5\beta)]\} \\ & + 3F^3u^7\{4n^2u[48s\alpha pu + 2suw(16\alpha + \beta) + 4sv(40\alpha + \beta) + pu^2w(8\alpha + \beta) \\ & + 8puv(10\alpha + \beta) + 132\alpha s^2] + 128\alpha n^3(2pu + 3s) - su^3v^3(8\alpha + \beta) \\ & + 2nu^2v[2puv(8\alpha + \beta) + 48\alpha s^2 + 3suw(8\alpha + \beta) + 2sv(44\alpha + 5\beta)]\} \\ & + 6F^4u^7\{4n^2(-32\alpha pu - 48\alpha s + \beta uw + 4\beta v) + 4\alpha su^2v^2 \\ & + nu[\beta v(8s + v) - 16\alpha(puv + suw + 5sv)]\} \\ & + 2F^5u^3\{3\beta u^5v^2 - 4n[s + 3\beta u^4(uw + 4v)]\} \\ & + 120F^2n^2s^2u^9[4\alpha n(pu + 4s) + suw(10\alpha + \beta)] - 8F^6nu^2 - 480\alpha n^3s^4u^{10}, \end{aligned} \quad (4.12)$$

$$\begin{aligned} \mathcal{B}\zeta \equiv & 6F^2u^5\{-4\alpha n^2[10v(pu + 5s) + uw(pu + 16s)] - su^2v^3(9\alpha + \beta) \\ & - 2nuw[puv(9\alpha + \beta) + 24\alpha s^2 + suw(21\alpha + 2\beta) + 6sv(14\alpha + \beta)]\} \\ & + 3F^3u^4\{16\alpha n^2(7uw + 8v) + 2nu[4\alpha v(6pu + 30s + 31v) + 4\alpha uw(6s + 25v) \\ & + 8\alpha u^2w^2 + \beta(u^2w^2 + 10uvw + 7v^2)] + u^2v^2[24\alpha s + uw(8\alpha + \beta) + 2v(10\alpha + \beta)]\} \\ & - 12F^4u^4[4\alpha n(7uw + 8v) + uv(2\alpha uw + 4\alpha v - \beta v)] \\ & + 30Fnsu^6[4\alpha n(puv + suw + 8sv) + suv^2(12\alpha + \beta)] - 240\alpha n^2s^3u^7v - 4F^5v, \end{aligned}$$

with denominators \mathcal{A} and \mathcal{B} of ξ and ζ , respectively given by

$$\mathcal{A} \equiv 12F^2n^2u^9 [8\alpha F^2 - 8\alpha nF - uvF(8\alpha + \beta) + 4\alpha nsu], \quad \mathcal{B} \equiv \mathcal{A}/(2u^3n). \quad (4.13)$$

From the expressions for \mathcal{A} and \mathcal{B} , the Morris-Throne condition $n(u_{\text{th}}) = 0$ implies that ξ and ζ simultaneously diverge. A wormhole throat is therefore generically a spontaneous singularity for the system (4.11), which is why we must ensure that the derivatives n', F', F'' are finite there, in turn ensuring the curvature is finite. In practice, the most annoying issue is that a singularity yields large numerical errors in the solution in its vicinity, especially for higher derivatives, which forbids us for obtaining those derivatives directly through numerical solutions, such as shooting methods usually do. We thus have to introduce another approach. For now, let us take a look at the initial value problems that we have to deal with.

4.3 Initial value problems

In general, shooting methods require tuning 6 parameters for our system. This number is halved if we limit our consideration to analytic local solutions at $u = 0$, namely, metric functions having the form

$$F(u) = F_2 u^2 + F_4 u^4 + \sum_{i=5}^{\infty} F_i u^i, \quad n(u) = 1 + \sum_{i=3}^{\infty} n_i u^i, \quad (4.14)$$

at $u = 0$. Solving (4.11) order by order in u in a neighbourhood of 0, we find

$$\Lambda_0 + 3/F_2 + 24\alpha/F_2^3 = 0, \quad \Lambda_0 + 2/F_2 = 0, \quad (4.15)$$

from the lowest two orders [121]. Note that these equations imply that there is no $\alpha \rightarrow 0$ limit for the solutions we obtain.

The coefficients $F_{i \geq 6}$ and $n_{i \geq 3}$ can be expressed in terms of F_2, F_4, F_5, β ; a few of these coefficients are explicitly presented in Appendix A.4. The physical interpretations of F_2, F_4, F_5 are given by

$$F_2 \equiv l^2 > 0, \quad F_4 \equiv -(1 + \delta)l^4 \in (-l^4, 0), \quad F_5 \equiv \frac{4l^4(2l^4 - 9\beta)}{9(l^4 - 2\beta)}M, \quad (4.16)$$

where F_2 and F_4 are determined such that the boundary condition (4.10) is satisfied; F_5 is proportional to the ADM mass M of the spacetime, which is identified as negative one-half the coefficient of $1/r$ in g^{rr} . The parameters F_2, F_4, F_5, β specify all initial conditions at $u = 0$ (and determine Λ_0 and α via (4.15)); hence their specification is all that is needed to obtain a solution under the analyticity assumption.

We emphasize that the above dependence of $F_{i \geq 6}$ and $n_{i \geq 3}$ on F_2, F_4, F_5 is only valid when $1/F_2 \neq 0$ and $\delta \neq 0$. If either condition is not satisfied, the analyticity (4.14) of both metric functions at $u = 0$ forces every $n_{i \geq 3}$ to be zero [121], which implies n is a constant function in the common convergent region of the series for F and n , and further indicates the product of $g_{tt}g_{rr}$ is a constant there. Arbitrary choices of F, F', F'' at $u = 0$ lead to black hole solutions when $g_{tt}g_{rr}$ is constant for the whole range of r . This implies, for initial conditions that are the same as for a given black hole solution, that wormholes can't exist when $g_{tt}g_{rr}$ is a constant in any neighbourhood of $u = 0$. This makes us particularly interested in asymptotically AdS solutions with non-zero δ , since this condition is required to obtain wormholes.

In practice, we introduce a tiny deviation parameter $\epsilon > 0$ to numerically integrate from $u = \epsilon$ to larger u with initial values $F(\epsilon), n(\epsilon), F'(\epsilon), n'(\epsilon), F''(\epsilon), n''(\epsilon)$ instead. The point of this is to avoid the trouble caused by the generic singularity at $u = 0$ leading to $\mathcal{A} = \mathcal{B} = 0$. In our construction ϵ is taken to be 0.00056. The part of the solution with $u < 0.00056$ can be obtained by integrating from 0.00056 to 0. The functions $n(u)$ and $F(u)/u^2$ both approach constants (matching (4.14) perfectly) until they eventually terminate at some rather tiny value limited by precision.

4.4 Wormhole identification

Figure 4.1 illustrates a numerical wormhole solution (solid curves), obtained from solving the initial value problem at $u = 0$ for a typical choice of F_2, F_4, F_5 and β . The wormhole throat u_{th} is located at the place where n vanishes. Both metric functions terminate at $u = u_{\text{th}}$, since u_{th} is generically a singular point, which causes numerical errors in evaluating higher derivatives of metric functions there. Consequently we need an alternative means for identifying u_{th} as a wormhole throat.

To this end, we first check the possibility that a series solution local at u_{th} not only satisfies desired boundary conditions discussed in Section 4.2 but also converges to the numerical solution at the terminal point. The local solution discovered in [121] is a Taylor series of the form

$$F(u) = \sum_{i=0}^{\infty} \tilde{F}_i (u - u_{\text{th}})^i, \quad n(u) = \sum_{i=1}^{\infty} \tilde{n}_i (u - u_{\text{th}})^i, \quad (4.17)$$

with coefficients obtained by solving the equations (4.11) order by order in $(u - u_{\text{th}})$. Similar to (4.14), higher order coefficients are uniquely characterized by the lower order ones $\{\tilde{F}_0, \tilde{n}_1, F_2, \beta, u_{\text{th}}\}$, as indicated in Appendix A.5. Thus 5 parameters in total need to be specified to obtain the series solution.

The dashed curves in Figure 4.1 represent different truncated series of the local solution (4.17) at $u_{\text{th}} = 3.19114$, which reads

$$\begin{aligned} F &= 4.10434 + 1.30746(u - u_{\text{th}}) - 0.133104(u - u_{\text{th}})^2 + 0.00189318(u - u_{\text{th}})^3 \\ &\quad + 0.00389799(u - u_{\text{th}})^4 - 0.00140705(u - u_{\text{th}})^5 + 0.000345987(u - u_{\text{th}})^6 + \dots, \\ n &= -0.456446(u - u_{\text{th}}) + 0.0130613(u - u_{\text{th}})^2 + 0.00718277(u - u_{\text{th}})^3 \\ &\quad - 0.00229803(u - u_{\text{th}})^4 + 0.000442028(u - u_{\text{th}})^5 - 0.0000556576(u - u_{\text{th}})^6 + \dots. \end{aligned} \quad (4.18)$$

The values of $F_2, \beta, u_{\text{th}}$ are taken from the numeric solution (shown as the solid curve), whereas the values of \tilde{F}_0, \tilde{n}_1 are induced from $F(u_{\text{th}})$ and $n'(u_{\text{th}})$ from the numerical solution. We find that even if we truncate the series at relatively low orders (blue dashed curves in Figure 4.1) the convergence with the numerical solution is very good, even near $u = 0$.

The close match between the series solution (4.18) and the numeric solution near the throat gives us confidence that the solid curve is indeed a numeric wormhole solution to the field equations. Improved accuracy can be obtained by further tuning the initial conditions to obtain a better match between the series and numeric solutions.

In fact, the solution in Figure 1 is found based on the “less singular” trick introduced in Appendix A, which indicates that the parameter F_4 is constrained in terms of $\{\beta, F_2, F_5\}$ so that the singularity at the throat is absent. To obtain such non-singular solutions we try different values of β, F_2, F_5 repeatedly until matching between numerical and series solutions over the range of u up to a certain level of numerical accuracy is realized, as shown in Figure 1. We used NDSolve in Mathematica with Accuracy and Precision goals of 10^{-20}

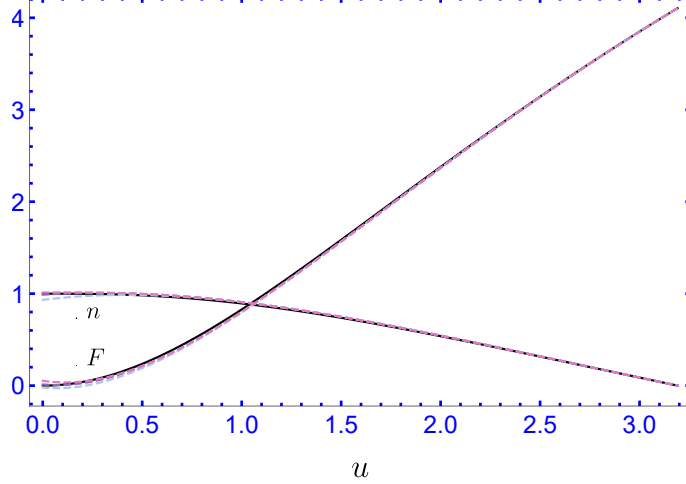


Figure 4.1: A wormhole solution with a positive mass M (4.16) is constructed subject to $\beta = 0.091, F_2 = 1, F_4 \approx -0.281186 \in (-1, 0), F_5 = 0.1, u_{\text{th}} \approx 3.19114$. The increasing and decreasing solid black curves correspond to the numerical solutions for $F(u)$ and $n(u)$ respectively. Dashed curves are truncations of the series (4.17). Truncation orders are 7, 12, 20 for the respective blue, pink, and purple curves for F ; and 8, 13, 21 for n . We see that pink and purple series curves overlap with the numeric ones for almost the entire domain of u , indicating the speed of convergence for the series (4.18).

and find in the vicinity of the throat ($u \sim 3.1$) that $\max\{|F_{\text{numerical}} - F_{\text{series}}|\} < 10^{-4}$ and $\max\{|n_{\text{numerical}} - n_{\text{series}}|\} < 10^{-5}$. The largest values we find across the entire range of u are $\max\{|F_{\text{numerical}} - F_{\text{series}}|\} < 0.03$, $\max\{|n_{\text{numerical}} - n_{\text{series}}|\} < 0.02$ for small u (i.e. near infinity).

4.5 Traversability of the wormhole

Since the series (4.18) provides a very good approximation of higher order derivatives near throat, we can use it to investigate the traversability [132, 146] of the numerical solution described in Figure 4.1.

Due to the power series form of (4.18), the factor $(F/n)^{1/2}$ of the proper radial distance $l(u) \equiv \int_{u_{\text{th}}}^u du (F/n)^{1/2} / u^2$ is no longer ill-defined at u_{th} . This can be seen by considering a small perturbation $\Delta u < 0$ around the throat, which implies $l \approx \sqrt{F(u_{\text{th}})\Delta u / n'(u_{\text{th}})} / u_{\text{th}}^2$ being regular. Therefore $l(u)$ is finite for all $0 < u \leq u_{\text{th}}$.

The Riemannian curvature tensor at the throat in an orthonormal basis has only four independent non-vanishing components

$$\begin{aligned}
 R_{\hat{t}\hat{r}\hat{t}\hat{r}} &= \frac{4nF'^2 - n'FF' - 2nFF''}{4F^3} = 0.918443, & R_{\hat{\theta}\hat{\phi}\hat{\theta}\hat{\phi}} &= \frac{F - n}{Fr^2} = 10.1834 \\
 R_{\hat{r}\hat{\theta}\hat{r}\hat{\theta}} &= R_{\hat{r}\hat{\phi}\hat{r}\hat{\phi}} = -\frac{1}{2r} \left(\frac{n}{F} \right)' = -1.80698, & R_{\hat{t}\hat{\theta}\hat{t}\hat{\theta}} &= R_{\hat{t}\hat{\phi}\hat{t}\hat{\phi}} = -\frac{nF'}{2F^2r} = 0,
 \end{aligned} \tag{4.19}$$

where $'$ indicates derivatives with respect to r . All of them are finite, implying regularity of the spacetime and of the tidal force experienced by a traveler moving at a slow speed when passing through the throat [132].

The flare-out condition [132] is easily visualized by considering the embedding of the wormhole geometry for a fixed t and $\theta = \pi/2$ into an AdS space

$$ds^2 = \left(1 + \delta + \frac{\rho^2}{l^2}\right) dz^2 + \left(1 + \delta + \frac{\rho^2}{l^2}\right)^{-1} d\rho^2 + \rho^2 d\psi^2, \quad (4.20)$$

with a deficit angle δ through the embedding relation

$$\rho = r, \quad \psi = \phi, \quad dz = \frac{\sqrt{F/n(1 + \delta + r^2/l^2) - 1}}{(1 + \delta + r^2/l^2)} dr. \quad (4.21)$$

This implies the throat truly corresponds to a local minimum in the radial coordinate since

$$\left. \frac{d}{dz} \left(\frac{dr}{dz} \right) \right|_{u_{\text{th}}} = 1.02888 > 0 \quad (4.22)$$

satisfying the flare-out condition $\left. \frac{d}{dz} \frac{dr}{dz} \right|_{u_{\text{th}}} > 0$.

4.6 Wormhole Candidates

Obtaining the value of F_4 in Figure 4.1 requires a trick in making the termination point of numerical methods “less singular”. Given β, F_2 and F_5 , a generic value of F_4 causes a “tip” in $F(u)$, bending it either up or down in the vicinity of a singularity, as shown in Figure 4.2 in blue or purple. This “tip” should be avoided as it is clearly not a part of a Taylor series expansion near the throat and implies a huge value for $F''(u_{\text{th}})$. The value of F_4 for the black curve in Figure 4.2 is determined by demanding that $F''(\tilde{u}_{\text{th}})$ has a small value at a point \tilde{u}_{th} close to u_{th} . For simplicity, we take $F''(0.9999999u_{\text{th}})$ to be 0. However other values less than $\sim 10^3$ will not make the result much different.

Two wormhole candidates with differing values of β and F_5 from those in Figure 4.1 are shown in Figure 4.3 based on the prescription for F_4 discussed above. From the figure, we see in each case that there is a segment of the series solution that converges to the corresponding numerical solution (near the throat) but otherwise departs from it. Since non-analytic solutions are allowed in non-linear systems, a mismatch with the series (4.17) does not forbid the numeric solutions from being wormholes. Since F'', F', n' appear to be finite from the figure, these solutions may also be regarded as wormholes. If we relax the wormhole criterion and regard all solutions with a vanishing “tip” to be wormholes, we arrive at Figure 4.4, which displays the size of the throat as a function of the mass M . We see that the throat slowly expands as M increases, apparently asymptoting to an upper bound. By this criterion, we obtain a family of wormhole candidates in Einstein cubic gravity. The increase in wormhole throat size with increasing mass suggests the presence of a potential repulsive effect. This intriguing phenomenon, along with the stability of these solutions, warrants further investigation.

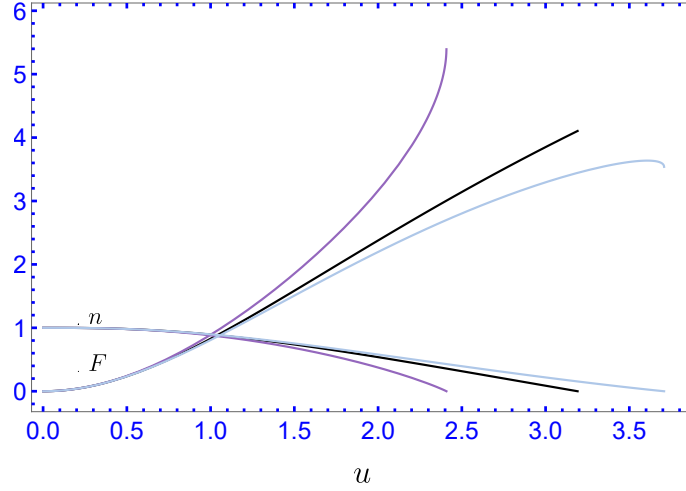


Figure 4.2: Solutions for different F_4 's. Rising and descending curves of the same color respectively correspond to $F(u)$ and $n(u)$ of a solution. The increasing and decreasing curves originating at $u = 0$ respectively correspond to $F(u)$ and $n(u)$. The wormhole solution in Figure 4.1 is in black, with $\beta = 0.091, F_2 = 1, F_4 \approx -0.281186, F_5 = 0.1$. The purple and the blue curves only differ the black ones in F_4 (purple: $F_4 = -0.1$; blue: $F_4 = -0.31$).

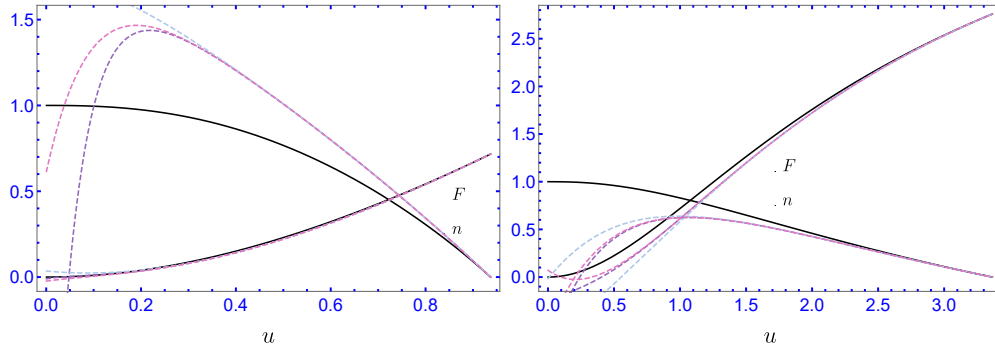


Figure 4.3: Wormhole candidates. The same labeling convention as in Figure 4.1 is applied here. Left: $\beta = 0.2, F_2 = F_5 = 1, F_4 \approx -0.635778, u_{\text{th}} \approx 0.937102$; Right: $\beta = 0.05, F_2 = F_5 = 1, F_4 \approx -0.648749, u_{\text{th}} \approx 3.36473$.

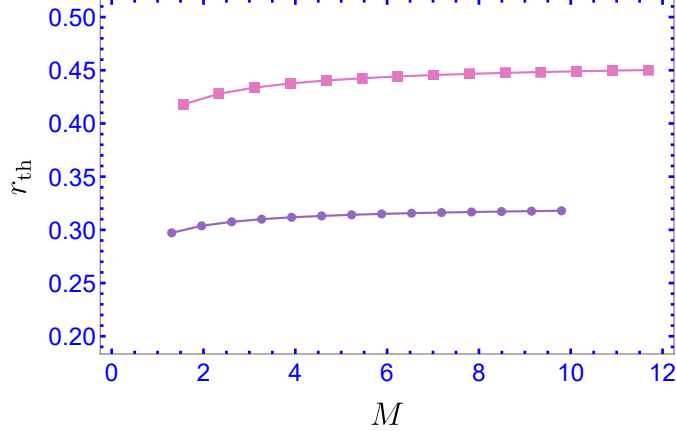


Figure 4.4: Relations between wormhole mass M and throat size r_{th} for $\beta = 0.05$ (purple) and 0.091 (pink). Both of them have the same $F_2 = 1$, and F_4 is obtained by the prescription in Section 4.6.

4.7 Comments

In general relativity, traversable wormholes solutions typically require the presence of exotic matter to exist. In this chapter, we have obtained for the first time a wormhole solution that requires no exotic matter in the framework of generalized quasi-topological gravity. Specifically, in Figure 4.1, we have shown that a traversable wormhole connecting two asymptotically AdS spacetimes exists as a solution to the field equations of 4D Einsteinian Cubic Gravity (ECG). The spacetime has a geometrical deficit δ , which can be interpreted as a global monopole. We also present some wormhole candidates in Appendix 4.6. Note that the coupling α is chosen to be a specific value that satisfies (4.15), which is achieved by demanding that the field equations be satisfied for asymptotically AdS solutions featuring a deficit angle [121]. The candidate wormhole solutions we find (given in Appendix 4.6) are constructed by specifying F_4 using the “less singular” technique for given values of β, F_2, F_5 .

During the course of our investigation, by varying the initial and boundary conditions, we also observed the possibility of numerical soliton solutions within the framework of 4D ECG. The metric for these solutions has neither an horizon nor a throat; the functions $F(u)$ and $n(u)$ both asymptotically approach finite values as $u \rightarrow \infty$. This new type of solution warrants further investigation; rather than present this here, we leave it for future study.

Another interesting aspect to consider is the exploration of 4D GQTG wormhole solutions that are asymptotically flat or de Sitter. These solutions are of greater physical interest.

Chapter 5

Final remarks

In this thesis, we have discussed various aspects of Generalized Quasi-Topological Gravities, advancing both their theoretical foundations and phenomenological implications. Our structural analysis has rigorously established the existence of exactly $n - 1$ inequivalent GQTG densities at order n in curvature for $D > 4$, while strongly supporting the uniqueness of the corresponding densities in four dimensions.

On the thermodynamic front, we introduced the K -rule—an extension of Maxwell’s equal area law—provides a powerful new tool to investigate multicritical phenomena in black hole phase space. Using this method, we have constructed novel examples of quadruple and quintuple points, and established bounds on the number of couplings required to support such complex criticality. These findings suggest intriguing parallels between the microscopic degrees of freedom of black holes and those of condensed matter systems with multiscale interactions.

Finally, we have shown that traversable wormholes can exist in GQTGs without the need for exotic matter. In particular, we presented the first such solution in four-dimensional Einsteinian Cubic Gravity, describing a wormhole connecting two asymptotically AdS regions, supported solely by the higher-curvature terms of the theory. These configurations exhibit a geometric deficit angle reminiscent of global monopoles and were constructed using refined numerical methods. These results indicate the study of nontrivial spacetime geometries in higher-curvature theories can also be fruitful.

Together, these results underline the promise of GQTGs as a fertile ground for addressing key questions in gravitational theory, black hole thermodynamics, and the quantum structure of spacetime. Future work may focus on connecting these work to the AdS/CFT correspondence.

References

- [1] Benjamin P Abbott, Richard Abbott, TD Abbott, MR Abernathy, Fausto Acernese, Kendall Ackley, Carl Adams, Thomas Adams, Paolo Addesso, RX Adhikari, et al. Observation of gravitational waves from a binary black hole merger. *Physical review letters*, 116(6):061102, 2016.
- [2] Connor Adair, Pablo Bueno, Pablo A. Cano, Robie A. Hennigar, and Robert B. Mann. Slowly rotating black holes in Einsteinian cubic gravity. *Phys. Rev. D*, 102(8):084001, 2020.
- [3] Jamil Ahmed, Robie A. Hennigar, Robert B. Mann, and Mozhgan Mir. Quintessential Quartic Quasi-topological Quartet. *JHEP*, 05:134, 2017.
- [4] Natacha Altamirano, David Kubiznak, and Robert B. Mann. Reentrant phase transitions in rotating anti-de Sitter black holes. *Phys. Rev. D*, 88(10):101502, 2013.
- [5] Natacha Altamirano, David Kubizňák, Robert B. Mann, and Zeinab Sherkatghanad. Kerr-AdS analogue of triple point and solid/liquid/gas phase transition. *Class. Quant. Grav.*, 31:042001, 2014.
- [6] Gustavo Arciniega, Pablo Bueno, Pablo A. Cano, José D. Edelstein, Robie A. Hennigar, and Luisa G. Jaime. Geometric Inflation. *Phys. Lett. B*, 802:135242, 2020.
- [7] Gustavo Arciniega, Jose D. Edelstein, and Luisa G. Jaime. Towards geometric inflation: the cubic case. *Phys. Lett. B*, 802:135272, 2020.
- [8] Gabriel Arenas-Henriquez, Robert B. Mann, Olivera Miskovic, and Rodrigo Olea. Mass in Lovelock Unique Vacuum gravity theories. *Phys. Rev. D*, 100(6):064038, 2019.
- [9] Gabriel Arenas-Henriquez, Olivera Miskovic, and Rodrigo Olea. Vacuum Degeneracy and Conformal Mass in Lovelock AdS Gravity. *JHEP*, 11:128, 2017.
- [10] R. Arnowitt, S. Deser, and C. W. Misner. Energy and the Criteria for Radiation in General Relativity. *Phys. Rev.*, 118:1100–1104, 1960.
- [11] Richard L. Arnowitt, Stanley Deser, and Charles W. Misner. Canonical variables for general relativity. *Phys. Rev.*, 117:1595–1602, 1960.

- [12] Richard L. Arnowitt, Stanley Deser, and Charles W. Misner. Coordinate invariance and energy expressions in general relativity. *Phys. Rev.*, 122:997, 1961.
- [13] Hamid R. Bakhtiarizadeh. Charged rotating black strings in Einsteinian quartic gravity. *Nucl. Phys. B*, 987:116083, 2023.
- [14] Vijay Balasubramanian and Per Kraus. A Stress tensor for Anti-de Sitter gravity. *Commun. Math. Phys.*, 208:413–428, 1999.
- [15] James M. Bardeen, B. Carter, and S. W. Hawking. The Four laws of black hole mechanics. *Commun. Math. Phys.*, 31:161–170, 1973.
- [16] Manuel Barriola and Alexander Vilenkin. Gravitational Field of a Global Monopole. *Phys. Rev. Lett.*, 63:341, 1989.
- [17] Emmanuele Battista, Salvatore Capozziello, and Abdelghani Errehymy. Generalized uncertainty principle corrections in Rastall–Rainbow Casimir wormholes. *Eur. Phys. J. C*, 84(12):1314, 2024.
- [18] Jacob D. Bekenstein. Black holes and entropy. *Phys. Rev.*, D7:2333–2346, 1973.
- [19] Jacob D. Bekenstein. Generalized second law of thermodynamics in black hole physics. *Phys. Rev.*, D9:3292–3300, 1974.
- [20] Snehasish Bhattacharjee. Baryogenesis in $f(P)$ Gravity. *Int. J. Mod. Phys. A*, 36:27, 3 2021.
- [21] Snehasish Bhattacharjee. Energy conditions in $f(P)$ gravity. *Int. J. Mod. Phys. D*, 31(03):2250014, 2022.
- [22] David G. Boulware and Stanley Deser. String Generated Gravity Models. *Phys. Rev. Lett.*, 55:2656, 1985.
- [23] K. A. Bronnikov. Scalar-tensor theory and scalar charge. *Acta Phys. Polon. B*, 4:251–266, 1973.
- [24] J. David Brown and C. Teitelboim. Neutralization of the Cosmological Constant by Membrane Creation. *Nucl. Phys. B*, 297:787–836, 1988.
- [25] Pablo Bueno and Pablo A. Cano. Einsteinian cubic gravity. *Phys. Rev. D*, 94(10):104005, 2016.
- [26] Pablo Bueno and Pablo A. Cano. Four-dimensional black holes in Einsteinian cubic gravity. *Phys. Rev.*, D94(12):124051, 2016.
- [27] Pablo Bueno and Pablo A. Cano. On black holes in higher-derivative gravities. *Class. Quant. Grav.*, 34(17):175008, 2017.
- [28] Pablo Bueno and Pablo A. Cano. Universal black hole stability in four dimensions. *Phys. Rev.*, D96(2):024034, 2017.

- [29] Pablo Bueno, Pablo A. Cano, and Robie A. Hennigar. (Generalized) quasi-topological gravities at all orders. *Class. Quant. Grav.*, 37(1):015002, 2020.
- [30] Pablo Bueno, Pablo A. Cano, Robie A. Hennigar, Mengqi Lu, and Javier Moreno. Generalized quasi-topological gravities: the whole shebang. *Class. Quant. Grav.*, 40(1):015004, 2023.
- [31] Pablo Bueno, Pablo A. Cano, Robie A. Hennigar, and Robert B. Mann. NUTs and bolts beyond Lovelock. *JHEP*, 10:095, 2018.
- [32] Pablo Bueno, Pablo A. Cano, Robie A. Hennigar, and Robert B. Mann. Universality of Squashed-Sphere Partition Functions. *Phys. Rev. Lett.*, 122(7):071602, 2019.
- [33] Pablo Bueno, Pablo A. Cano, Robie A. Hennigar, Victor A. Penas, and Alejandro Ruipérez. Partition functions on slightly squashed spheres and flux parameters. *JHEP*, 04:123, 2020.
- [34] Pablo Bueno, Pablo A. Cano, Quim Llorens, Javier Moreno, and Guido van der Velde. Aspects of three-dimensional higher curvatures gravities. *Class. Quant. Grav.*, 39(12):125002, 2022.
- [35] Pablo Bueno, Pablo A. Cano, Vincent S. Min, and Manus R. Visser. Aspects of general higher-order gravities. *Phys. Rev.*, D95(4):044010, 2017.
- [36] Pablo Bueno, Pablo A. Cano, Javier Moreno, and Ángel Murcia. All higher-curvature gravities as Generalized quasi-topological gravities. *JHEP*, 11:062, 2019.
- [37] Pablo Bueno, Pablo A. Cano, Javier Moreno, and Guido van der Velde. Regular black holes in three dimensions. *Phys. Rev. D*, 104(2):L021501, 2021.
- [38] Pablo Bueno, Pablo A. Cano, and Alejandro Ruipérez. Holographic studies of Einsteinian cubic gravity. *JHEP*, 03:150, 2018.
- [39] Daniel J. Burger, William T. Emond, and Nathan Moynihan. Rotating Black Holes in Cubic Gravity. *Phys. Rev. D*, 101(8):084009, 2020.
- [40] Elena Cáceres, Rodrigo Castillo Vásquez, and Alejandro Vilar López. Entanglement entropy in cubic gravitational theories. *JHEP*, 05:186, 2021.
- [41] Elena Caceres, Phuc H. Nguyen, and Juan F. Pedraza. Holographic entanglement entropy and the extended phase structure of STU black holes. *JHEP*, 09:184, 2015.
- [42] Marco M. Caldarelli, Guido Cognola, and Dietmar Klemm. Thermodynamics of Kerr-Newman-AdS black holes and conformal field theories. *Class. Quant. Grav.*, 17:399–420, 2000.
- [43] Pablo A. Cano, Kwinten Fransen, and Thomas Hertog. Novel higher-curvature variations of R^2 inflation. *Phys. Rev. D*, 103(10):103531, 2021.

- [44] Pablo A. Cano and Ángel Murcia. Electromagnetic Quasitopological Gravities. *JHEP*, 10:125, 2020.
- [45] Pablo A. Cano and Ángel Murcia. Resolution of Reissner-Nordström singularities by higher-derivative corrections. *Class. Quant. Grav.*, 38(7):075014, 2021.
- [46] Pablo A. Cano, Ángel J. Murcia, Alberto Rivadulla Sánchez, and Xuao Zhang. Higher-derivative holography with a chemical potential. *JHEP*, 07:010, 2022.
- [47] Pablo A. Cano and David Pereñiguez. Extremal Rotating Black Holes in Einsteinian Cubic Gravity. *Phys. Rev. D*, 101(4):044016, 2020.
- [48] Adolfo Cisterna, Nicolás Grandi, and Julio Oliva. On four-dimensional Einsteinian gravity, quasitopological gravity, cosmology and black holes. *Phys. Lett. B*, 805:135435, 2020.
- [49] Adolfo Cisterna, Luis Guajardo, Mokhtar Hassaine, and Julio Oliva. Quintic quasitopological gravity. *JHEP*, 04:066, 2017.
- [50] J Clerk-Maxwell. On the dynamical evidence of the molecular constitution of bodies. *Nature*, 11(279):357–359, 1875.
- [51] Event Horizon Telescope Collaboration et al. First m87 event horizon telescope results. i. the shadow of the supermassive black hole. *arXiv preprint arXiv:1906.11238*, 2019.
- [52] Jolien D. E. Creighton and Robert B. Mann. Quasilocal thermodynamics of dilaton gravity coupled to gauge fields. *Phys. Rev. D*, 52:4569–4587, 1995.
- [53] M. Cvetič, G. W. Gibbons, D. Kubiznak, and C. N. Pope. Black Hole Enthalpy and an Entropy Inequality for the Thermodynamic Volume. *Phys. Rev. D*, 84:024037, 2011.
- [54] Vittorio De Falco, Emmanuele Battista, Salvatore Capozziello, and Mariafelicia De Laurentis. Reconstructing wormhole solutions in curvature based Extended Theories of Gravity. *Eur. Phys. J. C*, 81(2):157, 2021.
- [55] Vittorio De Falco and Salvatore Capozziello. Static and spherically symmetric wormholes in metric-affine theories of gravity. *Phys. Rev. D*, 108(10):104030, 2023.
- [56] M. H. Dehghani, A. Bazrafshan, R. B. Mann, M. R. Mehdizadeh, M. Ghanaatian, and M. H. Vahidinia. Black Holes in Quartic Quasitopological Gravity. *Phys. Rev.*, D85:104009, 2012.
- [57] Stanley Deser and A. V. Ryzhov. Curvature invariants of static spherically symmetric geometries. *Class. Quant. Grav.*, 22:3315–3324, 2005.
- [58] Stanley Deser and Bayram Tekin. Energy in generic higher curvature gravity theories. *Phys. Rev.*, D67:084009, 2003.

- [59] Stanley Deser and Bayram Tekin. Shortcuts to high symmetry solutions in gravitational theories. *Class. Quant. Grav.*, 20:4877–4884, 2003.
- [60] Anshuman Dey, Pratim Roy, and Tapobrata Sarkar. On holographic Rényi entropy in some modified theories of gravity. *JHEP*, 04:098, 2018.
- [61] Elisabetta Di Grezia, Emmanuele Battista, Mattia Manfredonia, and Gennaro Miele. Spin, torsion and violation of null energy condition in traversable wormholes. *Eur. Phys. J. Plus*, 132(12):537, 2017.
- [62] Brian P. Dolan. The cosmological constant and the black hole equation of state. *Class. Quant. Grav.*, 28:125020, 2011.
- [63] Hannah Dykaar, Robie A. Hennigar, and Robert B. Mann. Hairy black holes in cubic quasi-topological gravity. *JHEP*, 05:045, 2017.
- [64] Arthur Stanley Eddington. The deflection of light during a solar eclipse. *Nature*, 104(2615):372–372, 1919.
- [65] Arthur Stanley Eddington. The total eclipse of 1919 may 29 and the influence of gravitation on light. *The Observatory*, 42:119–122, 1919.
- [66] José D. Edelstein, Nicolás Grandi, and Alberto Rivadulla Sánchez. Holographic superconductivity in Einsteinian Cubic Gravity. *JHEP*, 05:188, 2022.
- [67] José D. Edelstein, Robert B. Mann, David Vázquez Rodríguez, and Alejandro Vilar López. Small free field inflation in higher curvature gravity. *JHEP*, 01:029, 2021.
- [68] José D. Edelstein, David Vázquez Rodríguez, and Alejandro Vilar López. Aspects of Geometric Inflation. *JCAP*, 12:040, 2020.
- [69] Albert Einstein. *Relativity: the special and the general theory*. GENERAL PRESS, 2016.
- [70] Albert Einstein and N. Rosen. The Particle Problem in the General Theory of Relativity. *Phys. Rev.*, 48:73–77, 1935.
- [71] H. G. Ellis. Ether flow through a drainhole - a particle model in general relativity. *J. Math. Phys.*, 14:104–118, 1973.
- [72] H. G. Ellis. The evolving, flowless drain hole: a nongravitating particle model in general relativity theory. *Gen. Rel. Grav.*, 10:105–123, 1979.
- [73] William T. Emond and Nathan Moynihan. Scattering Amplitudes, Black Holes and Leading Singularities in Cubic Theories of Gravity. *JHEP*, 12:019, 2019.
- [74] Roberto Emparan, Clifford V. Johnson, and Robert C. Myers. Surface terms as counterterms in the AdS / CFT correspondence. *Phys. Rev.*, D60:104001, 1999.

- [75] Cristian Erices, Eleftherios Papantonopoulos, and Emmanuel N. Saridakis. Cosmology in cubic and $f(P)$ gravity. *Phys. Rev. D*, 99(12):123527, 2019.
- [76] Xing-Hui Feng, Hyat Huang, Zhan-Feng Mai, and H. Lu. Bounce Universe and Black Holes from Critical Einsteinian Cubic Gravity. *Phys. Rev.*, D96(10):104034, 2017.
- [77] Octavio Fierro, Nicolas Mora, and Julio Oliva. Slowly rotating black holes in quasitopological gravity. *Phys. Rev. D*, 103(6):064004, 2021.
- [78] Octavio Fierro, Daniela Narbona, Julio Oliva, Constanza Quijada, and Guillermo Rubilar. Scalar probes on wormholes in Lovelock theories with unique vacuum. *Phys. Rev. D*, 110(2):024027, 2024.
- [79] Antonia M. Frassino, David Kubiznak, Robert B. Mann, and Fil Simovic. Multiple Reentrant Phase Transitions and Triple Points in Lovelock Thermodynamics. *JHEP*, 09:080, 2014.
- [80] Antonia Micol Frassino and Jorge V. Rocha. Charged black holes in Einsteinian cubic gravity and nonuniqueness. *Phys. Rev. D*, 102(2):024035, 2020.
- [81] David H Frisch and James H Smith. Measurement of the relativistic time dilation using μ -mesons. *American Journal of Physics*, 31(5):342–355, 1963.
- [82] Changjun Gao. Black holes with many horizons in the theories of nonlinear electrodynamics. *Phys. Rev. D*, 104(6):064038, 2021.
- [83] Álvaro González García, Remco Tuinier, Jasper V Maring, Joeri Oudam, Henricus H Wensink, and Henk NW Lekkerkerker. Depletion-driven four-phase coexistences in discotic systems. *Molecular Physics*, 116(21-22):2757–2772, 2018.
- [84] Rahul Ghosh, Ujjal Debnath, and Shuvendu Chakraborty. Reconstructions of $f(P)$ gravity from (m, n) type ordinary and entropy-corrected holographic and Pilgrim dark energy models. *Int. J. Mod. Phys. A*, 36(29):2150198, 2021.
- [85] G. W. Gibbons and S. W. Hawking. Action Integrals and Partition Functions in Quantum Gravity. *Phys. Rev.*, D15:2752–2756, 1977.
- [86] Gary W. Gibbons, Renata Kallosh, and Barak Kol. Moduli, scalar charges, and the first law of black hole thermodynamics. *Phys. Rev. Lett.*, 77:4992–4995, 1996.
- [87] Finnian Gray, Robie A. Hennigar, David Kubiznak, Robert B. Mann, and Manu Srivastava. Generalized Lense-Thirring metrics: higher-curvature corrections and solutions with matter. *JHEP*, 04:070, 2022.
- [88] Tomáš Hale, David Kubizňák, Otakar Svítek, and Tayebah Tahamtan. Solutions and basic properties of regularized Maxwell theory. *Phys. Rev. D*, 107(12):124031, 2023.
- [89] Tiberiu Harko, Francisco S. N. Lobo, M. K. Mak, and Sergey V. Sushkov. Modified-gravity wormholes without exotic matter. *Phys. Rev. D*, 87(6):067504, 2013.

- [90] S. W. Hawking. Particle Creation by Black Holes. *Commun. Math. Phys.*, 43:199–220, 1975. [,167(1975)].
- [91] S. W. Hawking and Don N. Page. Thermodynamics of Black Holes in anti-De Sitter Space. *Commun. Math. Phys.*, 87:577, 1983.
- [92] Robie A. Hennigar. Criticality for charged black branes. *JHEP*, 09:082, 2017.
- [93] Robie A. Hennigar, David Kubizňák, and Robert B. Mann. Generalized quasitopological gravity. *Phys. Rev.*, D95(10):104042, 2017.
- [94] Robie A. Hennigar and Robert B. Mann. Black holes in Einsteinian cubic gravity. *Phys. Rev.*, D95(6):064055, 2017.
- [95] Robie A. Hennigar, Robert B. Mann, and Erickson Tjoa. Superfluid Black Holes. *Phys. Rev. Lett.*, 118(2):021301, 2017.
- [96] Robie A. Hennigar, Mohammad Bagher Jahani Poshteh, and Robert B. Mann. Shadows, Signals, and Stability in Einsteinian Cubic Gravity. *Phys. Rev.*, D97(6):064041, 2018.
- [97] Robie A. Hennigar, Erickson Tjoa, and Robert B. Mann. Thermodynamics of hairy black holes in Lovelock gravity. *JHEP*, 02:070, 2017.
- [98] Brayden R. Hull and Robert B. Mann. Thermodynamics of exotic black holes in Lovelock gravity. *Phys. Rev. D*, 104(8):084032, 2021.
- [99] Brayden R. Hull and Fil Simovic. Exotic black hole thermodynamics in third-order Lovelock gravity. *Class. Quant. Grav.*, 40(14):145016, 2023.
- [100] Vivek Iyer and Robert M. Wald. Some properties of Noether charge and a proposal for dynamical black hole entropy. *Phys. Rev.*, D50:846–864, 1994.
- [101] Vivek Iyer and Robert M. Wald. A Comparison of Noether charge and Euclidean methods for computing the entropy of stationary black holes. *Phys. Rev.*, D52:4430–4439, 1995.
- [102] Luisa G. Jaime and Gustavo Arciniega. A unified geometric description of the Universe: From inflation to late-time acceleration without an inflaton nor a cosmological constant. *Phys. Lett. B*, 827:136939, 2022.
- [103] Abdul Jawad and Sadaf Maqsood. Gravitationally induced particle creation in cubic gravity. *Int. J. Geom. Meth. Mod. Phys.*, 18(07):2150106, 2021.
- [104] Jie Jiang and Xiao-Wei Li. Adjusted complexity equals action conjecture. *Phys. Rev. D*, 100(6):066026, 2019.
- [105] Jose Beltrán Jiménez and Alejandro Jiménez-Cano. On the strong coupling of Einsteinian Cubic Gravity and its generalisations. *JCAP*, 01:069, 2021.

- [106] Zoya Khan, Shamaila Rani, Abdul Jawad, and G. Mustafa. Analysis of cubic gravity through cosmic aspects. *Int. J. Geom. Meth. Mod. Phys.*, 17(09):2050134, 2020.
- [107] H. Khodabakhshi, A. Giaimo, and Robert B. Mann. Einstein Quartic Gravity: Shadows, Signals, and Stability. *Phys. Rev. D*, 102(4):044038, 2020.
- [108] H. Khodabakhshi and Robert B. Mann. Gravitational Lensing by Black Holes in Einstein Quartic Gravity. *Phys. Rev. D*, 103(2):024017, 2021.
- [109] R. A. Konoplya, A. F. Zinhailo, and Z. Stuchlik. Quasinormal modes and Hawking radiation of black holes in cubic gravity. *Phys. Rev. D*, 102(4):044023, 2020.
- [110] M. Kord Zangeneh and A. Kazemi. Topological Born–Infeld charged black holes in Einsteinian cubic gravity. *Eur. Phys. J. C*, 80(8):794, 2020.
- [111] David Kubiznak and Robert B. Mann. P-V criticality of charged AdS black holes. *JHEP*, 07:033, 2012.
- [112] David Kubiznak and Robert B. Mann. Black hole chemistry. *Can. J. Phys.*, 93(9):999–1002, 2015.
- [113] David Kubiznak, Robert B. Mann, and Mae Teo. Black hole chemistry: thermodynamics with Lambda. *Class. Quant. Grav.*, 34(6):063001, 2017.
- [114] Cornelius Lanczos. Electricity as a natural property of Riemannian geometry. *Rev. Mod. Phys.*, 39:716–736, 1932.
- [115] Cornelius Lanczos. A Remarkable property of the Riemann-Christoffel tensor in four dimensions. *Annals Math.*, 39:842–850, 1938.
- [116] Yue-Zhou Li, H. Lu, and Liang Ma. Hidden relations of central charges and OPEs in holographic CFT. *JHEP*, 11:135, 2021.
- [117] D. Lovelock. The Einstein tensor and its generalizations. *J. Math. Phys.*, 12:498–501, 1971.
- [118] David Lovelock. Divergence-free tensorial concomitants. *Aequationes mathematicae*, 4(1):127–138, 1970.
- [119] Mengqi Lu and Robert B. Mann. Lagrangian Partition Functions Subject to a Fixed Spatial Volume Constraint in the Lovelock Theory. *Entropy*, 26(4):291, 2024.
- [120] Mengqi Lu and Robert B. Mann. Maxwell construction and multi-criticality in uncharged generalized quasi-topological black holes. *Class. Quant. Grav.*, 41(1):015016, 2024.
- [121] Mengqi Lu, Jiayue Yang, and Robert B. Mann. Gravitational Wormholes. *Universe*, 10:257, 2024.

- [122] Mengqi Lu, Jiayue Yang, and Robert B. Mann. Existence of vacuum wormholes in Einsteinian cubic gravity. *JHEP*, 03:073, 2025.
- [123] Robert B. Mann. The (Holographic) Chemistry of Black Holes. *Springer Proc. Phys.*, 392:97–132, 2024.
- [124] Robert B. Mann. Black hole chemistry: The first 15 years. *Int. J. Mod. Phys. D*, 34(09):2542001, 2025.
- [125] Mihai Marciu. Dynamical aspects for scalar fields coupled to cubic contractions of the Riemann tensor. *Phys. Rev. D*, 102(2):023517, 2020.
- [126] Mihai Marciu. Note on the dynamical features for the extended $f(P)$ cubic gravity. *Phys. Rev. D*, 101(10):103534, 2020.
- [127] Mohammad Reza Mehdizadeh and Amir Hadi Ziaie. Traversable wormholes in Einsteinian cubic gravity. *Mod. Phys. Lett. A*, 35(06):2050017, 2019.
- [128] Mozhgan Mir, Robie A. Hennigar, Jamil Ahmed, and Robert B. Mann. Black hole chemistry and holography in generalized quasi-topological gravity. *JHEP*, 08:068, 2019.
- [129] Mozhgan Mir, Robie A. Hennigar, Jamil Ahmed, and Robert B. Mann. Black hole chemistry and holography in generalized quasi-topological gravity. *JHEP*, 08:068, 2019.
- [130] Mozhgan Mir and Robert B. Mann. On generalized quasi-topological cubic-quartic gravity: thermodynamics and holography. *JHEP*, 07:012, 2019.
- [131] Javier Moreno and Ángel J. Murcia. Classification of generalized quasitopological gravities. *Phys. Rev. D*, 108(4):044016, 2023.
- [132] M. S. Morris and K. S. Thorne. Wormholes in space-time and their use for interstellar travel: A tool for teaching general relativity. *Am. J. Phys.*, 56:395–412, 1988.
- [133] G. Mustafa, Tie-Cheng Xia, Ibrar Hussain, and M. Farasat Shamir. Spherically symmetric static wormhole models in the Einsteinian cubic gravity. *Int. J. Geom. Meth. Mod. Phys.*, 17(14):2050214, 2020.
- [134] Robert C. Myers and M. J. Perry. Black Holes in Higher Dimensional Space-Times. *Annals Phys.*, 172:304, 1986.
- [135] Robert C. Myers and Brandon Robinson. Black Holes in Quasi-topological Gravity. *JHEP*, 08:067, 2010.
- [136] Ratbay Myrzakulov, Lorenzo Sebastiani, Sunny Vagnozzi, and Sergio Zerbini. Static spherically symmetric solutions in mimetic gravity: rotation curves and wormholes. *Class. Quant. Grav.*, 33(12):125005, 2016.

- [137] Julio Oliva and Sourya Ray. A new cubic theory of gravity in five dimensions: Black hole, Birkhoff's theorem and C-function. *Class. Quant. Grav.*, 27:225002, 2010.
- [138] M. Ostrogradsky. Mémoires sur les équations différentielles, relatives au problème des isopérimètres.
- [139] T. Padmanabhan and D. Kothawala. Lanczos-Lovelock models of gravity. *Phys. Rept.*, 531:115–171, 2013.
- [140] Richard S. Palais. The principle of symmetric criticality. *Commun. Math. Phys.*, 69(1):19–30, 1979.
- [141] VFD Peters, M Vis, Á González García, Henricus H Wensink, and R Tuinier. Defying the gibbs phase rule: Evidence for an entropy-driven quintuple point in colloid-polymer mixtures. *Physical Review Letters*, 125(12):127803, 2020.
- [142] Masroor C. Pookkillath, Antonio De Felice, and Alexei A. Starobinsky. Anisotropic instability in a higher order gravity theory. *JCAP*, 07:041, 2020.
- [143] Mohammad Bagher Jahani Poshteh and Robert B. Mann. Gravitational Lensing by Black Holes in Einsteinian Cubic Gravity. *Phys. Rev.*, D99(2):024035, 2019.
- [144] Israel Quiros, Roberto De Arcia, Ricardo García-Salcedo, Tame Gonzalez, Francisco X. Linares Cedeño, and Ulises Nucamendi. On the quantum origin of inflation in the geometric inflation model. *Phys. Rev. D*, 103(6):064043, 2021.
- [145] Israel Quiros, Ricardo García-Salcedo, Tame Gonzalez, Jorge Luis Morales Martínez, and Ulises Nucamendi. Global asymptotic dynamics of cosmological Einsteinian cubic gravity. *Phys. Rev. D*, 102(4):044018, 2020.
- [146] Ramesh Radhakrishnan, Patrick Brown, Jacob Mutulevich, Eric Davis, Delaram Mirfendereski, and Gerald Cleaver. A Review of Stable, Traversable Wormholes in $f(R)$ Gravity Theories. *Symmetry*, 16(8):1007, 2024.
- [147] João Luís Rosa, Nailya Ganiyeva, and Francisco S. N. Lobo. Non-exotic traversable wormholes in $f(R, T_{ab}T^{ab})$ gravity. *Eur. Phys. J. C*, 83(11):1040, 2023.
- [148] João Luís Rosa and Paul Martin Kull. Non-exotic traversable wormhole solutions in linear $f(R, T)$ gravity. *Eur. Phys. J. C*, 82(12):1154, 2022.
- [149] Andrei D Sakharov et al. Vacuum quantum fluctuations in curved space and the theory of gravitation. *Soviet Physics Uspekhi*, 34(5):394, 1991.
- [150] Alok Sardar and Ujjal Debnath. Reconstruction of extended $f(P)$ cubic gravity from other modified gravity models. *Phys. Dark Univ.*, 35:100926, 2022.
- [151] Larry Smarr. Mass formula for Kerr black holes. *Phys. Rev. Lett.*, 30:71–73, 1973. [Erratum: Phys.Rev.Lett. 30, 521–521 (1973)].

- [152] Thomas P. Sotiriou and Valerio Faraoni. $f(R)$ Theories Of Gravity. *Rev. Mod. Phys.*, 82:451–497, 2010.
- [153] Alexei A Starobinsky. A new type of isotropic cosmological models without singularity. *Physics Letters B*, 91(1):99–102, 1980.
- [154] K. S. Stelle. Renormalization of Higher Derivative Quantum Gravity. *Phys. Rev. D*, 16:953–969, 1977.
- [155] Masoumeh Tavakoli, Jerry Wu, and Robert B. Mann. Multi-critical points in black hole phase transitions. *JHEP*, 12:117, 2022.
- [156] C. Teitelboim. THE COSMOLOGICAL CONSTANT AS A THERMODYNAMIC BLACK HOLE PARAMETER. *Phys. Lett. B*, 158:293–297, 1985.
- [157] Daniel R. Terno. Inaccessibility of traversable wormholes. *Phys. Rev. D*, 106(4):044035, 2022.
- [158] Robert M. Wald. Black hole entropy is the Noether charge. *Phys. Rev.*, D48:3427–3431, 1993.
- [159] Shao-Wen Wei, Yu-Xiao Liu, and Robert B. Mann. Repulsive Interactions and Universal Properties of Charged Anti-de Sitter Black Hole Microstructures. *Phys. Rev. Lett.*, 123(7):071103, 2019.
- [160] Shao-Wen Wei, Yu-Xiao Liu, and Robert B. Mann. Ruppeiner Geometry, Phase Transitions, and the Microstructure of Charged AdS Black Holes. *Phys. Rev. D*, 100(12):124033, 2019.
- [161] James T. Wheeler. Symmetric Solutions to the Gauss-Bonnet Extended Einstein Equations. *Nucl. Phys.*, B268:737–746, 1986.
- [162] James T. Wheeler. Symmetric Solutions to the Maximally Gauss-Bonnet Extended Einstein Equations. *Nucl. Phys.*, B273:732, 1986.
- [163] Edward Witten. Anti-de Sitter space, thermal phase transition, and confinement in gauge theories. *Adv. Theor. Math. Phys.*, 2:505–532, 1998.
- [164] Richard P. Woodard. Avoiding dark energy with $1/r$ modifications of gravity. *Lect. Notes Phys.*, 720:403–433, 2007.
- [165] Richard P. Woodard. Ostrogradsky’s theorem on Hamiltonian instability. *Scholarpedia*, 10(8):32243, 2015.
- [166] Jerry Wu and Robert B. Mann. Multicritical phase transitions in Lovelock AdS black holes. *Phys. Rev. D*, 107(8):084035, 2023.
- [167] Jerry Wu and Robert B. Mann. Multicritical phase transitions in multiply rotating black holes. *Class. Quant. Grav.*, 40(6):06LT01, 2023.

- [168] Jerry Wu and Robert B. Mann. Thermodynamically stable phases of asymptotically flat Lovelock black holes. *Class. Quant. Grav.*, 40(14):145009, 2023.
- [169] Jiayue Yang and Robert B. Mann. Dynamic behaviours of black hole phase transitions near quadruple points. *JHEP*, 08:028, 2023.
- [170] Ming Zhang, Wen-Di Tan, Mengqi Lu, Dyuman Bhattacharya, Jiayue Yang, and Robert B. Mann. Finite-cutoff Holographic Thermodynamics. 7 2025.

APPENDICES

Appendix A

A.1 Explicit covariant genuine GQTG densities for $n = 4, 5, 6$ in $D = 5, 6$

In this appendix we present explicit GQT covariant densities of each of the $(n - 2)$ existing types for $n = 4, 5, 6$ in $D = 5$ and $D = 6$.

At quartic order, examples of representatives of the two inequivalent classes of GQT densities in $D = 5$ are (we use Roman numbers to label the different types)

$$\begin{aligned} \mathcal{S}_{[D=5,n=4]}^I = & + 12R^{abcd}R_{ab}{}^{ef}R_{ce}{}^{gh}R_{dgfh} + 3R^{abcd}R_{ac}{}^{ef}R_{bgdh}R_{ef}{}^{gh} \\ & - 6R^{abcd}R_{ac}{}^{ef}R_{eb}{}^{gh}R_{fgdh} - 9R^{ab}R_c{}^h{}_{ea}R_{dhfb}R^{cdef} + RR_{ab}{}^c{}^dR_{ef}{}^a{}^bR_{cd}{}^{ef}, \end{aligned} \quad (\text{A.1})$$

$$\begin{aligned} \mathcal{S}_{[D=5,n=4]}^{II} = & + 4R^{abcd}R_{ab}{}^{ef}R_{ce}{}^{gh}R_{dfgh} + 30R^{abcd}R_{ab}{}^{ef}R_{ce}{}^{gh}R_{dgfh} \\ & - 11R^{abcd}R_{ac}{}^{ef}R_{eb}{}^{gh}R_{fgdh} - 16R^{ab}R_c{}^h{}_{ea}R_{dhfb}R^{cdef} - R^{ab}R_{cd}{}^h{}_aR_{efhb}R^{cdef} \\ & - 3R^{ab}R_{ab}{}^c{}^dR_{efhc}R^{efh}{}_d + 3R^{ab}R^{cd}R_{ab}{}^e{}^fR_{ecfd} + R^{ab}R^{cd}R_{ac}{}^e{}^fR_{ebfd}, \end{aligned} \quad (\text{A.2})$$

which evaluated on the single-function ansatz reduce to linear combinations of $\mathcal{S}_{(4,j)}|_f$, as defined in eq. (2.11), with

$$\tau_{[D=5,n=4]}^I = 4\tau_{(4,1)} + 12\tau_{(4,3)} - 6\tau_{(4,4)}, \quad (\text{A.3})$$

$$\tau_{[D=5,n=4]}^{II} = 6\tau_{(4,2)} - \tau_{(4,4)}, \quad (\text{A.4})$$

respectively. It is straightforward to check that both satisfy conditions eq. (2.21) and eq. (2.23). In $D = 6$, we find

$$\begin{aligned} \mathcal{S}_{[D=6,n=4]}^I = & + 15R^{abcd}R_{ab}{}^{ef}R_{ce}{}^{gh}R_{dfgh} + 20R^{abcd}R_{ab}{}^{ef}R_{ce}{}^{gh}R_{dgfh} - 4R^{abcd}R_{ac}{}^{ef}R_{bgdh}R_{ef}{}^{gh} \\ & - 36R^{abcd}R_{ac}{}^{ef}R_{eb}{}^{gh}R_{fgdh} + 48R^{ab}R_c{}^h{}_{ea}R_{dhfb}R^{cdef} - 8R^{ab}R_{cd}{}^h{}_aR_{efhb}R^{cdef} \\ & - 8RR_{ab}{}^c{}^dR_{ef}{}^a{}^bR_{cd}{}^{ef} + 8R^{ab}R^{cd}R_{ac}{}^e{}^fR_{ebfd}, \end{aligned} \quad (\text{A.5})$$

$$\begin{aligned} \mathcal{S}_{[D=6,n=4]}^{II} = & - 5R^{abcd}R_{ab}{}^{ef}R_{ce}{}^{gh}R_{dfgh} - 28R^{abcd}R_{ab}{}^{ef}R_{ce}{}^{gh}R_{dgfh} - 20R^{abcd}R_{ac}{}^{ef}R_{bgdh}R_{ef}{}^{gh} \\ & + 52R^{abcd}R_{ac}{}^{ef}R_{eb}{}^{gh}R_{fgdh} - 16R^{ab}R_c{}^h{}_{ea}R_{dhfb}R^{cdef} + 8R^{ab}R_{cd}{}^h{}_aR_{efhb}R^{cdef} \\ & - 8R^{ab}R_{ab}{}^c{}^dR_{efhc}R^{efh}{}_d + 8R^{ab}R^{cd}R_{ab}{}^e{}^fR_{ecfd} - 8R^{ab}R^{cd}R_{ac}{}^e{}^fR_{ebfd}, \end{aligned} \quad (\text{A.6})$$

and for those

$$\tau_{[D=6,n=4]}^I = \tau_{(4,4)} - 2\tau_{(4,3)} - 2\tau_{(4,1)}. \quad (\text{A.7})$$

$$\tau_{[D=6,n=4]}^{II} = \tau_{(4,4)} - 4\tau_{(4,3)} - 6\tau_{(4,2)}. \quad (\text{A.8})$$

At quintic order, examples of the three inequivalent classes read

$$\begin{aligned} \mathcal{S}_{[D=5,n=5]}^I = & + 3235R^5 - 28409R^3R_a^bR_b^a + 46980R^2R_a^cR_b^aR_c^b - 93522RR_a^dR_b^aR_c^bR_d^c \\ & + 11928R_a^bR_b^aR_c^eR_d^cR_e^d + 98700RR_b^aR_d^bR_e^cR_{ac}^{de} + 2870R^3R_{ab}^{cd}R_{cd}^{ab} \\ & + 52080R_a^bR_b^aR_e^cR_f^dR_{cd}^{ef} - 151200RR_c^aR_d^bR_{ab}^{ef}R_{ef}^{cd} \\ & + 137655RR_b^aR_c^bR_{ad}^{ef}R_{ef}^{cd} - 5845RR_a^bR_b^aR_{cd}^{ef}R_{ef}^{cd} \\ & - 23940R_a^bR_b^aR_d^cR_{ce}^{fg}R_{fg}^{de}, \end{aligned} \quad (\text{A.9})$$

$$\begin{aligned} \mathcal{S}_{[D=5,n=5]}^{II} = & + 10505R^5 - 98197R^3R_a^bR_b^a + 242460R^2R_a^cR_b^aR_c^b - 362526RR_a^dR_b^aR_c^bR_d^c \\ & + 77784R_a^bR_b^aR_c^eR_d^cR_e^d + 77700RR_b^aR_d^bR_e^cR_{ac}^{de} + 1120R^3R_{ab}^{cd}R_{cd}^{ab} \\ & + 139440R_a^bR_b^aR_e^cR_f^dR_{cd}^{ef} - 173880RR_c^aR_d^bR_{ab}^{ef}R_{ef}^{cd} \\ & + 194985RR_b^aR_c^bR_{ad}^{ef}R_{ef}^{cd} + 12355RR_a^bR_b^aR_{cd}^{ef}R_{ef}^{cd} \\ & - 104580R_a^bR_b^aR_d^cR_{ce}^{fg}R_{fg}^{de} - 15120RR_b^aR_{ad}^{bc}R_{ce}^{fg}R_{fg}^{de} \\ & - 3780RR_b^aR_{ac}^{fg}R_{de}^{bc}R_{fg}^{de} + 11340R_a^bR_b^aR_{cd}^{gh}R_{ef}^{cd}R_{gh}^{ef}, \end{aligned} \quad (\text{A.10})$$

$$\begin{aligned} \mathcal{S}_{[D=5,n=5]}^{III} = & - 108751900R^5 + 1026499979R^3R_a^bR_b^a - 2724816480R^2R_a^cR_b^aR_c^b \\ & + 3743976918RR_a^dR_b^aR_c^bR_d^c - 981715812R_a^bR_b^aR_c^eR_d^cR_e^d \\ & + 241948812RR_b^aR_d^bR_e^cR_{ac}^{de} + 11124379R^3R_{ab}^{cd}R_{cd}^{ab} \\ & + 2523150RR_{ab}^{cd}R_{cd}^{ab} - 1472417016R_a^bR_b^aR_e^cR_f^dR_{cd}^{ef} \\ & + 442592640RR_c^aR_d^bR_{ab}^{ef}R_{ef}^{cd} - 1009017009RR_b^aR_c^bR_{ad}^{ef}R_{ef}^{cd} \\ & - 199666439RR_a^bR_b^aR_{cd}^{ef}R_{ef}^{cd} + 1327705722R_a^bR_b^aR_d^cR_{ce}^{fg}R_{fg}^{de} \\ & - 7998480RR_b^aR_{ad}^{bc}R_{ce}^{fg}R_{fg}^{de} + 151439400RR_b^aR_{ac}^{fg}R_{de}^{bc}R_{fg}^{de} \\ & - 197676360R_a^bR_b^aR_{cd}^{gh}R_{ef}^{cd}R_{gh}^{ef} + 35700000R_{ab}^{cd}R_{cd}^{ab}R_{ej}^{gh}R_{fh}^{ij}R_{gi}^{ef} \\ & + 121836960R_b^aR_{ad}^{bc}R_{cf}^{de}R_{eg}^{hi}R_{hi}^{fg} - 89250R_{ab}^{cd}R_{cd}^{ab}R_{ef}^{ij}R_{gh}^{ef}R_{ij}^{gh}, \end{aligned} \quad (\text{A.11})$$

And for them

$$\tau_{[D=5,n=5]}^I = +2\tau_{(5,0)} - \tau_{(5,1)} - 12\tau_{(5,2)} - 10\tau_{(5,3)} + 2\tau_{(5,4)} + 3\tau_{(5,5)}, \quad (\text{A.12})$$

$$\tau_{[D=5,n=5]}^{II} = -5\tau_{(5,0)} + 4\tau_{(5,1)} + 18\tau_{(5,2)} + 4\tau_{(5,3)} - 5\tau_{(5,4)}, \quad (\text{A.13})$$

$$\tau_{[D=5,n=5]}^{III} = +45\tau_{(5,0)} - 46\tau_{(5,1)} + 44(\tau_{(5,3)} - 3\tau_{(5,2)}). \quad (\text{A.14})$$

For $D = 6$, we find

$$\begin{aligned}
\mathcal{S}_{[D=6,n=5]}^{\text{I}} = & -123946191482880 R_a^b R_b^a R_c^e R_d^c R_e^d + 1472406237369312 R_a^d R_b^a R_c^b R_d^c R \\
& - 1080277675306560 R_a^c R_b^a R_c^b R^2 + 162174148310040 R_a^b R_b^a R^3 \\
& - 11444059832562 R^5 + 1702982503075584 R_b^a R_d^b R_e^c R R_{ac}^{de} \\
& + 75220642409760 R^3 R_{ab}^{cd} R_{cd}^{ab} + 12994390356246 R (R_{ab}^{cd} R_{cd}^{ab})^2 \\
& - 941724825600 R_a^b R_b^a R_e^c R_f^d R_{cd}^{ef} - 1826681030324352 R_c^a R_d^b R R_{ab}^{ef} R_{ef}^{cd} \\
& + 1161324617394816 R_b^a R_c^b R R_{ad}^{ef} R_{ef}^{cd} - 402058236112056 R_a^b R_b^a R R_{cd}^{ef} R_{ef}^{cd} \\
& + 796036321619712 R_b^a R R_{ad}^{bc} R_{ce}^{fg} R_{fg}^{de} \\
& - 226245709813248 R_b^a R R_{ac}^{fg} R_{de}^{bc} R_{fg}^{de} \\
& - 2713887813611520 R_{ag}^{cd} R_{bi}^{ef} R_{ce}^{ab} R_{dj}^{gh} R_{fh}^{ij} \\
& + 5441837051289600 R_{ag}^{cd} R_{bi}^{ef} R_{ce}^{ab} R_{dh}^{ij} R_{fj}^{gh} \\
& - 8516393811394560 R_{ag}^{cd} R_{bh}^{ij} R_{ce}^{ab} R_{di}^{ef} R_{fj}^{gh} \\
& - 9075154990067712 R_{aj}^{gh} R_{bd}^{ij} R_{ce}^{ab} R_{fg}^{cd} R_{hi}^{ef} , \tag{A.15}
\end{aligned}$$

$$\begin{aligned}
\mathcal{S}_{[D=6,n=5]}^{\text{II}} = & -39481565540352000 R_a^b R_b^a R_c^e R_d^c R_e^d + 496958473622415360 R_a^d R_b^a R_c^b R_d^c R \\
& - 366085018636185600 R_a^c R_b^a R_c^b R^2 + 56771103624384000 R_a^b R_b^a R^3 \\
& - 4236457006581120 R^5 + 605739537316331520 R_b^a R_d^b R_e^c R R_{ac}^{de} \\
& + 25066678861324800 R^3 R_{ab}^{cd} R_{cd}^{ab} + 2911274422692480 R (R_{ab}^{cd} R_{cd}^{ab})^2 \\
& - 9235519903334400 R_a^b R_b^a R_e^c R_f^d R_{cd}^{ef} \\
& - 654135376602562560 R_c^a R_d^b R R_{ab}^{ef} R_{ef}^{cd} \\
& + 384078592166215680 R_b^a R_c^b R R_{ad}^{ef} R_{ef}^{cd} \\
& - 128301089938030080 R_a^b R_b^a R R_{cd}^{ef} R_{ef}^{cd} \\
& + 247957574993141760 R_b^a R R_{ad}^{bc} R_{ce}^{fg} R_{fg}^{de} \\
& - 54410152259543040 R_b^a R R_{ac}^{fg} R_{de}^{bc} R_{fg}^{de} \\
& - 915942099386695680 R_{ag}^{cd} R_{bi}^{ef} R_{ce}^{ab} R_{dj}^{gh} R_{fh}^{ij} \\
& + 1855713735622656000 R_{ag}^{cd} R_{bi}^{ef} R_{ce}^{ab} R_{dh}^{ij} R_{fj}^{gh} \\
& - 2983978700100403200 R_{ag}^{cd} R_{bh}^{ij} R_{ce}^{ab} R_{di}^{ef} R_{fj}^{gh} \\
& - 3268733794665431040 R_{aj}^{gh} R_{bd}^{ij} R_{ce}^{ab} R_{fg}^{cd} R_{hi}^{ef} , \tag{A.16}
\end{aligned}$$

$$\begin{aligned}
\mathcal{S}_{[D=6,n=5]}^{\text{III}} = & -113245541360640R_a^b R_b^a R_c^e R_d^c R_e^d + 1060631652273264R_a^d R_b^a R_c^b R_d^c R \\
& - 903602985933600R_a^c R_b^a R_c^b R^2 + 127080097757820R_a^b R_b^a R^3 - 8955723921633R^5 \\
& + 1791407446201728R_b^a R_d^b R_e^c R R_{ac}^{de} + 65583784852200R^3 R_{ab}^{cd} R_{cd}^{ab} \\
& + 17709732531387R (R_{ab}^{cd} R_{cd}^{ab})^2 + 3780034053120 R_a^b R_b^a R_e^c R_f^d R_{cd}^{ef} \\
& - 2136457519124544R_c^a R_d^b R R_{ab}^{ef} R_{ef}^{cd} + 1548204355449792R_b^a R_c^b R R_{ad}^{ef} R_{ef}^{cd} \\
& - 341027462136492R_a^b R_b^a R R_{cd}^{ef} R_{ef}^{cd} + 601767492758784R_b^a R R_{ad}^{bc} R_{ce}^{fg} R_{fg}^{de} \\
& - 195741719323776R_b^a R R_{ac}^{fg} R_{de}^{bc} R_{fg}^{de} \\
& - 686045879580672R_{ag}^{cd} R_{bi}^{ef} R_{ce}^{ab} R_{dj}^{gh} R_{fh}^{ij} \\
& - 409211547264000R_{ag}^{cd} R_{bi}^{ef} R_{ce}^{ab} R_{dh}^{ij} R_{fj}^{gh} \\
& - 4137732154183680R_{ag}^{cd} R_{bh}^{ij} R_{ce}^{ab} R_{di}^{ef} R_{fj}^{gh} \\
& - 8161945395342336R_{aj}^{gh} R_{bd}^{ij} R_{ce}^{ab} R_{fg}^{cd} R_{hi}^{ef} , \tag{A.17}
\end{aligned}$$

and for them

$$\tau_{[D=6,n=5]}^{\text{I}} = \tau_{(5,5)} - 10\tau_{(5,2)} , \tag{A.18}$$

$$\tau_{[D=6,n=5]}^{\text{II}} = \tau_{(5,3)} - 3\tau_{(5,2)} + \tau_{(5,1)} , \tag{A.19}$$

$$\tau_{[D=6,n=5]}^{\text{III}} = \tau_{(5,4)} - \tau_{(5,3)} - 3\tau_{(5,2)} . \tag{A.20}$$

At order six we have four inequivalent GQT classes. Representatives in $D = 5$ are given by

$$\begin{aligned}
\mathcal{S}_{[D=5,n=6]}^{\text{I}} = & -73164000 (R_{ab}R^{ab})^3 - 1714893120R_{ab}R^{ab} R_c^e R_d^c R_e^d R \\
& + 1318812172R_{ab}R^{ab} R_c^d R_d^c R^2 + 271196208R_a^c R_b^a R_c^b R^3 \\
& - 317404865R_{ab}R^{ab} R^4 + 18018062R^6 + 300979224R_a^a R_d^b R^3 R_{ab}^{cd} \\
& + 248125440R_b^a R_d^b R_e^c R^2 R_{ac}^{de} + 170805000 (R_{ef}R^{ef})^2 R_{abcd}R^{abcd} \\
& - 452092811R_{ef}R^{ef} R^2 R_{abcd}R^{abcd} + 74766829R^4 R_{abcd}R^{abcd} \\
& - 139080000R_{ef}R^{ef} (R_{abcd}R^{abcd})^2 + 38179125R^2 (R_{abcd}R^{abcd})^2 \\
& + 35080000 (R_{abcd}R^{abcd})^3 - 2244499440R_{ab}R^{ab} R_e^c R_f^d R R_{cd}^{ef} \\
& - 445474968R_b^a R^3 R_{ac}^{de} R_{de}^{bc} - 87720000 (R_a^c R_b^d R_c^e R_d^f R_e^a R_f^b)^2 \\
& + 84746910R^3 R_{ab}^{ef} R_{cd}^{ab} R_{ef}^{cd} + 2407239480R_{ab}R^{ab} R_d^c R R_{ce}^{fg} R_{fg}^{de} \\
& - 88583040R_b^a R^2 R_{ad}^{bc} R_{ce}^{fg} R_{fg}^{de} - 410141550R_{ab}R^{ab} R R_{cd}^{gh} R_{ef}^{cd} R_{gh}^{ef} \\
& + 564422400R_b^a R R_{ad}^{bc} R_{cf}^{de} R_{eg}^{hi} R_{hi}^{fg} \\
& - 61305000R R_{abcd}R^{abcd} R_{ef}^{ij} R_{gh}^{ef} R_{ij}^{gh} \\
& + 727920000R^{de} R_{abcd}R^{abc} R_g^i R_h^j R_i^k R_j^l R_k^g R_l^h \\
& - 578160000R_{ab}^{cd} R_{cd}^{ef} R_{ef}^{ab} R_g^i R_h^j R_i^k R_j^l R_k^g R_l^h , \tag{A.21}
\end{aligned}$$

$$\begin{aligned}
\mathcal{S}_{[D=5,n=6]}^{\text{II}} = & -137140000 (R_{ab}R^{ab})^3 - 1947491520R_{ab}R^{ab}R_c^e R_d^c R_e^d R \\
& + 1751816692R_{ab}R^{ab}R_c^d R_d^c R^2 + 329051088R_a^c R_b^a R_c^b R^3 \\
& - 432438015R_{ab}R^{ab}R^4 + 25289682R^6 + 400229864R_c^a R_d^b R^3 R_{ab}^{cd} \\
& + 165181440R_b^a R_d^b R_e^c R^2 R_{ac}^{de} + 272619000 (R_{ef}R^{ef})^2 R_{abcd}R^{abcd} \\
& - 609591221R_{ef}R^{ef} R^2 R_{abcd}R^{abcd} + 100315219R^4 R_{abcd}R^{abcd} \\
& - 173400000R_{ef}R^{ef} (R_{abcd}R^{abcd})^2 + 46512875R^2 (R_{abcd}R^{abcd})^2 \\
& + 35600000 (R_{abcd}R^{abcd})^3 - 2869300240R_{ab}R^{ab}R_c^e R_f^d R R_{cd}^{ef} \\
& - 484473448R_b^a R^3 R_{ac}^{de} R_{de}^{bc} - 31320000 (R_a^c R_b^d R_c^e R_d^f R_e^a R_f^b)^2 \\
& + 55581410R^3 R_{ab}^{ef} R_{cd}^{ab} R_{ef}^{cd} + 2452251080R_{ab}R^{ab}R_d^c R R_{ce}^{fg} R_{fg}^{de} \\
& + 118104960R_b^a R^2 R_{ad}^{bc} R_{ce}^{fg} R_{fg}^{de} - 242892050R_{ab}R^{ab}R R_{cd}^{gh} R_{ef}^{cd} R_{gh}^{ef} \\
& + 425990400R_b^a R R_{ad}^{bc} R_{cf}^{de} R_{eg}^{hi} R_{hi}^{fg} \\
& - 77575000R R_{abcd}R^{abcd} R_{ef}^{ij} R_{gh}^{ef} R_{ij}^{gh} \\
& + 2129040000R^{de} R_{abcd}R^{abc} R_g^i R_h^j R_i^k R_j^l R_k^g R_l^h \\
& - 909840000R_{ab}^{cd} R_{cd}^{ef} R_{ef}^{ab} R_g^i R_h^j R_i^k R_j^l R_k^g R_l^h, \tag{A.22}
\end{aligned}$$

$$\begin{aligned}
\mathcal{S}_{[D=5,n=6]}^{\text{III}} = & -859300000 (R_{ab}R^{ab})^3 - 25179802560R_{ab}R^{ab}R_c^e R_d^c R_e^d R \\
& + 19703296676R_{ab}R^{ab}R_c^d R_d^c R^2 + 4227840144R_a^c R_b^a R_c^b R^3 \\
& - 4975158595R_{ab}R^{ab}R^4 + 291039066R^6 + 5123673672R_c^a R_d^b R^3 R_{ab}^{cd} \\
& + 1331589120R_b^a R_d^b R_e^c R^2 R_{ac}^{de} + 2222415000 (R_{ef}R^{ef})^2 R_{abcd}R^{abcd} \\
& - 6346768033R_{ef}R^{ef} R^2 R_{abcd}R^{abcd} + 1019618087R^4 R_{abcd}R^{abcd} \\
& - 1819320000R_{ef}R^{ef} (R_{abcd}R^{abcd})^2 + 513207375R^2 (R_{abcd}R^{abcd})^2 \\
& + 450800000 (R_{abcd}R^{abcd})^3 - 33156269520R_{ab}R^{ab}R_c^e R_f^d R R_{cd}^{ef} \\
& - 6081896904R_b^a R^3 R_{ac}^{de} R_{de}^{bc} + 4158600000 (R_a^c R_b^d R_c^e R_d^f R_e^a R_f^b)^2 \\
& + 1060299930R^3 R_{ab}^{ef} R_{cd}^{ab} R_{ef}^{cd} + 34472700840R_{ab}R^{ab}R_d^c R R_{ce}^{fg} R_{fg}^{de} \\
& - 834145920R_b^a R^2 R_{ad}^{bc} R_{ce}^{fg} R_{fg}^{de} - 5503384650R_{ab}R^{ab}R R_{cd}^{gh} R_{ef}^{cd} R_{gh}^{ef} \\
& + 6734419200R_b^a R R_{ad}^{bc} R_{cf}^{de} R_{eg}^{hi} R_{hi}^{fg} \\
& - 809475000R R_{abcd}R^{abcd} R_{ef}^{ij} R_{gh}^{ef} R_{ij}^{gh} \\
& + 15109200000R^{de} R_{abcd}R^{abc} R_g^i R_h^j R_i^k R_j^l R_k^g R_l^h \\
& - 9162000000R_{ab}^{cd} R_{cd}^{ef} R_{ef}^{ab} R_g^i R_h^j R_i^k R_j^l R_k^g R_l^h, \tag{A.23}
\end{aligned}$$

$$\begin{aligned}
\mathcal{S}_{[D=5,n=6]}^{\text{IV}} = & + 31500000 (R_{ab}R^{ab})^3 - 4028310720R_{ab}R^{ab}R_c{}^e R_d{}^c R_e{}^d R \\
& + 2252042612R_{ab}R^{ab}R_c{}^d R_d{}^c R^2 + 683314128R_a{}^c R_b{}^a R_c{}^b R^3 \\
& - 555694015R_{ab}R^{ab}R^4 + 27464642R^6 + 877183464R_c{}^a R_d{}^b R^3 R_{ab}{}^{cd} \\
& - 96706560R_b{}^a R_d{}^b R_e{}^c R^2 R_{ac}{}^{de} + 163995000 (R_{ef}R^{ef})^2 R_{abcd}R^{abcd} \\
& - 407173621R_{ef}R^{ef}R^2 R_{abcd}R^{abcd} + 62048819R^4 R_{abcd}R^{abcd} \\
& - 292440000R_{ef}R^{ef} (R_{abcd}R^{abcd})^2 + 28222875R^2 (R_{abcd}R^{abcd})^2 \\
& + 97600000 (R_{abcd}R^{abcd})^3 - 4629108240R_{ab}R^{ab}R_e{}^c R_f{}^d R R_{cd}{}^{ef} \\
& - 1045548648R_b{}^a R^3 R_{ac}{}^{de} R_{de}{}^{bc} + 2409000000 (R_a{}^c{}^d R_c{}^e{}^f R_e{}^a{}^b)^2 \\
& + 280021410R^3 R_{ab}{}^{ef} R_{cd}{}^{ab} R_{ef}{}^{cd} + 6317083080R_{ab}R^{ab}R_d{}^c R R_{ce}{}^{fg} R_{fg}{}^{de} \\
& - 655655040R_b{}^a R^2 R_{ad}{}^{bc} R_{ce}{}^{fg} R_{fg}{}^{de} - 1401052050R_{ab}R^{ab}R R_{cd}{}^{gh} R_{ef}{}^{cd} R_{gh}{}^{ef} \\
& + 664070400R_b{}^a R R_{ad}{}^{bc} R_{cf}{}^{de} R_{eg}{}^{hi} R_{hi}{}^{fg} - 46575000R R_{abcd}R^{abcd} R_{ef}{}^{ij} R_{gh}{}^{ef} R_{ij}{}^{gh} \\
& + 1414800000R^{de} R_{abcd}R^{abc} R_g{}^i{}^j R_i{}^k{}^l R_k{}^g{}^l \\
& - 1832400000R_{ab}{}^{cd} R_{cd}{}^{ef} R_{ef}{}^{ab} R_g{}^i{}^j R_i{}^k{}^l R_k{}^g{}^l . \tag{A.24}
\end{aligned}$$

And the corresponding $\tau(r)$ are given by

$$\tau_{[D=5,n=6]}^{\text{I}} = +\tau_{(6,0)} + 12\tau_{(6,5)} - 8\tau_{(6,6)} , \tag{A.25}$$

$$\tau_{[D=5,n=6]}^{\text{II}} = -5\tau_{(6,2)} - 16\tau_{(6,5)} + 11\tau_{(6,6)} , \tag{A.26}$$

$$\tau_{[D=5,n=6]}^{\text{III}} = -5\tau_{(6,3)} - 3\tau_{(6,5)} + 3\tau_{(6,6)} , \tag{A.27}$$

$$\tau_{[D=5,n=6]}^{\text{IV}} = +15\tau_{(6,4)} - 2(6\tau_{(6,5)} - \tau_{(6,6)}) . \tag{A.28}$$

For $D = 6$ we find

$$\begin{aligned}
\mathcal{S}_{[D=6,n=6]}^I = & - 14096679060821760 R_a^b R_b^c R_c^d R_d^e R_e^f R_f^a \\
& + 14852647970900544 R_c^e R_d^c R_e^d R_i^j R_j^i R \\
& - 5617985150718012 (R_i^j R_j^i)^2 R^2 - 1124843605416416 R_a^c R_b^a R_c^b R^3 \\
& + 1005726172300248 R_{ab} R^{ab} R^4 - 29156254184830 R^6 \\
& - 1438756007591232 R_c^a R_d^b R^3 R_{ab}^{cd} + 2380028275859520 R^2 R_b^a R_d^b R_e^c R_{ac}^{de} \\
& + 1254308457170736 R_{ef} R^{ef} R^2 R_{abcd} R^{abcd} - 168004022190642 R^4 R_{ab}^{cd} R_{cd}^{ab} \\
& + 3230088574927500 R_i^j R_j^i (R_{ab}^{cd} R_{cd}^{ab})^2 - 607399901908371 R^2 (R_{ab}^{cd} R_{cd}^{ab})^2 \\
& + 721416483693312 R_e^c R_f^d R_i^j R_j^i R R_{cd}^{ef} + 1133891404354368 R_b^a R^3 R_{ac}^{de} R_{de}^{bc} \\
& - 682346981951712 R^3 R_{ab}^{ef} R_{cd}^{ab} R_{ef}^{cd} + 9376966635379200 R^{ab} R^{cd} R_i^j R_j^i R_{ecfd} R_a^e R_b^f \\
& - 8990642116684800 R^{ab} R_i^j R_j^i R_a^c R_b^d R_{efgc} R^{efg}_d \\
& - 6299359808303232 R_d^c R_i^j R_j^i R R_{ce}^{fg} R_{fg}^{de} \\
& + 1901604108792960 R_b^a R^2 R_{ad}^{bc} R_{ce}^{fg} R_{fg}^{de} \\
& + 3847116811602240 R_i^j R_j^i R R_{cd}^{gh} R_{ef}^{cd} R_{gh}^{ef} \\
& - 10134930764312640 R_a^b R_b^c R_c^d R_d^a R_{ef}^{hi} R_{hi}^{eg} \\
& - 2178824133657600 R_b^a R R_{ad}^{bc} R_{cf}^{de} R_{eg}^{hi} R_{hi}^{fg} \\
& + 304956123151680 R R_{ab}^{cd} R_{cd}^{ab} R_{ef}^{ij} R_{gh}^{ef} R_{ij}^{gh} \\
& - 1895257162656000 R_{ab}^{cd} R_{cd}^{ef} R_{ef}^{gh} R_{gh}^{ij} R_{ij}^{kl} R_{kl}^{ab} \\
& + 1259726446836000 R_{ab}^{cd} R_{cd}^{ef} R_{ef}^{gh} R_{gh}^{ab} R_{ij}^{kl} R_{kl}^{ij}, \tag{A.29}
\end{aligned}$$

$$\begin{aligned}
\mathcal{S}_{[D=6,n=6]}^{\text{II}} = & - 31836692340236160 R_a^b R_b^c R_c^d R_d^e R_e^f R_f^a \\
& + 34439506371202464 R_c^e R_d^c R_e^d R_i^j R_j^i R - 13557698416858564 (R_i^j R_j^i)^2 R^2 \\
& - 2849781769779440 R_a^c R_b^a R_c^b R^3 + 2611991351109630 R_{ab} R^{ab} R^4 \\
& - 88399029128845 R^6 - 3677104626840832 R_c^a R_d^b R^3 R_{ab}^{cd} \\
& + 6132894365769600 R^2 R_b^a R_d^b R_e^c R_{ac}^{de} + 3157451844617752 R_{ef} R^{ef} R^2 R_{abcd} R^{abcd} \\
& - 441312471667562 R^4 R_{ab}^{cd} R_{cd}^{ab} + 7146998363226150 R_i^j R_j^i (R_{ab}^{cd} R_{cd}^{ab})^2 \\
& - 1314167139538110 R^2 (R_{ab}^{cd} R_{cd}^{ab})^2 + 2087392939560192 R_e^c R_f^d R_i^j R_j^i R R_{cd}^{ef} \\
& + 2787439490093632 R_b^a R^3 R_{ac}^{de} R_{de}^{bc} - 1533575360560320 R^3 R_{ab}^{ef} R_{cd}^{ab} R_{ef}^{cd} \\
& + 22373284326307200 R^{ab} R^{cd} R_i^j R_j^i R_{ecfd} R_a^e R_b^f \\
& - 20005506406828800 R^{ab} R_i^j R_j^i R_a^c R_b^d R_{efgc} R^{efg}_d \\
& - 15079987603900032 R_d^c R_i^j R_j^i R R_{ce}^{fg} R_{fg}^{de} \\
& + 3611210786726400 R_b^a R^2 R_{ad}^{bc} R_{ce}^{fg} R_{fg}^{de} \\
& + 8724416327193600 R_i^j R_j^i R R_{cd}^{gh} R_{ef}^{cd} R_{gh}^{ef} \\
& - 23212861724463840 R_a^b R_b^c R_c^d R_d^a R_{ef}^{hi} R_{hi}^{eg} \\
& - 3819771274176000 R_b^a R R_{ad}^{bc} R_{cf}^{de} R_{eg}^{hi} R_{hi}^{fg} \\
& + 616693394116800 R R_{ab}^{cd} R_{cd}^{ab} R_{ef}^{ij} R_{gh}^{ef} R_{ij}^{gh} \\
& - 4293178347744000 R_{ab}^{cd} R_{cd}^{ef} R_{ef}^{gh} R_{gh}^{ij} R_{ij}^{kl} R_{kl}^{ab} \\
& + 2871990255420000 R_{ab}^{cd} R_{cd}^{ef} R_{ef}^{gh} R_{gh}^{ab} R_{ij}^{kl} R_{kl}^{ij}, \tag{A.30}
\end{aligned}$$

$$\begin{aligned}
\mathcal{S}_{[D=6,n=6]}^{\text{III}} = & -6943970290757760 R_a^b R_b^c R_c^d R_d^e R_e^f R_f^a \\
& + 5474732611842144 R_c^e R_d^c R_e^d R_i^j R_j^i R - 2281174181020312 (R_i^j R_j^i)^2 R^2 \\
& - 355850581360016 R_a^c R_b^a R_c^b R^3 + 372382664514798 R_{ab} R^{ab} R^4 - 8079133402255 R^6 \\
& - 724084260087232 R_c^a R_d^b R^3 R_{ab}{}^{cd} + 680829460259520 R^2 R_b^a R_d^b R_e^c R_{ac}{}^{de} \\
& + 397223834424736 R_{ef} R^{ef} R^2 R_{abcd} R^{abcd} - 65621870854892 R^4 R_{ab}{}^{cd} R_{cd}{}^{ab} \\
& + 656091001244250 R_i^j R_j^i (R_{ab}{}^{cd} R_{cd}{}^{ab})^2 - 121001538886371 R^2 (R_{ab}{}^{cd} R_{cd}{}^{ab})^2 \\
& + 2073302769914112 R_e^c R_f^d R_i^j R_j^i R R_{cd}{}^{ef} + 671781101071168 R_b^a R^3 R_{ac}{}^{de} R_{de}{}^{bc} \\
& - 224552737043712 R^3 R_{ab}{}^{ef} R_{cd}{}^{ab} R_{ef}{}^{cd} \\
& + 2768431158979200 R^{ab} R^{cd} R_i^j R_j^i R_{ecfd} R_a^e R_b^f \\
& - 2668237319404800 R^{ab} R_i^j R_j^i R_a^c R_b^d R_{efgc} R^{efg}{}_d \\
& - 3774533321404032 R_d^c R_i^j R_j^i R R_{ce}{}^{fg} R_{fg}{}^{de} \\
& + 523902114552960 R_b^a R^2 R_{ad}{}^{bc} R_{ce}{}^{fg} R_{fg}{}^{de} \\
& + 1290427980114240 R_i^j R_j^i R R_{cd}{}^{gh} R_{ef}{}^{cd} R_{gh}{}^{ef} \\
& - 849014886788640 R_a^b R_b^c R_c^d R_d^a R_{ef}{}^{hi} R_{hi}{}^{eg} \\
& - 965396466777600 R_b^a R R_{ad}{}^{bc} R_{cf}{}^{de} R_{eg}{}^{hi} R_{hi}{}^{fg} \\
& + 70932032851680 R R_{ab}{}^{cd} R_{cd}{}^{ab} R_{ef}{}^{ij} R_{gh}{}^{ef} R_{ij}{}^{gh} \\
& - 336455941536000 R_{ab}{}^{cd} R_{cd}{}^{ef} R_{ef}{}^{gh} R_{gh}{}^{ij} R_{ij}{}^{kl} R_{kl}{}^{ab} \\
& + 219456058536000 R_{ab}{}^{cd} R_{cd}{}^{ef} R_{ef}{}^{gh} R_{gh}{}^{ab} R_{ij}{}^{kl} R_{kl}{}^{ij}, \tag{A.31}
\end{aligned}$$

$$\begin{aligned}
\mathcal{S}_{[D=6,n=6]}^{\text{IV}} = & -14096679060821760 R_a^b R_b^c R_c^d R_d^e R_e^f R_f^a \\
& + 14852647970900544 R_c^e R_d^c R_e^d R_i^j R_j^i R - 5617985150718012 (R_i^j R_j^i)^2 R^2 \\
& - 1124843605416416 R_a^c R_b^a R_c^b R^3 + 1005726172300248 R_{ab} R^{ab} R^4 \\
& - 29156254184830 R^6 - 1438756007591232 R_c^a R_d^b R^3 R_{ab}^{cd} \\
& + 2380028275859520 R^2 R_b^a R_d^b R_e^c R_{ac}^{de} + 1254308457170736 R_{ef} R^{ef} R^2 R_{abcd} R^{abcd} \\
& - 168004022190642 R^4 R_{ab}^{cd} R_{cd}^{ab} + 3230088574927500 R_i^j R_j^i (R_{ab}^{cd} R_{cd}^{ab})^2 \\
& - 607399901908371 R^2 (R_{ab}^{cd} R_{cd}^{ab})^2 + 721416483693312 R_e^c R_f^d R_i^j R_j^i R R_{cd}^{ef} \\
& + 1133891404354368 R_b^a R^3 R_{ac}^{de} R_{de}^{bc} - 682346981951712 R^3 R_{ab}^{ef} R_{cd}^{ab} R_{ef}^{cd} \\
& + 9376966635379200 R^{ab} R^{cd} R_i^j R_j^i R_{ecfd} R_a^e R_b^f - \\
& 8990642116684800 R^{ab} R_i^j R_j^i R_a^c R_b^d R_{efgc} R^{efg}_d \\
& - 6299359808303232 R_d^c R_i^j R_j^i R R_{ce}^{fg} R_{fg}^{de} \\
& + 1901604108792960 R_b^a R^2 R_{ad}^{bc} R_{ce}^{fg} R_{fg}^{de} \\
& + 3847116811602240 R_i^j R_j^i R R_{cd}^{gh} R_{ef}^{cd} R_{gh}^{ef} \\
& - 10134930764312640 R_a^b R_b^c R_c^d R_d^a R_{ef}^{hi} R_{hi}^{eg} \\
& - 2178824133657600 R_b^a R R_{ad}^{bc} R_{cf}^{de} R_{eg}^{hi} R_{hi}^{fg} \\
& + 304956123151680 R R_{ab}^{cd} R_{cd}^{ab} R_{ef}^{ij} R_{gh}^{ef} R_{ij}^{gh} \\
& - 1895257162656000 R_{ab}^{cd} R_{cd}^{ef} R_{ef}^{gh} R_{gh}^{ij} R_{ij}^{kl} R_{kl}^{ab} \\
& + 1259726446836000 R_{ab}^{cd} R_{cd}^{ef} R_{ef}^{gh} R_{gh}^{ab} R_{ij}^{kl} R_{kl}^{ij}, \tag{A.32}
\end{aligned}$$

and for them

$$\tau_{[D=6,n=6]}^{\text{I}} = \tau_{(6,6)} - 15\tau_{(6,2)} + 4\tau_{(6,1)}, \tag{A.33}$$

$$\tau_{[D=6,n=6]}^{\text{II}} = \tau_{(6,5)} - 10\tau_{(6,2)} + 3\tau_{(6,1)}, \tag{A.34}$$

$$\tau_{[D=6,n=6]}^{\text{III}} = \tau_{(6,4)} - 6\tau_{(6,2)} + 2\tau_{(6,1)}, \tag{A.35}$$

$$\tau_{[D=6,n=6]}^{\text{IV}} = \tau_{(6,3)} - 3\tau_{(6,2)} + \tau_{(6,1)}. \tag{A.36}$$

A.2 Physical constraints for GQTG black holes

The equation of motion for $f(r)$ with non-zero black hole mass admits asymptotically AdS solutions of the form

$$f(r) = \kappa + f_\infty \frac{r^2}{\ell^2} + \frac{m}{h'(f_\infty) r^{D-3}} + \dots, \tag{A.37}$$

with omitted terms decaying faster than $1/r^{d-3}$. The parameter m is related to the ADM mass M via

$$M = \frac{(D-2)\Omega_{D-2}}{16\pi} m.$$

The constant f_∞ satisfies the polynomial equation

$$h(f_\infty) \equiv 1 - f_\infty + \sum_{n \geq 2} \sum_{k=1}^{n_{\max}} \frac{(-1)^n 2\alpha_{n,k}}{\ell^{2n-2}} \frac{D-2n}{D-2} f_\infty^n = 0, \quad (\text{A.38})$$

whose first derivative with respect to f_∞ is

$$h'(f_\infty) = -1 + \sum_{n \geq 2} \sum_{k=1}^{n_{\max}} \frac{(-1)^n 2\alpha_{n,k}}{L^{2n-2}} \frac{D-2n}{D-2} n f_\infty^{n-1}. \quad (\text{A.39})$$

These conditions ensure that the graviton is not a ghost in a constant curvature background. In some theories $h'(f_\infty)$ vanishes identically [8, 9], in which cases the asymptotic expansion (3.14) is no longer valid. We shall not consider this situation here, leaving it for future investigation.

For the QT class, a positive value of f_∞ that solves (A.38) is sufficient to impose asymptotically AdS boundary conditions, but is insufficient for a theory with genuine GQT densities. This is because of the non-algebraic nature of equation (3.6). Since this is a differential equation, the expansion (3.14) only represents one particular solution for $f(r)$. To gain a complete version of the asymptotic solution, we must find the homogenous part f_h , which solves the differential equation

$$f_h'' - \frac{4}{r} f_h' - \gamma^2 r^{D-3} f_h = 0. \quad (\text{A.40})$$

Although the structure of (A.40) is general for any genuine GQT theories, the expression for the coefficient γ^2 here depends on the choice of higher-curvature couplings. For example, the expression

$$\gamma^2 = \frac{4[h'(f_\infty)]^2 f_\infty^2}{3(D-1)m[h(f_\infty) + f_\infty - 1]L^2} \quad (\text{A.41})$$

holds for theories that have $\{\alpha_{n,k=2}\}$ as the only non-zero couplings, but becomes invalid if any coupling with $k \geq 3$ is turned on.

Hence for GQT theories, in addition to the sign of f_∞ , we require that f_h have only decaying modes faster than $1/r^{D-3}$ to preserve the correct asymptotic condition at the boundary. Solving (A.40) at far region yields

$$f_h = \begin{cases} r^{5/2} \left[\mathcal{A} I_{\frac{5}{(D-1)}} \left(2\gamma \frac{r^{(D-1)/2}}{D-1} \right) + \mathcal{B} K_{\frac{5}{(D-1)}} \left(2\gamma \frac{r^{(D-1)/2}}{D-1} \right) \right] & \text{if } \gamma^2 > 0 \\ r^{5/2} \left[\mathcal{C} J_{\frac{5}{(D-1)}} \left(2\gamma \frac{r^{(d-1)/2}}{D-1} \right) + \mathcal{D} Y_{\frac{5}{(D-1)}} \left(2\gamma \frac{r^{(D-1)/2}}{D-1} \right) \right] & \text{if } \gamma^2 < 0, \end{cases}$$

where \mathcal{A} , \mathcal{B} , \mathcal{C} and \mathcal{D} are constants fixed by boundary conditions and $I_k(x)$, $K_k(x)$, $J_k(x)$ and $Y_k(x)$ are Bessel functions of order k . In the large- r limit they become

$$f_h^{(+)} \sim \mathcal{A} r^{\frac{11-D}{4}} \exp\left(\frac{2|\gamma|r^{\frac{D-1}{2}}}{D-1}\right) + \mathcal{B} r^{\frac{11-D}{4}} \exp\left(-\frac{2|\gamma|r^{\frac{D-1}{2}}}{D-1}\right),$$

$$f_h^{(-)} \sim \mathcal{C}r^{\frac{11-D}{4}} \cos\left(\frac{2|\gamma|r^{\frac{D-1}{2}}}{D-1} + \frac{(3D-13)\pi}{4(D-1)}\right) + \mathcal{D}r^{\frac{11-D}{4}} \sin\left(\frac{2|\gamma|r^{\frac{D-1}{2}}}{D-1} + \frac{(3D-13)\pi}{4(D-1)}\right),$$

where the superscripts (\pm) indicate the sign of γ^2 . In order that the homogenous part is subdominant at large r , we require $\gamma^2 > 0$ and $\mathcal{A} = 0$.

Apart from the correct asymptote, physical theories should only propagate one type of massless spin-2 graviton on constant curvature backgrounds. This implies the effective Newtonian constant must have the same sign as the one in general relativity, which means the third term in (3.14) should become negative for positive mass, that is $h'(f_\infty) < 0$ [93].

Summarizing, we only consider black holes with $f_\infty > 0$, $h'(f_\infty) < 0$ and $\gamma^2 > 0$ as satisfying the requisite physical criteria.

A.3 Field Equations

The equations of motion $\mathcal{E}_F = 0 = \mathcal{E}_n$ for the two metric functions in (4.9) are obtained by the variation of the on shell action with respect to F and n respectively, where the explicit forms of \mathcal{E}_F and \mathcal{E}_n are given by

$$\begin{aligned} 4F^7 \mathcal{E}_F / u^3 &\equiv 3F^3 u^4 \{2nu[24\alpha un'F'' + 10(10\alpha + \beta)un'n'' + u^2 n' n^{(3)}(8\alpha + \beta) \\ &+ 24\alpha F'(un'' + 5n') + (124\alpha + 7\beta)n'^2 + u^2(8\alpha + \beta)n''^2] \\ &+ u^2 n'^2 [24\alpha F' + 2(10\alpha + \beta)n' + u(8\alpha + \beta)n''] + 16\alpha n^2 [u(n^{(3)}u + 7n'') + 8n']\} \\ &+ 30u^6 n F F' \{u(12\alpha + \beta)F'n'^2 + 4\alpha n [uF''n' + F'(un'' + 8n')]\} - 240\alpha n^2 u^7 F'^3 n' \\ &- 6F^2 u^5 \{u^2(9\alpha + \beta)F'n'^3 + 4\alpha n^2 [F'(n^{(3)}u^2 + 16un'' + 50n') + uF''(un'' + 10n')]\} \\ &+ 2nun' [24\alpha F'^2 + 6(14\alpha + \beta)n'F' + u(21\alpha + 2\beta)F'n'' + u(9\alpha + \beta)F''n'] \\ &- 12F^4 u^4 \{un'[(4\alpha - \beta)n' + 2\alpha un''] + 4\alpha n [u(n^{(3)}u + 7n'') + 8n']\} - 4F^5 n', \end{aligned}$$

$$\begin{aligned} 8F^7 n \mathcal{E}_n &\equiv 8F^7 (\Lambda_0 - u^2) - 120F n^2 u^9 F'^2 [u(10\alpha + \beta)F'n' + 4\alpha n (uF'' + 4F')] \\ &+ 6F^2 n u^8 \{u^2(58\alpha + 7\beta)F'^2 n'^2 + 8\alpha n^2 [u^2 F''^2 + uF'(F^{(3)}u + 26F'') + 54F'^2] \\ &+ 4nuF' [24\alpha F'^2 + 2(62\alpha + 5\beta)F'n' + u(10\alpha + \beta)F'n'' + 4u(9\alpha + \beta)F''n']\} \\ &+ 6F^4 u^7 \{-4\alpha u^2 F'n'^2 + 4n^2 [48\alpha F' + u(32\alpha F'' + 4\alpha F^{(3)}u - \beta n'') - 4\beta n'] \\ &+ nu [8(10\alpha - 1\beta)F'n' + 16\alpha un'F'' - \beta n'^2 + 16\alpha uF'n'']\} \\ &+ F^5 \{8nu^3 [F' + 3\beta u^4 (un'' + 4n')] - 6\beta u^8 n'^2\} + 8F^6 nu^2 + 480\alpha n^3 u^{10} F'^4 \\ &- 3F^3 u^7 \{2nu^2 n' [48\alpha F'^2 + 2(44\alpha + 5\beta)n'F' + 3u(8\alpha + \beta)F'n'' + 2u(8\alpha + \beta)F''n'] \\ &+ 4n^2 u [132\alpha F'^2 + 48\alpha uF'F'' + 4(40\alpha + \beta)F'n' + 2u(16\alpha + \beta)F'n''] \\ &+ 8(10\alpha + \beta)un'F'' + u^2(8\alpha + \beta)n''F'' + F^{(3)}u^2(8\alpha + \beta)n'] - u^3(8\alpha + \beta)F'n'^3 \\ &+ 32\alpha n^3 [u(F^{(3)}u + 8F'') + 12F']\}. \end{aligned}$$

(A.42)

A.4 Taylor Series Solution at $u = 0$

The field equations imply that the series ansatz (4.14) and (4.15) have the coefficients given in (4.14). These all depend only on F_2, F_4, F_5 and β , with a few of the leading terms being

$$n_3 = \frac{5F_2F_5}{18\beta - 4F_2^2} \quad (\text{A.43})$$

$$n_4 = \frac{135F_2F_5^2(3F_2^2 - 11\beta)}{16(9\beta - 2F_2^2)^2(F_2^2 + F_4)} \quad (\text{A.44})$$

$$n_5 = \frac{27F_2F_5^3(11916\beta^2 - 6621\beta F_2^2 + 919F_2^4)}{64(F_2^2 + F_4)^2(9\beta - 2F_2^2)^3} + \frac{3F_4F_5}{9\beta - 2F_2^2} \quad (\text{A.45})$$

$$n_6 = \frac{45F_2F_5^4(-3217212\beta^3 + 2700468\beta^2F_2^2 - 755109\beta F_2^4 + 70339F_2^6)}{448(F_2^2 + F_4)^3(9\beta - 2F_2^2)^4} + \frac{25F_5^2[F_2^2(96\beta + 175F_4) - 630\beta F_4 - 22F_2^4]}{112(F_2^2 + F_4)(9\beta - 2F_2^2)^2} \quad (\text{A.46})$$

...

$$F_6 = \frac{F_4^2}{F_2} - \frac{9F_5^2(828\beta^2 - 363\beta F_2^2 + 37F_2^4)}{32(F_2^2 + F_4)(9\beta - 2F_2^2)^2} \quad (\text{A.47})$$

$$F_7 = \frac{9F_5^3(268164\beta^3 - 184383\beta^2F_2^2 + 40020\beta F_2^4 - 2641F_2^6)}{224(F_2^2 + F_4)^2(9\beta - 2F_2^2)^3} + \frac{F_4F_5(34F_2^2 - 135\beta)}{7(2F_2^3 - 9\beta F_2)} \quad (\text{A.48})$$

...

A.5 Taylor Series Solution at $u = u_{\text{th}}$

Similarly, we can obtain the coefficients in the series (4.17) by solving (A.42) order by order. A few coefficients are given by

$$\tilde{F}_1 = -\frac{1}{\tilde{n}_1^2 u_{\text{th}}^9 \mathcal{D}} [6\tilde{F}_0^2 \beta \tilde{n}_1^2 F_2 u_{\text{th}}^8 + 8\tilde{F}_0^4 (F_2 u_{\text{th}}^2 + 2)] \quad (\text{A.49})$$

$$\begin{aligned} \tilde{n}_2 = & \frac{1}{4\tilde{n}_1 F_2 u_{\text{th}}^9 \mathcal{D}^2} [4\tilde{F}_0^3 \tilde{n}_1 u_{\text{th}} (48\beta + 24\beta F_2 u_{\text{th}}^2 - 7F_2^3 u_{\text{th}}^2 - 18F_2^2) \\ & + \tilde{n}_1^4 F_2 (-36\beta^2 + 27\beta F_2^2 - 5F_2^4) u_{\text{th}}^{10} + 48\tilde{F}_0^4 F_2^2 (F_2 u_{\text{th}}^2 + 2) \\ & + 9\tilde{F}_0 \tilde{n}_1^3 F_2^3 (F_2^2 - 3\beta) u_{\text{th}}^9 - 4\tilde{F}_0^2 \tilde{n}_1^2 F_2 (F_2^2 - 3\beta) u_{\text{th}}^4 (F_2^2 u_{\text{th}}^4 + 2)], \end{aligned} \quad (\text{A.50})$$

where \mathcal{D} is defined as

$$\mathcal{D} \equiv \tilde{n}_1 F_2 (F_2^2 - 3\beta) u_{\text{th}} - \tilde{F}_0 F_2^3 \quad (\text{A.51})$$